

Chiara Guardasoni

# Wave Propagation Analysis

with

# Boundary Element Method

PhD Thesis

June 10, 2010



*Three important years have been spent  
and for all thanks to  
my father Fabio and my mother Raffaella  
my grandparents  
Michele  
Alessandra  
Prof. M. Diligenti and Prof. A. Aimi ...*



# Preface

Time-dependent problems, that are frequently modelled by hyperbolic partial differential equations, can be dealt with the boundary integral equations (BIEs) method. The ideal situation is when the partial differential equation is homogeneous with constant coefficients, the initial conditions vanish and the data are given only on the boundary of a domain independent of time. In this situation the transformation of the differential problem to a BIE follows the same well-known method for elliptic boundary value problems. In fact the starting point for a BIE method is the representation of the differential problem solution in terms of single layer and double layer potentials using the fundamental solution of the hyperbolic partial differential operator.

There are, however, specific difficulties due to the additional time dimension: apart from the practical problems of increased complexity related to the higher dimension, new stability problems can appear [14, 26]. In the time-dependent case, instabilities have been observed in practice and due to the absence of ellipticity, the stability analysis is more difficult and fewer theoretical results are available.

For what concerns the discretization of the obtained BIEs, boundary element methods (BEMs) have been successfully applied to many time-dependent problems from fields as electromagnetic wave propagation, computation of transient acoustic wave, linear elastodynamics, fluid dynamics, etc. [7, 9, 24, 42, 49]. Frequently claimed advantages over domain approaches are the dimensionality reduction of the discretization, the easy implicit enforcement for radiation conditions at infinity, the reduction of an unbounded exterior domain to a bounded boundary, the high accuracy achievable and simple pre- and post-processing for input and output data.

In the case of hyperbolic initial-boundary value problems, one can distinguish three approaches to the application of boundary integral methods: Laplace-transform methods, time-stepping methods and space-time integral equations. I refer to the surveys [19, 20] for a more complete bibliography on the subject.

- Most earlier contributions concerned direct formulations of BEM in the frequency domain, often using the Laplace or Fourier transforms. After this transformation a standard boundary integral method for an elliptic (Helmoltz) problem is applied and then the transformation back to time domain employs special techniques for the inversion of Laplace or Fourier transforms.

- Time-stepping methods start from a time discretization of the original initial-boundary value problem via an implicit scheme and then use boundary integral equations to solve the resulting elliptic problems for each time step. Here a difficulty lies in the form of the problem for every simple time step which has non-zero initial data and thus it is not in the ideal form for an application of the boundary integral method, namely vanishing initial conditions and volume forces and non-homogeneous boundary data.

The convolution quadrature method for the time discretization, that has been developed in [39, 40, 41], overcomes this problem providing a straightforward way to obtain a stable time stepping scheme using the Laplace transform of the kernel function.

- The consideration of the time-domain (transient) problem yields directly the unknown time-dependent quantities. Usual numerical discretization methods include collocation methods in addition to some stabilization techniques and Laplace-Fourier methods coupled with Galerkin boundary elements in space.

The application of Galerkin boundary elements in both space and time has been implemented by several authors but in this direction only the weak formulation due to Bamberger and Ha Duong [10, 11, 29, 30] furnishes genuine convergence results. They obtain the well-posedness of the retarded BIE and stability of the BEM approximations thanks to a coerciveness property of a suitable quadratic form in the unknown density closely related to the energy functional of the wave equation. Their approach relies, via Laplace transform, on uniform estimates with respect to complex frequencies of the corresponding Helmholtz problem.

The stability analysis for all known algorithms, for the space-time integral equation methods as for the time-stepping schemes, passes through the transformation to the frequency domain and uses corresponding estimates for the stability of BIE methods for elliptic problems.

The aim of this thesis is to develop an efficient procedure for the application of BEM to transient scalar wave propagation problems, investigating the coerciveness property of the related energy functional, avoiding the analysis in the frequency domain. Thus is of great interest both from the theoretical and the numerical point of view. In fact, a formulation based on the direct analysis in time of the energy functional would hopefully provide, even for the multidimensional problems, an effective alternative to that proposed in [10], where the passage to complex frequencies leads to stability constants that grow exponentially in time, as stated in [20].

In the first chapter, firstly I recall the analytical properties of the starting differential problem that is the transient scalar wave equation in a domain  $\Omega$  with homogeneous initial conditions and Dirichlet and/or Neumann conditions on the boundary of  $\Omega$ .

Then various tables summarize the wide range of possible retarded BIEs with time-dependent densities as unknowns reformulating the wave problem at hand.

The technique used by Bamberger and Ha Duong to find the weak formulation and to prove stability is described in section 1.2 and it can be resumed in the following steps: Fourier-Laplace transform in time variable of the differential problem; uniform estimates with respect to complex frequencies of the corresponding Helmholtz

problem; application of Paley-Wiener theorem and Parseval identity. In particular this final step provides a space-time weak formulation closely related to the energy functional of the wave equation, whose associated quadratic form turns out to be coercive with respect to a suitable weighted Sobolev norm.

At this stage the passage to complex frequencies can be avoided exploiting the well-known energy-flux relation that allows to infer a suitable space-time weak formulation for the integral problems with a natural quadratic form  $a_{\mathcal{E}}$ .

For suitable geometries of the boundary, and thanks to the finite speed of propagation property, the square root of the energy defines a norm, through which one can study continuity and coerciveness properties of the energy functional in order to verify the stability of further Galerkin approximation:

- In chapter 2, for the simple case of one dimensional problems, precise estimates of continuity and coerciveness in  $L^2$  have been presented for every sort of boundary conditions and consequently, unconditionally stable schemes with well-behaved stability constants, even for large times, have been found.
- In chapter 3, considering the extension to two dimensional problems, there are no difficulties concerning the continuity but only some partial results have been obtained, via Fourier transform, in the case of a flat obstacle for what concern coercivity. On the other hand the presented theoretical analysis of the energetic weak formulation has its natural counterpart in the context of three dimensional problems: in fact these theoretical results can be extended without modifications to any spatial dimension  $n \geq 3$ .

Further, with the “energetic” formulation, I have obtained several numerical results which seem to be very interesting in comparison with other ones found in literature either in one dimensional or two dimensional cases ([12, 26]): typical instability phenomena are never present with the energetic procedure.

These numerical results have been obtained using the Galerkin discretization of the energetic weak problems as reported in chapter 4. Representing the approximate solution of the integral problem with piecewise polynomial functions in the space-time domain, the applied element by element technique produces a linear system with a Toeplitz block lower triangular matrix easily solvable with appropriate accuracy without high computational costs.

The implementation of this procedure implies, during the calculation of the matrix elements, a double analytic integration in time variables and then numerical integration of weakly singular, singular and hypersingular double integrals in space variables with several troubles concerning their approximation. Therefore I have developed some suitable quadrature techniques in order to achieve satisfactory precision. In particular some quadrature formulas illustrated in [5, 44, 45, 46], already tested for the elliptic problems, have been coupled with a regularization technique after a careful subdivision of the integration domain due to the presence of the Heaviside function in the integral kernels. The introduced numerical schemes are a valid alternative to those proposed in [28, 53].

Numerical results, compared with literature benchmarks whenever possible, are given throughout the thesis.

*Milan, February 2010*

*Chiara Guardasoni*





# Contents

<b>1</b>	<b>Basic theory</b> .....	1
1.1	The differential problem and the space-time integral reformulation .	1
1.2	The Bamberger-Ha Duong method .....	8
<b>2</b>	<b>The one-dimensional wave problem</b> .....	15
2.1	The Dirichlet problem .....	15
2.1.1	Energetic weak problem related to the BIE .....	16
2.1.2	Numerical results .....	20
2.2	Neumann problem .....	25
2.3	Mixed Boundary Value Problems .....	27
2.3.1	Energetic weak problem related to the BIEs .....	29
2.3.2	Numerical results .....	34
<b>3</b>	<b>The two dimensional wave problem</b> .....	41
3.1	Exterior Dirichlet problem .....	41
3.1.1	Numerical results .....	54
3.2	Exterior Neumann problem .....	59
3.2.1	Numerical results .....	60
3.3	Mixed Boundary Value Problems .....	67
3.3.1	Numerical results .....	68
<b>4</b>	<b>Discretization</b> .....	75
4.1	Galerkin BEM discretization .....	75
4.2	Evaluation of Galerkin matrix elements .....	80
4.3	Basic quadrature rules .....	88
4.4	Numerical integration schemes .....	90
<b>A</b>	<b>Appendix</b> .....	103
A.1	Remarks on energy coerciveness in 1D .....	103
A.2	Integration over disjoint elements ( $\bar{e}_i \cap \bar{e}_j = \emptyset$ ) .....	107
A.3	Recurrence relations for product rules .....	109
A.4	Numerical integration of (4.45) .....	112
	<b>References</b> .....	116



# Chapter 1

## Basic theory

This first chapter has the aim to give an overview of the theoretical analysis present in literature of the properties of the differential and integral transient wave problem useful to investigate boundary integral methods. In this context I will focus only on Bamberger and Ha Duong space-time weak formulation for the strictly connection with the energetic weak formulation which is the subject of my research, leaving out the other above cited methods.

### 1.1 The differential problem and the space-time integral reformulation

The transient wave problem treated in this thesis describes the propagation of the displacement field  $u$  with velocity equal to one without external forces action, beginning from a state of rest (vanishing initial conditions) with Dirichlet and/or Neumann boundary conditions.

The reference results about existence, uniqueness and regularity for the solution of this differential problem are in [37] and [38], then there are some improvements in recent papers as [35] for the Dirichlet problems, [33], [34] for Neumann problems and [47], [16] for mixed boundary value problems.

Let  $\Omega$  be an open set of  $\mathbb{R}^n$  with infinitely differentiable boundary  $\Gamma$  of dimension  $n - 1$  ( $\Omega$  takes up locally only one side of  $\Gamma$ ).

#### • Dirichlet Problem

$$(P_{\mathcal{D}}) \begin{cases} u_{tt}(\mathbf{x}, t) - \Delta u(\mathbf{x}, t) = 0 & \mathbf{x} \in \Omega, t \in (0, T) \\ u(\mathbf{x}, 0) = u_t(\mathbf{x}, 0) = 0 & \mathbf{x} \in \Omega \\ u(\mathbf{x}, t) = g_{\mathcal{D}}(\mathbf{x}, t) & (\mathbf{x}, t) \in \Sigma = \Gamma \times [0, T] \end{cases}$$

For the problem  $(P_{\mathcal{D}})$  with the compatibility condition  $g_{\mathcal{D}}|_{t=0} = 0$ , the basic theoretical result is

**Theorem 1** *If  $g_{\mathcal{D}} \in L^2(\Sigma)$  then  $u \in C([0, T]; L^2(\Omega)) \cap C^1([0, T]; H^{-1}(\Omega))$  and  $\partial u / \partial \mathbf{n} \in H^{-1}(\Sigma)$ . If  $g_{\mathcal{D}} \in H^1(\Sigma)$  then  $u \in C([0, T]; H^1(\Omega)) \cap C^1([0, T]; L^2(\Omega))$  and  $\partial u / \partial \mathbf{n} \in L^2(\Sigma)$ .*

If we need to consider  $\Gamma$  non-smooth we can refer to [31].

• Neumann Problem:

$$(P_{\mathcal{N}}) \begin{cases} u_{tt}(\mathbf{x}, t) - \Delta u(\mathbf{x}, t) = 0 & \mathbf{x} \in \Omega, t \in (0, T) \\ u(\mathbf{x}, 0) = u_t(\mathbf{x}, 0) = 0 & \mathbf{x} \in \Omega \\ \frac{\partial u}{\partial \mathbf{n}}(\mathbf{x}, t) = g_{\mathcal{N}}(\mathbf{x}, t) & (\mathbf{x}, t) \in \Sigma := \Gamma \times [0, T] \end{cases}$$

**Theorem 2** *If  $g_{\mathcal{N}} \in L^2(\Sigma)$  then  $u \in C([0, T]; H^{1/2}(\Omega)) \cap C^1([0, T]; H^{-1/2}(\Omega))$ <sup>1</sup> and  $u \in L^2(\Sigma)$ . If  $g_{\mathcal{N}} \in L^2(\Sigma)$  then  $u \in H^{3/5-\varepsilon}([0, T] \times \Omega)$  and  $u \in H^{1/5-\varepsilon}(\Sigma)$  with  $\varepsilon > 0$ .*

This last result can be extended also to the case of a parallelepiped  $\Omega$  obtaining

**Theorem 3** *If  $g_{\mathcal{N}} \in L^2(\Sigma)$  then  $u \in H^{3/4-\varepsilon}([0, T] \times \Omega)$  and  $u \in H^{2/3-\varepsilon}(\Sigma)$  with  $\varepsilon > 0$ .*

Defining  $\Gamma_{\mathcal{D}}$  and  $\Gamma_{\mathcal{N}}$  (the portions of the boundary  $\Gamma$  where Dirichlet or Neumann data are respectively given) in a way such that  $\bar{\Gamma} = \bar{\Gamma}_{\mathcal{D}} \cup \bar{\Gamma}_{\mathcal{N}}$  and  $\Gamma_{\mathcal{D}} \cap \Gamma_{\mathcal{N}} = \emptyset$  we can cope with

• Problem with Mixed Boundary Conditions

$$(P_{\mathcal{D}\mathcal{N}}) \begin{cases} u_{tt}(\mathbf{x}, t) - \Delta u(\mathbf{x}, t) = 0 & \mathbf{x} \in \Omega, t \in (0, T) \\ u(\mathbf{x}, 0) = u_t(\mathbf{x}, 0) = 0 & \mathbf{x} \in \Omega \\ u(\mathbf{x}, t) = g_{\mathcal{D}}(\mathbf{x}, t) & (\mathbf{x}, t) \in \Sigma_{\mathcal{D}} := \Gamma_{\mathcal{D}} \times [0, T] \\ \frac{\partial u}{\partial \mathbf{n}}(\mathbf{x}, t) = g_{\mathcal{N}}(\mathbf{x}, t) & (\mathbf{x}, t) \in \Sigma_{\mathcal{N}} := \Gamma_{\mathcal{N}} \times [0, T] \end{cases}$$

Few of articles can be found in literature, referring to existence and uniqueness of the solution of this kind of problems. I don't describe here the related statements because of the complexity of theory necessary to explain them, for reference look at [47] and [16].

The same benchmark problems can be posed in exterior domains; the above reported results can be naturally extended to problems whose domain is considered outside the boundary  $\Gamma$  ( $\Omega^e := \mathbb{R}^n \setminus \Omega$ ): thanks to well-known property of finite velocity of wave propagation, with respect to time interval of observation  $[0, T]$ , we can reduce all the problems to some interior problems.

<sup>1</sup> A fortiori  $u \in H^{1/2}([0, T] \times \Omega)$ .

Talking about the integral reformulation of the differential wave problem, the crucial point is the integral representation theorem that allows us to obtain an analytical expression of the solution by means of an unknown function on the boundary. In order to apply this theorem we need the second Gauss-Green formula

**Theorem 4** (Second Gauss-Green Formula) *Let  $\Omega$  be a bounded domain in  $\mathbb{R}^n$  with piecewise-smooth boundary  $\Gamma$ . Let  $\mathbf{n} = (\mathbf{n}_1, \mathbf{n}_2, \dots, \mathbf{n}_n)$  denote the outward unit normal vector field on  $\Gamma$  which exists everywhere except at finitely many nonsmooth points of  $\Gamma$ . Let  $f$  and  $g$  be sufficiently regular functions defined on  $\Omega$  (e.g.,  $f, g \in H^1(\Omega)$ ). then the integration-by-parts in multi dimensional space*

$$\int_{\Omega} \frac{\partial f(\mathbf{x})}{\partial \mathbf{x}_i} g(\mathbf{x}) d\mathbf{x} = \int_{\Gamma} f(\mathbf{x}) g(\mathbf{x}) \mathbf{n}_i(\mathbf{x}) d\mathbf{x}_{\Gamma} - \int_{\Omega} f(\mathbf{x}) \frac{\partial g(\mathbf{x})}{\partial \mathbf{x}_i} d\mathbf{x}$$

and, as a consequence, the second Gauss-Green formula

$$\int_{\Omega} \{f(\mathbf{x}) \Delta g(\mathbf{x}) - g(\mathbf{x}) \Delta f(\mathbf{x})\} d\mathbf{x} = \int_{\Gamma} \left\{ f(\mathbf{x}) \frac{\partial g(\mathbf{x})}{\partial \mathbf{n}} - g(\mathbf{x}) \frac{\partial f(\mathbf{x})}{\partial \mathbf{n}} \right\} d\mathbf{x}_{\Gamma}$$

holds.

and the knowledge of the fundamental solution that is, by definition, the solution  $G$  in the point  $\mathbf{x} \in \mathbb{R}^n$  at the time  $t > 0$  of:

$$G_{tt}(\mathbf{x}, t) - \Delta G(\mathbf{x}, t) = \delta(\mathbf{x} - \xi) \delta(t - \tau) \quad (1.1)$$

where  $\delta$  is the Dirac distribution centered in the point  $\xi$  and in the time instant  $\tau$ . The solutions of (1.1) are respectively

- $n = 1$

$$G(x, \xi, t, \tau) = \frac{1}{2} H[t - \tau - |x - \xi|] \quad (1.2)$$

- $n = 2$

$$G(\mathbf{x}, \xi, t, \tau) = \frac{1}{2\pi} \frac{H[t - \tau - |\mathbf{x} - \xi|]}{[(t - \tau)^2 - |\mathbf{x} - \xi|^2]^{1/2}} \quad (1.3)$$

- $n = 3$

$$G(\mathbf{x}, \xi, t, \tau) = \frac{1}{4\pi} \frac{\delta[t - \tau - |\mathbf{x} - \xi|]}{|\mathbf{x} - \xi|} \quad (1.4)$$

with  $H[\cdot]$ , Heaviside step function.

Now, consider the wave equation and its initial conditions in a domain  $\Omega \subset \mathbb{R}^n$  satisfying the hypothesis to apply the Gauss-Green formula

$$\begin{cases} u_{tt}(\mathbf{x}, t) - \Delta u(\mathbf{x}, t) = 0, & t \in \mathbb{R}^+ \\ u(\mathbf{x}, 0) = u_t(\mathbf{x}, 0) = 0 \end{cases} \quad (1.5)$$

multiply the equation by the fundamental solution  $G$  and integrate in time and space

$$\int_0^t \int_{\Omega} u_{\tau\tau}(\xi, \tau) G(\mathbf{x}, \xi, t, \tau) d\xi d\tau - \int_0^t \int_{\Omega} \Delta u(\xi, \tau) G(\mathbf{x}, \xi, t, \tau) d\xi d\tau = 0 \quad (1.6)$$

then integrate by-parts twice in time, noticing that  $G$  and  $G_{\tau}$  vanish when  $\tau = t$  and that the initial conditions are homogeneous

$$\begin{aligned} & - \int_0^t \int_{\Omega} \Delta u G d\xi d\tau + \int_{\Omega} u_{\tau} G d\xi \Big|_0^t - \int_0^t \int_{\Omega} u_{\tau} G_{\tau} d\xi d\tau = 0, \\ & - \int_0^t \int_{\Omega} \Delta u G d\xi d\tau + \int_{\Omega} u_{\tau} G d\xi \Big|_0^t - \int_{\Omega} u G_{\tau} d\xi \Big|_0^t + \int_0^t \int_{\Omega} u G_{\tau\tau} d\xi d\tau = 0, \\ & - \int_0^t \int_{\Omega} \Delta u G d\xi d\tau + \int_0^t \int_{\Omega} u G_{\tau\tau} d\xi d\tau = 0. \end{aligned}$$

Applying the second Gauss-Green formula and the equation (1.1)

$$\begin{aligned} & - \int_0^t \int_{\Omega} \Delta u G d\xi d\tau + \int_0^t \int_{\Omega} u G_{\tau\tau} d\xi d\tau = 0, \\ & \int_0^t \int_{\Gamma} \left\{ u \frac{\partial G}{\partial \mathbf{n}_{\xi}} - G \frac{\partial u}{\partial \mathbf{n}_{\xi}} \right\} d\xi_{\Gamma} d\tau - \int_0^t \int_{\Omega} u \Delta G d\xi d\tau + \int_0^t \int_{\Omega} u G_{\tau\tau} d\xi d\tau = 0, \\ & \int_0^t \int_{\Gamma} \left\{ u \frac{\partial G}{\partial \mathbf{n}_{\xi}} - G \frac{\partial u}{\partial \mathbf{n}_{\xi}} \right\} d\xi_{\Gamma} d\tau + \int_0^t \int_{\Omega} u \delta(\mathbf{x} - \xi) \delta(t - \tau) d\xi d\tau = 0 \end{aligned}$$

we obtain an integral representation of the solutions  $u$  of (1.5) with  $\mathbf{x} \in \Omega$  and  $t \in \mathbb{R}^+$ :

$$u(\mathbf{x}, t) = \int_0^t \int_{\Gamma} \left\{ G(\mathbf{x}, \xi, t, \tau) \frac{\partial u(\xi, \tau)}{\partial \mathbf{n}_{\xi}} - u(\xi, \tau) \frac{\partial G(\mathbf{x}, \xi, t, \tau)}{\partial \mathbf{n}_{\xi}} \right\} d\xi_{\Gamma} d\tau. \quad (1.7)$$

An analogous representation can be found in the exterior problem defined for  $\mathbf{x} \in \Omega^e := \mathbb{R}^n \setminus \Omega$  and  $t \in \mathbb{R}^+$  with a change in sign

$$u(\mathbf{x}, t) = \int_0^t \int_{\Gamma} \left\{ -G(\mathbf{x}, \xi, t, \tau) \frac{\partial u(\xi, \tau)}{\partial \mathbf{n}_{\xi}} + u(\xi, \tau) \frac{\partial G(\mathbf{x}, \xi, t, \tau)}{\partial \mathbf{n}_{\xi}} \right\} d\xi_{\Gamma} d\tau. \quad (1.8)$$

The above expressions can be collected in the following theorem (see [13] and [20]):

**Theorem 5** *If  $u$  is a classical solution of (1.5) in the domain  $(\Omega^e \cup \Omega) \times \mathbb{R}^+$  with regular traces on  $\Gamma \times \mathbb{R}^+$  then:  $\forall (\mathbf{x}, t) \in (\Omega^e \cup \Omega) \times \mathbb{R}^+$*

$$u(\mathbf{x}, t) = \int_0^t \int_{\Gamma} \left\{ G(\mathbf{x}, \xi, t, \tau) \left[ \frac{\partial u(\xi, \tau)}{\partial \mathbf{n}_{\xi}} \right]_{\Gamma} - \frac{\partial G(\mathbf{x}, \xi, t, \tau)}{\partial \mathbf{n}_{\xi}} [u(\xi, \tau)]_{\Gamma} \right\} d\xi_{\Gamma} d\tau \quad (1.9)$$

where the square brackets  $[\ ]_{\Gamma}$  define the jump of their argument function on  $\Gamma$ .

Now I'm going to introduce some notations through which I will formulate the Boundary Integral Equations (BIEs) (for references see [13], [15], [16], [19] and [20]).

When  $\mathbf{x} \in \Omega$ , introducing the single layer potential operator  $\mathcal{V}$

$$(\mathcal{V}\psi)(\mathbf{x}, t) = \int_0^t \int_{\Gamma} G(\mathbf{x}, \xi, t, \tau) \psi(\xi, \tau) d\xi_{\Gamma} d\tau \quad (1.10)$$

and the double layer potential operator  $\mathcal{K}$

$$(\mathcal{K}\psi)(\mathbf{x}, t) = \int_0^t \int_{\Gamma} \frac{\partial G(\mathbf{x}, \xi, t, \tau)}{\partial \mathbf{n}_{\xi}} \psi(\xi, \tau) d\xi_{\Gamma} d\tau \quad (1.11)$$

the representation formula (1.9) can be rewritten in a compact form as

$$u = \mathcal{V}[\partial_{\mathbf{n}_{\xi}} u]_{\Gamma} - \mathcal{K}[u]_{\Gamma} \quad (1.12)$$

with the classical jump relations

$$\begin{aligned} [\mathcal{V}\psi]_{\Gamma} &= 0 & [\partial_{\mathbf{n}_{\mathbf{x}}}\mathcal{V}\psi]_{\Gamma} &= -\psi, \\ [\mathcal{K}\psi]_{\Gamma} &= \psi & [\partial_{\mathbf{n}_{\mathbf{x}}}\mathcal{K}\psi]_{\Gamma} &= 0. \end{aligned} \quad (1.13)$$

It appears therefore natural to introduce the boundary operators by sums and differences of the one-sided traces on the exterior ( $\Gamma^+$ ) and interior ( $\Gamma^-$ ) of  $\Gamma$ :

$$\begin{aligned} V &:= \mathcal{V}|_{\Gamma} \\ K &:= \frac{1}{2}(\mathcal{K}|_{\Gamma^+} + \mathcal{K}|_{\Gamma^-}) \\ K' &:= \frac{1}{2}(\partial_{\mathbf{n}_{\mathbf{x}}}\mathcal{V}|_{\Gamma^+} + \partial_{\mathbf{n}_{\mathbf{x}}}\mathcal{V}|_{\Gamma^-}) \\ D &:= \partial_{\mathbf{n}_{\mathbf{x}}}\mathcal{K}|_{\Gamma} \end{aligned} \quad (1.14)$$

To interior or exterior differential problems with any of the boundary conditions mentioned in this section can be associated one or more Representation Formulas (RFs) for the solution  $u$  and, as consequence, making the point  $\mathbf{x}$  of the domain tending to a point on the boundary, the related BIEs. Typically one has a choice of at least four BIEs for each problem: the first two come from taking the traces in the representation formula (1.12) (“direct method”), the third one comes from a single layer representation

$$u = \mathcal{V}\psi \quad \text{with unknown } \psi$$

and the fourth one from a double layer representation

$$u = \mathcal{K}\omega \quad \text{with unknown } \omega.$$

Everything is resumed in the following tables:

- Dirichlet Problem

- Domain  $\Omega \times [0, T]$ :

$u|_{\Gamma} = g_{\mathcal{D}}$  given and  $\varphi := \partial_{\mathbf{n}} u|_{\Gamma^-}$ ,  $\psi$ ,  $\omega$  boundary unknowns

	$\forall (\mathbf{x}, t) \in \Omega \times \mathbb{R}^+$		$\forall (\mathbf{x}, t) \in \Gamma^- \times \mathbb{R}^+$	
RF	$\partial_{\mathbf{n}_{\mathbf{x}}} u = \partial_{\mathbf{n}_{\mathbf{x}}} (\mathcal{V} \varphi - \mathcal{K} u)$	BIE	$(-\frac{1}{2} + K') \varphi = D g_{\mathcal{D}}$	(D1a)
RF	$u = \mathcal{V} \varphi - \mathcal{K} u$	BIE	$V \varphi = (K + \frac{1}{2}) g_{\mathcal{D}}$	(D1b)
RF	$u = \mathcal{V} \psi$	BIE	$V \psi = g_{\mathcal{D}}$	(D1c)
RF	$u = -\mathcal{K} \omega$	BIE	$(\frac{1}{2} - K) \omega = g_{\mathcal{D}}$	(D1d)

- Domain  $\Omega^e \times [0, T]$ :

$u|_{\Gamma} = g_{\mathcal{D}}$  given and  $\varphi := \partial_{\mathbf{n}} u|_{\Gamma^+}$ ,  $\psi$ ,  $\omega$  boundary unknowns

	$\forall (\mathbf{x}, t) \in \Omega^e \times \mathbb{R}^+$		$\forall (\mathbf{x}, t) \in \Gamma^+ \times \mathbb{R}^+$	
RF	$\partial_{\mathbf{n}_{\mathbf{x}}} u = \partial_{\mathbf{n}_{\mathbf{x}}} (-\mathcal{V} \varphi + \mathcal{K} u)$	BIE	$(\frac{1}{2} + K') \varphi = D g_{\mathcal{D}}$	(D2a)
RF	$u = -\mathcal{V} \varphi + \mathcal{K} u$	BIE	$V \varphi = (K - \frac{1}{2}) g_{\mathcal{D}}$	(D2b)
RF	$u = -\mathcal{V} \psi$	BIE	$V \psi = -g_{\mathcal{D}}$	(D2c)
RF	$u = \mathcal{K} \omega$	BIE	$(\frac{1}{2} + K) \omega = g_{\mathcal{D}}$	(D2d)

- Domain  $(\Omega^e \cup \Omega) \times [0, T]$ :

$u|_{\Gamma} = g_{\mathcal{D}}$  given and  $\varphi := [\partial_{\mathbf{n}} u]_{\Gamma}$  boundary unknown

	$\forall (\mathbf{x}, t) \in (\Omega^e \cup \Omega) \times \mathbb{R}^+$		$\forall (\mathbf{x}, t) \in \Gamma \times \mathbb{R}^+$	
RF	$u = \mathcal{V} \varphi$	BIE	$V \varphi = g_{\mathcal{D}}$	(D3a)

- Neumann Problem

- Domain  $\Omega \times [0, T]$ :

$\partial_{\mathbf{n}} u|_{\Gamma} = g_{\mathcal{N}}$  given and  $\phi := u|_{\Gamma^-}$ ,  $\psi$ ,  $\omega$  boundary unknowns

	$\forall (\mathbf{x}, t) \in \Omega \times \mathbb{R}^+$		$\forall (\mathbf{x}, t) \in \Gamma^- \times \mathbb{R}^+$	
RF	$\partial_{\mathbf{n}_{\mathbf{x}}} u = \partial_{\mathbf{n}_{\mathbf{x}}} (\mathcal{V} \partial_{\mathbf{n}_{\xi}} u - \mathcal{K} \phi)$	BIE	$D \phi = (-\frac{1}{2} + K') g_{\mathcal{N}}$	(N1a)
RF	$u = \mathcal{V} \partial_{\mathbf{n}_{\xi}} u - \mathcal{K} \phi$	BIE	$(K + \frac{1}{2}) \phi = V g_{\mathcal{N}}$	(N1b)
RF	$\partial_{\mathbf{n}_{\mathbf{x}}} u = \partial_{\mathbf{n}_{\mathbf{x}}} \mathcal{V} \psi$	BIE	$(\frac{1}{2} + K') \psi = g_{\mathcal{N}}$	(N1c)
RF	$\partial_{\mathbf{n}_{\mathbf{x}}} u = -\partial_{\mathbf{n}_{\mathbf{x}}} \mathcal{K} \omega$	BIE	$D \omega = -g_{\mathcal{N}}$	(N1d)

- Domain  $\Omega^e \times [0, T]$ :

$\partial_{\mathbf{n}} u|_{\Gamma} = g_{\mathcal{N}}$  given and  $\phi := u|_{\Gamma^+}$ ,  $\psi$ ,  $\omega$  boundary unknowns

	$\forall (\mathbf{x}, t) \in \Omega^e \times \mathbb{R}^+$		$\forall (\mathbf{x}, t) \in \Gamma^+ \times \mathbb{R}^+$	
RF	$\partial_{\mathbf{n}_{\mathbf{x}}} u = \partial_{\mathbf{n}_{\mathbf{x}}} (-\mathcal{V} \partial_{\mathbf{n}_{\xi}} u + \mathcal{K} \phi)$	BIE	$D \phi = (\frac{1}{2} + K') g_{\mathcal{N}}$	(N2a)
RF	$u = -\mathcal{V} \partial_{\mathbf{n}_{\xi}} u + \mathcal{K} \phi$	BIE	$(K - \frac{1}{2}) \phi = V g_{\mathcal{N}}$	(N2b)
RF	$\partial_{\mathbf{n}_{\mathbf{x}}} u = -\partial_{\mathbf{n}_{\mathbf{x}}} \mathcal{V} \psi$	BIE	$(\frac{1}{2} - K') \psi = g_{\mathcal{N}}$	(N2c)
RF	$\partial_{\mathbf{n}_{\mathbf{x}}} u = \partial_{\mathbf{n}_{\mathbf{x}}} \mathcal{K} \omega$	BIE	$D \omega = g_{\mathcal{N}}$	(N2d)



- Domain  $(\Omega^e \cup \Omega) \times [0, T]$ :  
 $\partial_{\mathbf{n}} u|_{\Gamma} = g_{\mathcal{N}}$  given and  $\phi := [u]_{\Gamma}$  boundary unknown

	$\forall (\mathbf{x}, t) \in (\Omega^e \cup \Omega) \times \mathbb{R}^+$		$\forall (\mathbf{x}, t) \in \Gamma \times \mathbb{R}^+$	
RF	$\partial_{\mathbf{n}_x} u = \partial_{\mathbf{n}_x} \mathcal{K} \phi$	BIE	$D\phi = g_{\mathcal{N}}$	(N3a)

- Mixed Boundary Value Problems

Dealing with representation formulas and boundary integral equations for problems with mixed boundary conditions, we have to take into consideration the RF  $u = \mathcal{V} \partial_{\mathbf{n}_\xi} u - \mathcal{K} u$  and its normal derivative and then couple in a system the limit of the RF, for  $\mathbf{x}$  tending to a point of  $\Gamma_{\mathcal{D}}$  and the limit of the derivative of the RF, for  $\mathbf{x}$  tending to a point of  $\Gamma_{\mathcal{N}}$ . Solving this system we obtain, as result,  $u|_{\Gamma_{\mathcal{N}}}$  and  $\partial_{\mathbf{n}} u|_{\Gamma_{\mathcal{D}}}$  that inserted in the RF are sufficient to get the solution  $u$  over the whole domain. Resuming

- Domain  $\Omega \times [0, T]$ :  
 $\partial_{\mathbf{n}} u|_{\Gamma_{\mathcal{N}}} = g_{\mathcal{N}}$  and  $u|_{\Gamma_{\mathcal{D}}} = g_{\mathcal{D}}$  given  
 $\phi := u|_{\Gamma_{\mathcal{N}}^-}$  and  $\varphi := \partial_{\mathbf{n}} u|_{\Gamma_{\mathcal{D}}^-}$  boundary unknowns

	$\forall (\mathbf{x}, t) \in \Omega \times \mathbb{R}^+$		$\forall (\mathbf{x}, t) \in \Gamma^- \times \mathbb{R}^+$	
RF	$u = \mathcal{V} \partial_{\mathbf{n}_\xi} u - \mathcal{K} u$	BIE	$\begin{cases} V \partial_{\mathbf{n}_\xi} u - Ku = \frac{1}{2} g_{\mathcal{D}} \\ -K' \partial_{\mathbf{n}_\xi} u + Du = -\frac{1}{2} g_{\mathcal{N}} \end{cases}$	(M1)

- Domain  $\Omega^e \times [0, T]$ :  
 $\partial_{\mathbf{n}} u|_{\Gamma_{\mathcal{N}}} = g_{\mathcal{N}}$  and  $u|_{\Gamma_{\mathcal{D}}} = g_{\mathcal{D}}$  given  
 $\phi := u|_{\Gamma_{\mathcal{N}}^+}$  and  $\varphi := \partial_{\mathbf{n}} u|_{\Gamma_{\mathcal{D}}^+}$  boundary unknowns

	$\forall (\mathbf{x}, t) \in \Omega \times \mathbb{R}^+$		$\forall (\mathbf{x}, t) \in \Gamma^+ \times \mathbb{R}^+$	
RF	$u = -\mathcal{V} \partial_{\mathbf{n}_\xi} u + \mathcal{K} u$	BIE	$\begin{cases} -V \partial_{\mathbf{n}_\xi} u + Ku = \frac{1}{2} g_{\mathcal{D}} \\ K' \partial_{\mathbf{n}_\xi} u - Du = -\frac{1}{2} g_{\mathcal{N}} \end{cases}$	(M2)

As told in [16], during last decades, a number of paper dealing with the numerical solution of non-stationary boundary equations have appeared but without proofs of convergence of approximate solutions to the exact ones. On the other hand, up to very recently, existence theorems for the corresponding non-stationary boundary equations were absent as well. This was connected to the fact that the boundary operators that correspond to the boundary equations in the dynamic case differ essentially from the analogous operators in the static (elliptic) case. In particular, their ranges are not closed in some natural function spaces. This does not make it possible to use the Fredholm alternative in studying their properties.

The earlier results can be found in [10] and in [11] where two theorems state existence and uniqueness of solutions in a Sobolev type functional space respectively for the BIEs (D1c)/(D2c)/(D3a) reformulations of the Dirichlet problem and for the BIEs (N1d)/(N2d)/(N3a) reformulations of the Neumann problem in inte-

rior/exterior domains of  $\mathbb{R}^3$ . The method introduced by the authors, Bamberger and Ha Duong, has then been applied by Chudinovich in a wider variety of non stationary boundary equations in  $\mathbb{R}^3$  as summarized in [16].

This method, thanks to its general nature, can be easily extended also to problems in  $\mathbb{R}^1$  and  $\mathbb{R}^2$  and moreover it gives us a numerical stable scheme to perform numerical implementations so I cannot prescind from going into details.

## 1.2 The Bamberger-Ha Duong method

The basic idea of the method can be outlined in four steps:

1. transform the starting differential transient wave problem into the Helmholtz problem
2. reformulate the Helmholtz problem via BIEs
3. write the BIE in a continuous and coercive weak form
4. antitransform it obtaining a time-space variational formulation for the transient wave problem with stability and convergence properties.

To explain the procedure, I'll take into consideration the exterior Dirichlet problem (see [10])

$$(P_{\mathcal{D}}^e) \begin{cases} u_{tt}(\mathbf{x}, t) - \Delta u(\mathbf{x}, t) = 0 & \mathbf{x} \in \Omega^e \subset \mathbb{R}^n, t \in (0, T) \\ u(\mathbf{x}, 0) = u_t(\mathbf{x}, 0) = 0 & \mathbf{x} \in \Omega^e \\ u(\mathbf{x}, t) = g_{\mathcal{D}}(\mathbf{x}, t) & (\mathbf{x}, t) \in \Sigma = \Gamma \times [0, T] \end{cases}$$

Suppose that extending  $g_{\mathcal{D}}$  and  $u$  to 0 for  $t < 0$  on obtains Laplace transformable<sup>2</sup> distributional functions with values in  $H^{1/2}(\Gamma)$  and  $H^1(\Omega^e)$  respectively; so, considering

$$\mathcal{L}[u](\mathbf{x}, s) := \int_{-\infty}^{+\infty} u(\mathbf{x}, t) e^{-st} dt, s \in \mathbb{C}, \quad (1.15)$$

for every  $s$  such that  $s = -i\omega$ ,  $\omega = \eta + i\sigma$  and  $\sigma > \sigma_0$  we can define

$$\hat{u}(\mathbf{x}, \omega) := \mathcal{L}[u](\mathbf{x}, \omega) = \int_{-\infty}^{+\infty} u(\mathbf{x}, t) e^{i\omega t} dt \quad \text{and} \quad \hat{g}_{\mathcal{D}}(\mathbf{x}, \omega) := \int_{-\infty}^{+\infty} g_{\mathcal{D}}(\mathbf{x}, t) e^{i\omega t} dt \quad (1.16)$$

with the properties

$$\mathcal{L}[\Delta u](\mathbf{x}, \omega) = \Delta \hat{u}(\mathbf{x}, \omega) \quad \mathcal{L}[u_{tt}](\mathbf{x}, \omega) = -\omega^2 \hat{u}(\mathbf{x}, \omega) \quad (1.17)$$

and we can convert the problem  $(P_{\mathcal{D}}^e)$  into the Helmholtz problem:

<sup>2</sup> It means that there exists a constant  $\sigma_0 \in \mathbb{R}$  that is infimum of the set where the improper integrals of  $e^{-\sigma_0 t} g_{\mathcal{D}}$  and  $e^{-\sigma_0 t} u$  defining the Laplace transforms converge.

$$(P_{\mathcal{D}}^{\omega}) \begin{cases} \hat{u}(\mathbf{x}, \omega) \in H^1(\Omega^e) \\ \Delta \hat{u}(\mathbf{x}, \omega) + \omega^2 \hat{u}(\mathbf{x}, \omega) = 0 & x \in \Omega^e \\ \hat{u}(\mathbf{x}, \omega) = \hat{g}_{\mathcal{D}}(\mathbf{x}, \omega) & x \in \Gamma \end{cases}$$

It is well known that in the half space  $\sigma > 0$  (we can always take  $\sigma_0 \geq 0$ ) the problem  $(P_{\mathcal{D}}^{\omega})$  admits a unique solution provided that the Sommerfield radiation condition is satisfied (here replaced by the condition  $\hat{u}(\mathbf{x}, \omega) \in H^1(\Omega^e)$ ) and in [10] the following proposition has been proved

**Theorem 6** *The problem  $(P_{\mathcal{D}}^{\omega})$  has a unique solution in  $H^1(\Omega^e)$  for every  $\omega$  with  $\sigma > 0$ . This solution verifies*

$$\|\hat{u}\|_{\Omega^e, \omega} := \left( \int_{\Omega} |\nabla \hat{u}|^2 + |\omega \hat{u}|^2 \right)^{1/2} \leq C \frac{1}{\sigma^2} \max\left(\frac{1}{\sigma_0}, 1\right) |\omega|^3 |g_{\mathcal{D}}|_{1/2}^2 \quad (1.18)$$

for every  $\omega \in \{\sigma \geq \sigma_0 > 0\}$ . The constant  $C$  is dependent only on  $\Gamma$ .

Same results are obtained also considering the problem  $(P_{\mathcal{D}}^e)$  as a problem in the interior domain  $(P_{\mathcal{D}})$  and, thus the classical single layer representation formula for the Helmholtz problem gives us, for  $\hat{u} \in C^1(\overline{\Omega^e}) \cap C^1(\overline{\Omega})$ :

$$\hat{u}(\mathbf{x}, \omega) = \int_{\Gamma} G_{\omega}(\mathbf{x}, \xi) \hat{\varphi}(\xi, \omega) d\xi_{\Gamma} \quad \mathbf{x} \in \Omega^e \cup \Omega \quad (1.19)$$

with  $G_{\omega}$  fundamental solution of the Helmholtz equation in  $\mathbb{R}^n$  and  $\hat{\varphi} := \left[ \frac{\partial \hat{u}}{\partial \mathbf{n}} \right]_{\Gamma}$  jump across the boundary.

Thanks to the continuity of this potential across  $\Gamma$  the integral equation for  $\hat{\varphi}$  is

$$\hat{g}_{\mathcal{D}}(\mathbf{x}, \omega) = \int_{\Gamma} G_{\omega}(\mathbf{x}, \xi) \hat{\varphi}(\xi, \omega) d\xi_{\Gamma} =: (V_{\omega} \hat{\varphi})(\mathbf{x}, \omega) \quad \mathbf{x} \in \Gamma \quad (1.20)$$

and the operator  $V_{\omega}$  has the properties to be inverse of the isomorphisme from  $H^{1/2}(\Gamma)$  to  $H^{-1/2}(\Gamma)$  that associates the jump  $\hat{\varphi}$  to the datum  $\hat{g}_{\mathcal{D}}$  and it holds that

$$\|V_{\omega}^{-1}\| \leq C \frac{1}{\sigma_0} \max\left(\frac{1}{\sigma_0}, 1\right) |\omega|^2 \quad \forall \omega \in \{\Im \omega \geq \sigma_0 > 0\}. \quad (1.21)$$

So  $\hat{u}$  has strictly one single layer representation as (1.19) and its density  $\hat{\varphi}$  is solution of the variational problem

$$\begin{cases} \hat{\varphi} \in H^{-1/2}(\Gamma) \\ \langle \psi, -i\omega V_{\omega} \hat{\varphi} \rangle = \langle \psi, -i\omega \hat{g}_{\mathcal{D}} \rangle \quad \forall \psi \in H^{-1/2}(\Gamma) \end{cases} \quad (1.22)$$

equivalent to (1.20) for which Bamberger and Ha Duong have proved a coerciveness property ( $\langle \dots \rangle$  is the antiduality between  $H^{-1/2}(\Gamma)$  and  $H^{1/2}(\Gamma)$ ). Then, using the Paley-Wiener theorem,

**Theorem 7 (Paley-Wiener Theorem)** *Let  $E$  be a Banach space, then the following assertions are equivalent:*

- i)  $h(\omega) = \widehat{f}(\omega)$  with  $f \in \mathcal{L}'(E)$
- ii) -  $h$  is holomorphic in a complex half plane  $\{\Im \omega > \sigma_0\}$  with values in  $E$
- $\exists \sigma_1 > \sigma_0, C > 0$  and  $k \geq 0$  s.t.  $\|h(\omega)\|_E \leq C(1 + |\omega|)^k \quad \forall \omega : \Im \omega \geq \sigma_1$ .

the authors have proved that

**Theorem 8 (Existence and Uniqueness)** *For every  $g \in \mathcal{L}'(H^{1/2}(\Gamma))^3$  the problem  $(P_{\mathcal{D}}^e)$  has a unique solution in  $\mathcal{L}'(H^1(\Omega^e))$  that is representable in a unique way with a simple layer retarded potential as in (D3a)*

$$u(\mathbf{x}, t) = \int_{\Sigma} G(\mathbf{x}, \xi, t, \tau) \varphi(\xi, \tau) d\xi_{\Gamma} d\tau := (\mathcal{V}\varphi)(\mathbf{x}, t) \quad \mathbf{x} \in \Omega^e, t \in [0, T]$$

The density  $\varphi$  of this potential is in  $\mathcal{L}'(H^{-1/2}(\Gamma))$ .

*Proof.* In consideration of the kernel of  $V_{\omega}$  the function  $\omega \mapsto V_{\omega}$ , defined in  $\mathbb{C}$ , with values in  $\mathcal{L}(H^{-1/2}(\Gamma), H^{1/2}(\Gamma))$  is holomorphic and the same is for  $V_{\omega}^{-1}$  on the half plane  $\{\Im \omega > 0\}$ . So if  $\widehat{g}$  is holomorphic in a half plane  $\{\Im \omega > \sigma_0\}$  with values in  $H^{1/2}(\Gamma)$ , the solution  $\widehat{\varphi}$  of (1.20), that exists for  $\Im \omega > 0$ , is an holomorphic function in the half plane  $\{\Im \omega > (0 \vee \sigma_0)\}$  with values in  $H^{-1/2}(\Gamma)$ . The representation formula (1.19) implies that  $\widehat{u}$  is holomorphic in the same half plane with values in  $H^1(\Omega^e)$ . Moreover, thanks to inequalities (1.18) and (1.21),  $\widehat{u}$  and  $\widehat{\varphi}$  verify the second statement of Paley-Wiener theorem and therefore they are Laplace transforms of distributions in  $\mathcal{L}(H^1(\Omega^e))$  and  $\mathcal{L}'(H^{-1/2}(\Gamma))$  that are the solution of problem  $(P_{\mathcal{D}}^e)$  and its retarded potential density respectively.

But this result can be specified considering the definition below whenever  $E$  is an Hilbert space

$$H_{\sigma}^s(\mathbb{R}^+, E) = \{f \in \mathcal{L}'(E); e^{-\sigma t} \Lambda^s f \in L^2(\mathbb{R}, E)\} \quad (1.23)$$

with the norm  $|\cdot|_{\sigma, s, r}$  if  $E = H^r(\Gamma)$ , where  $\sigma > 0, s \in \mathbb{R}$  and the operator  $\Lambda^s : \mathcal{L}'(E) \rightarrow \mathcal{L}'(E)$  is defined by  $\Lambda^s f := \mathcal{L}^{-1}[(-i\omega)^s \widehat{f}(\omega)]$ , obtaining

**Theorem 9** *If it exists a constant  $\sigma_0 > 0$  such that  $g_{\mathcal{D}} \in H_{\sigma_0}^{3/2}(\mathbb{R}^+, H^{1/2}(\Gamma))$ , the problem  $(P_{\mathcal{D}}^e)$  has a unique solution in  $H_{\sigma_0}^0(\mathbb{R}^+, H^1(\Omega^e))$  verifying the energy inequality:*

$$\int_{-\infty}^{+\infty} e^{-2\sigma t} \mathcal{E}^e(t) dt \leq C \frac{1}{\sigma^2} \max\left(\frac{1}{\sigma_0}, 1\right) |g_{\mathcal{D}}|_{\sigma, 3/2, 1/2}^2 \quad (1.24)$$

for all  $\sigma \geq \sigma_0 > 0$ , where  $C$  is a constant dependent on  $\Gamma$  only and

<sup>3</sup> Let the Laplace transform be  $\mathcal{L}[f](\sigma) = \int_{-\infty}^{+\infty} f(t) e^{-\sigma t} dt$ , let  $E$  be a Banach space, then  $\mathcal{L}'(E)$  denotes the set of distributions  $f : \mathbb{R} \rightarrow E$  that are null in  $\mathbb{R}^-$  and that are Laplace transformable for every  $\sigma \geq \sigma_0$  with  $\sigma_0(f) \in \mathbb{R}$ .

$$\mathcal{E}^e(t) = \int_{\Omega^e} \left( |\nabla u(t, \mathbf{x})|^2 + \left| u_t(t, \mathbf{x}) \right|^2 \right) d\mathbf{x}. \quad (1.25)$$

The same result holds also for the interior problem  $(P_{\mathcal{D}})$ . Therefore the solution  $u$  of  $(P_{\mathcal{D}}^e) \cup (P_{\mathcal{D}})$  is representable in a unique way as simple layer retarded potential on  $\Gamma$ . The density  $\varphi$  of this potential, defined by  $\varphi = [\partial u / \partial \mathbf{n}]$ , is such that, for all  $\sigma \geq \sigma_0 > 0$

$$|\varphi|_{\sigma, -1/2, -1/2} \leq C \frac{1}{\sigma} \max \left( \frac{1}{\sigma_0}, 1 \right) |g_{\mathcal{D}}|_{\sigma, 3/2, 1/2}. \quad (1.26)$$

With this theorem the mathematical expression of energy  $\mathcal{E}$ , that will be very important in next chapters to introduce the energy space-time variational formulation, makes the scene for the first time in this thesis.

Anyway, the variational formulation proposed by Bamberger and Ha Duong to find the density  $\varphi$  for  $x \in \Gamma$  in the boundary integral equation (D3a)  $V\varphi = g_{\mathcal{D}}$  is obtained anti-transforming the result (1.22) found in the frequencies domain, keeping a coerciveness property. In fact, as

$$\mathcal{L}[V\varphi_t] = \mathcal{L}[(V\varphi)_t] = -i\omega V_{\omega} \widehat{\varphi} \quad (1.27)$$

and, thanks to the Parseval formula<sup>4</sup>,

$$\frac{1}{2\pi} \int_{-\infty+i\sigma}^{+\infty+i\sigma} \langle \widehat{\varphi}, -i\omega V_{\omega} \widehat{\varphi} \rangle d\omega = \int_{-\infty}^{+\infty} e^{-2\sigma t} \langle \varphi, (V\varphi)_t \rangle dt \quad (1.28)$$

### Theorem 10

- $V : H_{\sigma}^1(\mathbb{R}^+, H^{-1/2}(\Gamma)) \rightarrow H_{\sigma}^0(\mathbb{R}^+, H^{1/2}(\Gamma))$  is a linear continuous operator with bounded norm independent of the constant  $\sigma \geq \sigma_0 > 0$ . More precisely

$$\int_{-\infty}^{+\infty} e^{-2\sigma t} |V\varphi|_{1/2}^2 dt \leq C \frac{1}{\sigma_0^2} \max \left( \frac{1}{\sigma_0^4}, 1 \right) \int_{-\infty}^{+\infty} e^{-2\sigma t} |\varphi_t|_{-1/2}^2 dt. \quad (1.29)$$

- Let  $\varphi \in \{ \varphi \in H_{\sigma}^1(\mathbb{R}^+, H^{-1/2}(\Gamma)) : V\varphi \in H_{\sigma}^1(\mathbb{R}^+, H^{1/2}(\Gamma)) \}$  then it holds the coerciveness inequality

$$\int_{-\infty}^{+\infty} e^{-2\sigma t} \langle \varphi, V\varphi_t \rangle dt \geq C \min(\sigma_0, 1) |\varphi|_{\sigma, -1/2, -1/2}^2. \quad (1.30)$$

<sup>4</sup> Let  $f$  and  $g$  be two distributions in  $\mathcal{L}'(E)$

$$\frac{1}{2\pi} \int_{-\infty+i\sigma}^{+\infty+i\sigma} \langle \widehat{f}(\omega), \widehat{g}(\omega) \rangle_E d\omega = \int_{-\infty}^{+\infty} e^{-2\sigma t} \langle f(t), g(t) \rangle_E dt.$$

This allows to conclude that the boundary integral equation (D3a) connected to the problem  $(P_{\mathcal{D}}^e) \cup (P_{\mathcal{D}})$ :

$$(V\varphi)(\mathbf{x}, t) = \int_{\Sigma} G(\mathbf{x}, \xi, t, \tau) \varphi(\xi, \tau) d\xi_{\Gamma} d\tau = g_{\mathcal{D}}(\mathbf{x}, t) \quad \mathbf{x} \in \Gamma, t \in [0, T]$$

can be replaced by a variational equation:

**Theorem 11 (Variational Formulation)** *If  $\varphi \in \{\varphi \in H_{\sigma}^1(\mathbb{R}^+, H^{-1/2}(\Gamma)) : V\varphi \in H_{\sigma}^1(\mathbb{R}^+, H^{1/2}(\Gamma))\}$  is solution of (D3a) then is solution of*

$$\int_{-\infty}^{+\infty} e^{-2\sigma t} \langle V\varphi_t, \psi \rangle dt = \int_{-\infty}^{+\infty} e^{-2\sigma t} \langle g_{\mathcal{D}t}, \psi \rangle dt \quad \forall \psi \in H_{\sigma}^1(\mathbb{R}^+, H^{-1/2}(\Gamma)). \quad (1.31)$$

(1.31) has been the first one and anyway, at now, one of few variational formulations for this time-dependent wave boundary integral problem whose stability and convergence have been proven.

Then, considering  $\Delta t$  and  $\mathbf{x}$  the discretization parameters, in time and space respectively and naming  $\varphi_{\Delta \mathbf{x}, \Delta t}$  the standard Galerkin approximation of  $\varphi$ , a stability result for the Galerkin scheme associated to (1.31) holds:

**Theorem 12 (Stability)** *If  $g_{\mathcal{D}t}^{\Delta \mathbf{x}, \Delta t}$  is an approximation of  $g_{\mathcal{D}t}$  in  $H_{\sigma}^{1/2}(\mathbb{R}^+, H^{1/2}(\Gamma))$ , the scheme is stable, that is:*

$$|\varphi_{\Delta \mathbf{x}, \Delta t}|_{\sigma, -1/2, -1/2} \leq C \quad \text{for} \quad \Delta \mathbf{x}, \Delta t \rightarrow 0. \quad (1.32)$$

and a convergence result

**Theorem 13 (Convergence)** *If the solution  $\varphi$  of the boundary integral equation (D3a) is such that  $\varphi \in H_{\sigma}^1(\mathbb{R}^+, H^{d_2+1}(\Gamma)) \cup H_{\sigma}^{d_1+1}(\mathbb{R}^+, L^2(\Gamma))$  then*

$$|\varphi - \varphi_{\Delta \mathbf{x}, \Delta t}|_{\sigma, 0, 0} \leq C \left[ \frac{|g_{\mathcal{D}t}^{\Delta \mathbf{x}, \Delta t} - g_{\mathcal{D}t}|_{\sigma, 1/2, 1/2}}{\sqrt{\Delta \mathbf{x} \Delta t}} + \Delta \mathbf{x}^{d_2 + \frac{1}{2}} \frac{|\varphi|_{\sigma, 1, d_2+1}}{\sqrt{\Delta t}} + \Delta t^{d_1 - \frac{1}{2}} \frac{|\varphi|_{\sigma, d_1+1, 0}}{\sqrt{\Delta \mathbf{x}}} \right]. \quad (1.33)$$

In [11] the method has been applied to the Neumann problem

$$(P_{\mathcal{N}}^e) \cup (P_{\mathcal{N}}) \begin{cases} u_{tt}(\mathbf{x}, t) - \Delta u(\mathbf{x}, t) = 0 & \mathbf{x} \in \Omega^e \cup \Omega, t \in (0, T) \\ u(\mathbf{x}, 0) = u_t(\mathbf{x}, 0) = 0 & \mathbf{x} \in \Omega^e \cup \Omega \\ \frac{\partial u}{\partial \mathbf{n}}(\mathbf{x}, t) = g_{\mathcal{N}}(\mathbf{x}, t) & (\mathbf{x}, t) \in \Sigma = \Gamma \times [0, T] \end{cases}$$

**Theorem 14 (Existence and Uniqueness)** *If  $g_{\mathcal{N}} \in H_{\sigma}^{\tau_0}(\mathbb{R}^+, H^{-1/2}(\Gamma))$  with  $\sigma \geq \sigma_0 > 0$ , the problem  $(P_{\mathcal{N}}^e) \cup (P_{\mathcal{N}})$  has a unique solution  $u \in H_{\sigma}^{\tau_0-1}$ , representable in a unique way by the double layer retarded potential*

$$u(\mathbf{x}, t) = \int_{\Sigma} \frac{\partial G(\mathbf{x}, \xi, t, \tau)}{\partial \mathbf{n}_{\xi}} \phi(\xi, \tau) d\xi_{\Gamma} d\tau := (\mathcal{K}\phi)(\mathbf{x}, t) \quad \mathbf{x} \in \Omega^e \cup \Omega, t \in [0, T]$$

where  $\phi$  is the function defined by the boundary integral equation (N3a):

$$g_{\mathcal{N}}(\mathbf{x}, t) = \int_{\Sigma} \frac{\partial^2 G(\mathbf{x}, \xi, t, \tau)}{\partial \mathbf{n}_{\mathbf{x}} \partial \mathbf{n}_{\xi}} \phi(\xi, \tau) d\xi_{\Gamma} d\tau := (D\phi)(\mathbf{x}, t) \quad \mathbf{x} \in \Gamma, t \in [0, T].$$

So, the scheme proposed by authors to calculate the approximate solution of the problem is performed with the before illustrated passage through the Helmholtz problem and then the use of the Laplace-Fourier anti-transform, obtaining the following coercive variational formulation

**Theorem 15 (Variational Formulation)** *If  $g_{\mathcal{N}} \in H_{\sigma}^3(\mathbb{R}^+, H^{-1/2}(\Gamma))$ , the solution  $\phi$  of (N3a) is the unique solution of the variational problem*

$$\left\{ \begin{array}{l} \text{Find } \phi \in H_{\sigma}^2(\mathbb{R}^+, H^{1/2}(\Gamma)) \text{ such that} \\ \int_{-\infty}^{+\infty} e^{-2\sigma t} \langle D\phi, \psi_t \rangle dt = \int_{-\infty}^{+\infty} e^{-2\sigma t} \langle g_{\mathcal{N}}, \psi_t \rangle dt \quad \forall \psi \in H_{\sigma}^2(\mathbb{R}^+, H^{1/2}(\Gamma)) \end{array} \right. \quad (1.34)$$

with favorable results of stability and convergence of the approximate solution  $\phi_{\Delta \mathbf{x}, \Delta t}$  obtained as explained for the Dirichlet problem

**Theorem 16 (Stability)** *If  $g_{\mathcal{N}}^{\Delta \mathbf{x}, \Delta t}$  is an approximation of  $g_{\mathcal{N}}$  in  $H_{\sigma}^1(\mathbb{R}^+, H^{-1/2}(\Gamma))$ , the schema is stable, that is:*

$$|\phi_{\Delta \mathbf{x}, \Delta t}|_{\sigma, 0, 1/2} \leq C \quad \text{for} \quad \Delta \mathbf{x}, \Delta t \rightarrow 0. \quad (1.35)$$

**Theorem 17 (Convergence)** *If the solution  $\phi$  of the boundary integral equation (N3a) is enough regular then*

$$\begin{aligned} |\phi - \phi_{\Delta \mathbf{x}, \Delta t}|_{\sigma, 0, 1/2} \leq C & \left[ |g_{\mathcal{N}}^{\Delta \mathbf{x}, \Delta t} - g_{\mathcal{N}}|_{\sigma, 1, -1/2} \right. \\ & \left. + \frac{\Delta \mathbf{x}^{d_2 + \frac{1}{2}}}{\Delta t} |\varphi|_{\sigma, 2, d_2 + 1} + \Delta t^{d_1 - 2} |\varphi|_{\sigma, d_1 + 1, 1/2} \right]. \end{aligned} \quad (1.36)$$

For completeness, numerical examples of how this method behaves, applied to a problem with mixed boundary conditions, have been inserted in section 3.3.1 with a comparison of the Bamberger-Ha Duong variational formulation depending on the parameter  $\sigma$  with the variational formulation based on the energy expression that I'm going to introduce.





## Chapter 2

### The one-dimensional wave problem

In this section I will take into consideration boundary problems for one dimensional wave propagation reformulated in terms of boundary integral equations (BIEs) with retarded potential. Then, starting from a natural energy identity, I will introduce a space-time weak formulation for the BIEs with some theoretical results about the continuity and coerciveness properties of the related bilinear form. All enriched with some numerical results, obtained using different approximation techniques that will be presented and discussed.

#### 2.1 The Dirichlet problem

Let  $\Omega = (0, L) \subset \mathbb{R}$  with boundary  $\Gamma = \{0, L\}$  and let  $u(x, t)$  be the solution to the wave problem

$$(P_{\mathcal{D}}^e) \cup (P_{\mathcal{D}}) \begin{cases} u_{tt}(x, t) - u_{xx}(x, t) = 0 & x \in \mathbb{R} \setminus \Gamma, \quad t \in (0, T), \\ u(x, 0) = u_t(x, 0) = 0 & x \in \mathbb{R} \setminus \Gamma, \\ u(x, t) = g_{\mathcal{D}}(x, t) & (x, t) \in \Sigma = \Gamma \times [0, T] \end{cases} \quad (2.1)$$

where the subscript index  $x$  denotes the space-derivative. Note that  $u$  is considered as the solution on the whole  $\mathbb{R}$ , not only in  $\Omega$ . Whenever necessary, I shall distinguish the internal solution  $u^-$ , i.e. for  $x \in \Omega$ , from the external one  $u^+$ , i.e. for  $x \in \mathbb{R} \setminus \Omega$ . In order to rewrite problem (2.1) as a boundary integral equation, I need to recall the expression of the forward fundamental solution  $G(x, t)$  of the wave operator written in (1.2):

$$G(x, t) = \frac{1}{2}H[t - |x|] = \frac{1}{2}H[t] (H[x + t] - H[x - t]). \quad (2.2)$$

Using (2.2) one obtains the single layer representation formula (D3a) introduced in page 6 for the solution of the wave equation, for  $t \in \mathbb{R}$ ,  $x \in \mathbb{R} \setminus \Gamma$ :

$$\begin{aligned}
u(x,t) &= (\mathcal{V}\varphi)(x,t) = \int_{-\infty}^{+\infty} G(x,t-\tau)\varphi(0,\tau)d\tau + \int_{-\infty}^{+\infty} G(x-L,t-\tau)\varphi(L,\tau)d\tau \\
&= \frac{1}{2} \int_{-\infty}^t H[t-\tau-|x|]\varphi(0,\tau)d\tau + \frac{1}{2} \int_{-\infty}^t H[t-\tau-|x-L|]\varphi(L,\tau)d\tau \\
&= \frac{1}{2} \int_{-\infty}^{t-|x|} \varphi(0,\tau)d\tau + \frac{1}{2} \int_{-\infty}^{t-|x-L|} \varphi(L,\tau)d\tau, \tag{2.3}
\end{aligned}$$

where

$$\varphi = \left[ \frac{\partial u}{\partial \mathbf{n}} \right] := \frac{\partial u^-}{\partial \mathbf{n}} - \frac{\partial u^+}{\partial \mathbf{n}} \tag{2.4}$$

is the jump of the normal derivatives of  $u$  at  $x=0$  and  $x=L$ , and  $\mathbf{n}$  is fixed as the unitary outward normal with respect to the boundary of  $\Omega$ .

Since problem (2.1) is formulated on the time interval  $[0, T]$ , in order to keep the notations as simple as possible, hereafter I shall consider functions  $\varphi$  defined on the whole real line but having support only in the fixed time interval  $[0, T]$ . From formula (2.3), taking the limits as  $x \rightarrow 0$  and  $x \rightarrow L$ , one obtains the following system of boundary integral equations at the endpoints of the interval  $(0, L)$ :

$$\begin{aligned}
(V\varphi)(0,t) &= \frac{1}{2} \left[ \int_0^t \varphi(0,\tau)d\tau + \int_0^{t-L} \varphi(L,\tau)d\tau \right] = g_{\mathcal{D}}(0,t) \\
(V\varphi)(L,t) &= \frac{1}{2} \left[ \int_0^{t-L} \varphi(0,\tau)d\tau + \int_0^t \varphi(L,\tau)d\tau \right] = g_{\mathcal{D}}(L,t)
\end{aligned} \tag{2.5}$$

$t \in [0, T]$ .

The system (2.5) can be written with the compact notation

$$V\varphi = g_{\mathcal{D}}, \tag{2.6}$$

where  $\varphi(t) = (\varphi(0,t), \varphi(L,t))^{\top}$  and  $g_{\mathcal{D}}(t) = (g_{\mathcal{D}}(0,t), g_{\mathcal{D}}(L,t))^{\top}$  represent the unknown vector valued function and the given boundary function in  $x=0$  and  $x=L$ , respectively. In order to formulate the equation (2.6) in a suitable functional framework, assume  $V$  as defined in  $L^2(\Sigma)$ . With this choice, from (2.5) it is easy to verify that the range of  $V$  lies in  $H_{\{0\}}^1(\Sigma)$ , the space of  $H^1(\Sigma)$  functions vanishing at  $t=0$ . Hence hereafter I shall consider  $V : L^2(\Sigma) \rightarrow H_{\{0\}}^1(\Sigma)$ .

### 2.1.1 Energetic weak problem related to the BIE

A classical way to introduce a weak formulation for the BIE (2.6) is to project the BIE using  $L^2(\Sigma)$  scalar product. Now, considering the bilinear form  $a_{L^2}(\varphi, \psi) :$

$L^2(\Sigma) \times L^2(\Sigma) \rightarrow \mathbb{R}$  defined by

$$a_{L^2}(\varphi, \psi) := \langle V\varphi, \psi \rangle_{L^2(\Sigma)} = \int_0^T \psi(0,t) (V\varphi)(0,t) dt + \int_0^T \psi(L,t) (V\varphi)(L,t) dt, \quad (2.7)$$

it's possible to write the following weak problem:

given  $g_{\mathcal{D}} \in H_{\{0\}}^1(\Sigma)$ , find  $\varphi \in L^2(\Sigma)$  such that

$$a_{L^2}(\varphi, \psi) = \langle g_{\mathcal{D}}, \psi \rangle_{L^2(\Sigma)}, \quad \forall \psi \in L^2(\Sigma). \quad (2.8)$$

There are two major drawbacks in the above formulation: the bilinear form  $a_{L^2}(\cdot, \cdot)$  is not coercive, in fact choosing  $\varphi \equiv \psi$ , the formula (2.7) does not give a positive definite expression<sup>1</sup>; further, it is implicit in problem (2.8) that the equation (2.6) must be understood considering the compact operator  $V : L^2(\Sigma) \rightarrow L^2(\Sigma)$ , which obviously cannot have continuous inverse. As a consequence, it is not surprising that problem (2.8) gives rise to instability phenomena in the discretization phase, as it will be shown in the next section.

An alternative approach is suggested by the well-known conservation law satisfied by the (real-valued) solutions to the d'Alembert equation:

$$0 = u_t(u_{tt} - u_{xx}) = \frac{\partial}{\partial t} \left( \frac{1}{2}u_t^2 + \frac{1}{2}u_x^2 \right) - \frac{\partial}{\partial x} (u_t u_x). \quad (2.9)$$

Integrating with respect to space-time in  $\mathbb{R} \times (0, T)$  and taking into account that  $u$  and  $u_t$  vanish for  $t = 0$ , we get the energy identity

$$\mathcal{E}(T) = \frac{1}{2} \int_{-\infty}^{+\infty} (u_t^2 + u_x^2) dx \Big|_{t=T} = \int_0^T u_t \cdot \left[ \frac{\partial u}{\partial \mathbf{n}} \right] dt = \int_0^T (V\varphi)_t \cdot \varphi dt, \quad (2.10)$$

where the dot denotes the scalar product in  $\mathbb{R}^2$ .

The quadratic form appearing in the last term of (2.10) leads to a natural space-time weak formulation of the corresponding boundary integral equation (2.6) with robust theoretical properties. In fact, the main advantage of this approach is that the quadratic form given by the energy, i.e.

$$\mathcal{E}(T) = \langle (V\varphi)_t, \varphi \rangle_{L^2(\Sigma)},$$

is, in the one dimensional case, both continuous and coercive in the appropriate spaces, i.e. exactly the functional spaces where the Dirichlet problem is well-posed as reported at page 2. In order to derive continuity and coerciveness properties of the total energy  $\mathcal{E}(T)$ , the analysis has to be concentrated on the operator  $A : L^2(\Sigma) \rightarrow L^2(\Sigma)$ , defined as

<sup>1</sup> For example, choosing  $\varphi(0,t) = \varphi(L,t) = \cos(\frac{\pi t}{T})$ ,  $a_{L^2}(\varphi, \varphi) < 0$  when  $T > L$ .

$$A\varphi(t) := (V\varphi)_t(t) = \begin{bmatrix} (V\varphi)_t(0,t) \\ (V\varphi)_t(L,t) \end{bmatrix} = \frac{1}{2} \begin{bmatrix} \varphi(0,t) + H[t-L]\varphi(L,t-L) \\ H[t-L]\varphi(0,t-L) + \varphi(L,t) \end{bmatrix}, \quad (2.11)$$

for  $t \in [0, T]$ . By an application of the Cauchy-Schwarz inequality, it results immediately that  $A$  is a continuous operator:

**Theorem 18** *For any given time  $T$ , the operator  $A : L^2(\Sigma) \rightarrow L^2(\Sigma)$ , defined in (2.11) is bounded, with norm  $\|A\| \leq 1$ .*

More interesting are the positivity properties of the quadratic form associated to the operator  $A$ . Instead of the non-symmetric operator  $A$ , consider its symmetric part

$$A_s = \frac{A + A^*}{2},$$

where the asterisk denotes the adjoint of an operator. Having introduced the bilinear form  $a_{\mathcal{E}}(\varphi, \psi) : L^2(\Sigma) \times L^2(\Sigma) \rightarrow \mathbb{R}$  defined by

$$a_{\mathcal{E}}(\varphi, \psi) := \langle A\varphi, \psi \rangle_{L^2(\Sigma)} = \int_0^T \psi(0,t) (V\varphi)_t(0,t) dt + \int_0^T \psi(L,t) (V\varphi)_t(L,t) dt, \quad (2.12)$$

for every  $\varphi \in L^2(\Sigma)$ , we have

$$a_{\mathcal{E}}(\varphi, \varphi) = \langle A_s \varphi, \varphi \rangle_{L^2(\Sigma)}. \quad (2.13)$$

Introducing the modified anticipated and retarded shift operators:

$$(S_+ f)(t) := H[T-L-t]f(t+L), \quad (S_- f)(t) := H[t-L]f(t-L).$$

and denoting by  $\mathcal{R}$  the reflection matrix, from a straightforward calculation on obtains

$$A^* \varphi(t) = \frac{1}{2} [\varphi(t) + S_+ \mathcal{R} \varphi(t)].$$

Therefore the symmetric part of  $A$  has the following expression:

$$2A_s \varphi(t) = \varphi(t) + \frac{1}{2} (S_- + S_+) \mathcal{R} \varphi(t), \quad t \in [0, T]. \quad (2.14)$$

**Theorem 19** *For every  $T > 0$ , there exists a positive constant  $c(T)$  such that*

$$a_{\mathcal{E}}(\varphi, \varphi) \geq c(T) \|\varphi\|_{L^2(\Sigma)}^2, \quad \varphi \in L^2(\Sigma). \quad (2.15)$$

*Moreover, let  $N$  be the least positive integer such that  $T \leq NL$ ; then one has the explicit bound:*

$$c(T) \geq \sin^2 \left( \frac{\pi}{2(N+1)} \right). \quad (2.16)$$

*Proof.* There is a clear analogy between the formulation (2.14) of the operator  $A_s$  and the usual second order finite differences scheme. In what follows I proceed to make clear this analogy and eventually I shall reduce the action of  $A_s$  to that of a matrix operator closely connected to finite differences. First of all assume  $T = NL$  for some positive integer  $N$  otherwise trivially extend  $\varphi$  up to  $NL$  where  $N = [T/L] + 1$ . Then (2.14) can be reformulated in the following equivalent way:

$$2(S_+^k A_s \varphi)(t) = S_+^k \varphi(t) + \frac{1}{2} (S_- + S_+) \mathcal{R} S_+^k \varphi(t), \quad t \in [0, L], \quad k = 0, 1, \dots, N-1. \quad (2.17)$$

Let define, for  $k = 0, 1, \dots, N-1$ ,

$$\Phi_k(t) := (\Phi_k(0, t), \Phi_k(L, t))^\top := \mathcal{R}^k S_+^k \varphi(t), \quad t \in [0, L],$$

that is

$$\Phi(0, t) = (\varphi(0, t), S_+ \varphi(L, t), S_+^2 \varphi(0, t), \dots, S_+^{N-1} \varphi_{m_1}(L, t)), \quad t \in [0, L],$$

$$\Phi(L, t) = (\varphi(L, t), S_+ \varphi(0, t), S_+^2 \varphi(L, t), \dots, S_+^{N-1} \varphi_{m_2}(L, t)), \quad t \in [0, L],$$

where:  $m_1 = [(N-1) - 2[\frac{N-1}{2}]]$  and  $m_2 = m_1 + (-1)^{N-1}$ . Similarly, for the left-hand side in (2.17), set

$$\Psi_k(t) := (\Psi_k(0, t), \Psi_k(L, t))^\top := 2(\mathcal{R}^k S_+^k A_s \varphi)(t).$$

Finally, observe that multiplying both sides of formula (2.17) by  $\mathcal{R}^k$ , we obtain ( $\Phi_{-1}(t) \equiv \Phi_N(t) \equiv 0$ ):

$$\Psi_k(t) = \frac{1}{2} \Phi_{k-1}(t) + \Phi_k(t) + \frac{1}{2} \Phi_{k+1}(t), \quad t \in [0, L], \quad k = 0, 1, \dots, N-1.$$

Thus each component of  $\Psi(t)$  can be expressed as

$$\Psi_0(t) = \mathcal{M} \Phi_0(t), \quad \Psi_L(t) = \mathcal{M} \Phi_L(t),$$

where  $\mathcal{M} = \text{tridiag}[\frac{1}{2}, 1, \frac{1}{2}]$  is a tridiagonal matrix of order  $N$ . Note that the only difference between the matrix  $\mathcal{M}$  and the usual finite difference matrix is the sign of the  $\frac{1}{2}$ 's. In fact, the two matrices are similar through the diagonal matrix which alternates 1 and  $-1$  along the principal diagonal. It is well known that the  $N \times N$  finite difference matrix is positive definite and its spectrum is given by the  $N$  eigenvalues [17]

$$\omega_k^2 = 2 \sin^2 \left( \frac{k\pi}{2(N+1)} \right), \quad k = 1, \dots, N.$$

Now, having set  $\Phi(t) = (\Phi_0(t), \Phi_L(t))^\top$ , the conclusion follows from the following identity

$$\int_0^T |\varphi(t)|^2 dt = \sum_{k=0}^{N-1} \int_0^L |\mathcal{R}^k S_+^k \varphi(t)|^2 dt = \sum_{k=0}^{N-1} \int_0^L |\Phi_k(t)|^2 dt = \int_0^L |\Phi(t)|^2 dt,$$

and from the inequality

$$\begin{aligned} 2 \langle A_s \varphi, \varphi \rangle_{L^2(\Sigma)} &= \sum_{k=0}^{N-1} \int_0^L (\mathcal{R}^k S_+^k A_s \varphi)(t) \cdot (\mathcal{R}^k S_+^k \varphi)(t) dt \\ &= \sum_{k=0}^{N-1} \int_0^L \Psi_k(t) \cdot \Phi_k(t) dt = \int_0^L \mathcal{M} \Phi_0(t) \cdot \Phi_0(t) dt + \\ &+ \int_0^L \mathcal{M} \Phi_L(t) \cdot \Phi_L(t) dt \geq \omega_1^2 \int_0^L |\Phi(t)|^2 dt = \omega_1^2 |\varphi|_{L^2(\Sigma)}^2, \end{aligned}$$

remembering (2.13).

At this point we can write down the energetic weak problem related to the BIE (2.6), which admits a unique, stable solution:

given  $g_{\mathcal{D}} \in H_{\{0\}}^1(\Sigma)$ , find  $\varphi \in L^2(\Sigma)$  such that

$$a_{\mathcal{E}}(\varphi, \psi) = \langle g_{\mathcal{D},t}, \psi \rangle_{L^2(\Sigma)}, \quad \forall \psi \in L^2(\Sigma). \quad (2.18)$$

### 2.1.2 Numerical results

Denoting by  $\mathcal{P}_{d_k}$  the space of algebraic polynomials of degree  $d_k \geq 0$ , consider the standard finite element space

$$X_{-1,\Delta t} := \{v_{\Delta t}(t) \in L^2(0, T) : v_{\Delta t}|_{[t_k, t_{k+1}]} \in \mathcal{P}_{d_k}, d_k \geq 0, k = 0, \dots, N_{\Delta t} - 1\}.$$

Then, considering the finite dimensional space  $W_{-1,\Delta t} = X_{-1,\Delta t} \times X_{-1,\Delta t} \subset L^2(\Sigma)$ , we can write down the discrete form of the previously introduced weak problems. For instance, referring to (2.18) we have:

given  $g_{\mathcal{D}} \in H_{\{0\}}^1(\Sigma)$ , find  $\varphi_{\Delta t} \in W_{-1,\Delta t}$  such that

$$a_{\mathcal{E}}(\varphi_{\Delta t}, \psi_{\Delta t}) = \langle g_{\mathcal{D},t}, \psi_{\Delta t} \rangle_{L^2(\Sigma)}, \quad \forall \psi_{\Delta t} \in W_{-1,\Delta t}. \quad (2.19)$$

Denoting with  $\{v_k\}$  a basis for  $X_{-1,\Delta t}$ , the unknown function  $\varphi_{\Delta t}$  can be expressed as:

$$\varphi_{\Delta t}(0, t) = \sum_k \varphi_k^0 v_k(t), \quad \varphi_{\Delta t}(L, t) = \sum_k \varphi_k^L v_k(t)$$

and the discrete problems, associated to (2.8) and to (2.18) respectively, can be equivalently written, respectively, as linear systems

$$\mathbb{E}_{L^2} \alpha_{L^2} = \mathbf{b}_{L^2}, \quad \mathbb{E}_{\mathcal{E}} \alpha_{\mathcal{E}} = \mathbf{b}_{\mathcal{E}}, \quad (2.20)$$

in the unknowns the coefficients  $\varphi_k^0$  and  $\varphi_k^L$ .

- As test problem, consider a one dimensional domain of length  $L = \frac{\pi}{2}$ , subject to the Dirichlet boundary conditions:

$$g_{\mathcal{D}}(0,t) = 0, \quad g_{\mathcal{D}}(L,t) = \sin^2(t)H(t)H\left(\frac{\pi}{2}-t\right) + H\left(t-\frac{\pi}{2}\right).$$

The observation time interval is  $(0, 6L) = (0, 3\pi)$ . For the discretization, the time steps considered are of the type  $\Delta t = \frac{\pi}{2p}$ ,  $p \in \mathbb{N}^+$ , such that the time  $\frac{\pi}{2}$  required by the wave, travelling with unitary speed, to cover the distance between the two end-points of the domain is a multiple of  $\Delta t$ . Tractions in  $x = 0$  and  $x = L$  have been approximated by constant or linear shape functions. In figure 2.1 on the left there is the numerical solution obtained with  $\Delta t = \frac{\pi}{32}$  and constant shape functions, solving  $\mathbb{E}_{\mathcal{E}} \alpha_{\mathcal{E}} = \mathbf{b}_{\mathcal{E}}$ ; refining the time mesh, choosing  $\Delta t = \frac{\pi}{128}$ , the numerical approximation improves, as shown in figure 2.1 on the right. In figure 2.2 on the left

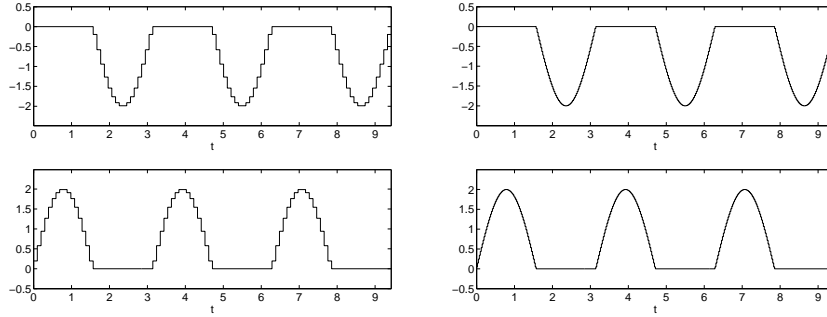


Fig. 2.1: Piece-wise constant approximations of  $\varphi(0,t)$  above and  $\varphi(L,t)$  below, obtained solving  $\mathbb{E}_{\mathcal{E}} \alpha_{\mathcal{E}} = \mathbf{b}_{\mathcal{E}}$  with  $\Delta t = \frac{\pi}{32}$  on the left and  $\Delta t = \frac{\pi}{128}$  on the right.

instability phenomena arising solving  $\mathbb{E}_{L^2} \alpha_{L^2} = \mathbf{b}_{L^2}$  with the coarse time grid, are presented. This instability still remains even using the smaller time step, as shown in figure 2.2 on the right, while it disappears choosing an odd parameter  $p$  in the time step  $\Delta t$  or if we use linear shape functions. The numerical solutions obtained by any of the above linear systems, with  $\Delta t = \frac{\pi}{30}$  and constant shape functions, and with  $\Delta t = \frac{\pi}{32}$  and linear shape functions, are reported in figures 2.3. If the observation time interval is  $(0, 10)$  it could be natural to choose the submultiple time step  $\Delta t = 0.1$ , even if the time  $\frac{\pi}{2}$  required by the wave to cover the distance between the two end-points of the domain is not a multiple of it and in figure 2.4

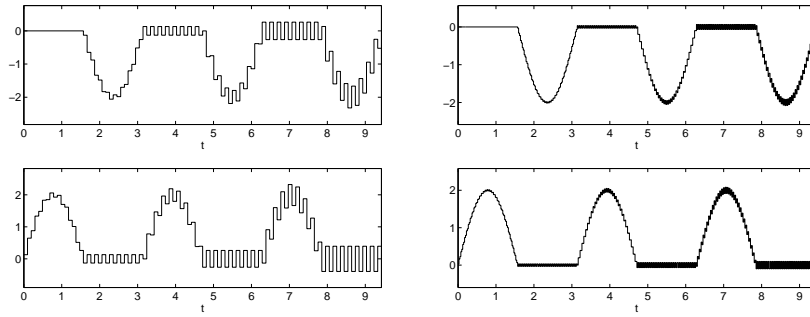


Fig. 2.2: Piece-wise constant unstable approximations of  $\varphi(0,t)$  above and  $\varphi(L,t)$  below, obtained solving  $\mathbb{E}_{L^2} \alpha_{L^2} = \mathbf{b}_{L^2}$  with  $\Delta t = \frac{\pi}{32}$  on the left and  $\Delta t = \frac{\pi}{128}$  on the right.

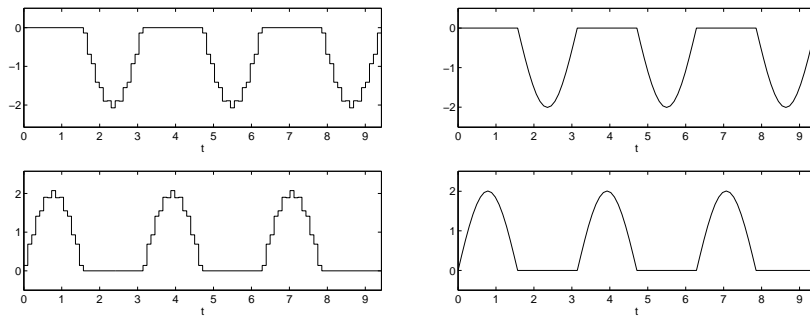


Fig. 2.3: On the left piece-wise constant approximations of  $\varphi(0,t)$  and  $\varphi(L,t)$  with  $\Delta t = \frac{\pi}{30}$ , on the right piece-wise linear approximations of  $\varphi(0,t)$  and  $\varphi(L,t)$  with  $\Delta t = \frac{\pi}{32}$  obtained solving  $\mathbb{E}_{L^2} \alpha_{L^2} = \mathbf{b}_{L^2}$ .

there is the numerical solution obtained solving  $\mathbb{E}_{\mathcal{E}} \alpha_{\mathcal{E}} = \mathbf{b}_{\mathcal{E}}$ , using this time step and linear shape functions compared with the huge instability phenomena arising solving  $\mathbb{E}_{L^2} \alpha_{L^2} = \mathbf{b}_{L^2}$ . At last, in figure 2.5, the sparsity structure of the above two matrices are reported, together with their spectral condition number.

**Remark.** The energetic procedure appears to be unconditionally stable. In fact, even though the stability constant  $1/c(T)$ , with  $c(T)$  given as in theorem 19, has an asymptotic behavior of the type  $O(T^2)$  when  $T \rightarrow \infty$ , the approximate solution remains stable even for large times: in figure 2.6 the numerical solution of the test problem, obtained with  $\Delta t = 0.1$  and linear shape functions, has been calculated till the final time  $T = 100$ .

- Further, figure 2.7 presents the numerical solution referred to another Dirichlet test problem on the time interval  $(0,100)$ , related to a one dimensional domain of



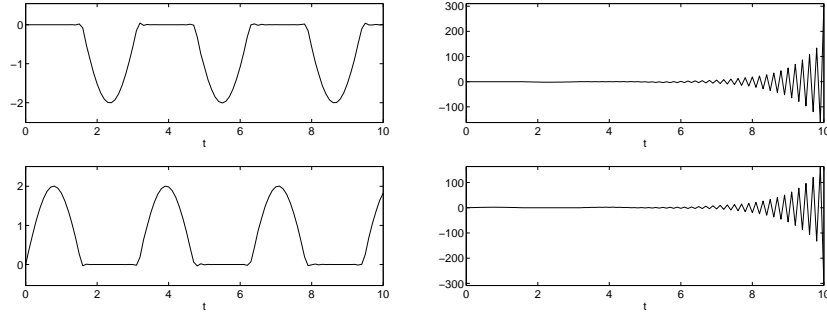


Fig. 2.4: Piece-wise linear approximations of  $\varphi(0,t)$  and  $\varphi(L,t)$  obtained with  $\Delta t = 0.1$  solving  $\mathbb{E}_{\mathcal{E}} \alpha_{\mathcal{E}} = \mathbf{b}_{\mathcal{E}}$  on the left and  $\mathbb{E}_{L^2} \alpha_{L^2} = \mathbf{b}_{L^2}$  on the right with the instability phenomena arising from classical  $L^2$  weak formulation.

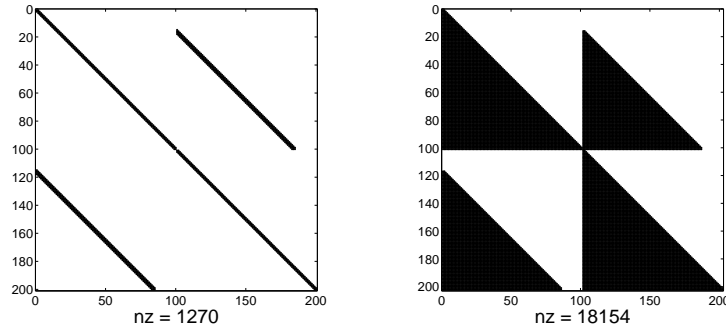


Fig. 2.5: Matrices  $\mathbb{E}_{\mathcal{E}}, \mathbb{E}_{L^2}$ , with  $\mu_2(\mathbb{E}_{\mathcal{E}}) \simeq 15.3$  and  $\mu_2(\mathbb{E}_{L^2}) \simeq 8.6 \cdot 10^7$ .

unitary length subject to the boundary conditions:

$$g_{\mathcal{D}}(0,t) = 0, \quad g_{\mathcal{D}}(L,t) = H(t) \sin(t).$$

The new challenging features of the datum  $g_{\mathcal{D}}(L,t)$  with respect to the previous one are: the fact that it never collapses to a constant for  $t > \bar{t} > 0$  and its jump in the first derivative for  $t = 0$ , which is reproduced in the solution after reflection at time intervals of unitary length. The approximation is carried out starting from the energetic weak formulation, using  $\Delta t = 0.1$  and constant shape functions in the discretization phase. In this case, the analytical solution is

$$\varphi^0(t) = -2 \sum_{k=0}^{49} H(t-2k-1) \cos(t-2k-1), \quad \varphi^L(t) = 2 \sum_{k=0}^{50} H(t-2k) \cos(t-2k).$$

and it is possible to evaluate the approximation error, which turns out to be

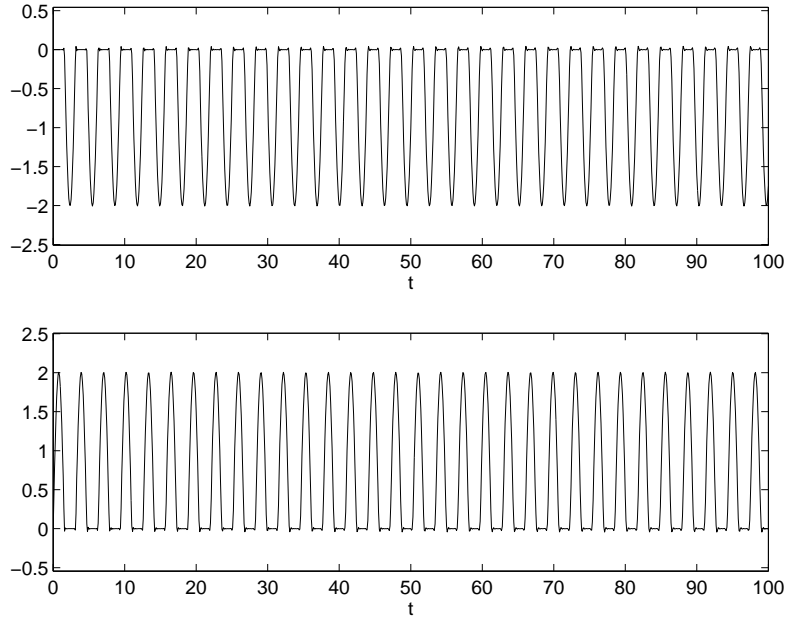


Fig. 2.6: Numerical stability of the energetic approach approximate solution for large times obtained with linear shape functions.

$$\max_{t \in (0,100)} |\varphi(t) - \varphi_{0.1}(t)| \approx 8.98 \cdot 10^{-4}.$$

**Remark.** The energetic weak formulation for one dimensional problems has been introduced as a one-shot analysis till final time  $T$ . In fact, the linear system  $\mathbb{E}_{\mathcal{E}} \alpha_{\mathcal{E}} = \mathbf{b}_{\mathcal{E}}$  has a vector solution which allow to recover the whole time histories  $\varphi_{\Delta t}(0,t)$  and  $\varphi_{\Delta t}(L,t)$  till the final instant of the observation time interval. If instead we search the approximate solution step by step, for instance using constant or linear basis functions, i.e. we analyze the problem on each time interval of the type  $(0, h\Delta t)$ , for  $h = 1, \dots, N_{\Delta t}$ , we will have to solve  $N_{\Delta t}$  linear systems of order two, with the same coefficient matrix, in the unknown vector  $(\varphi_h^0 \ \varphi_h^L)^\top$ , using the approximate solutions obtained in the previous steps to update the right-hand sides. This time marching procedure is formally equivalent to solve a global linear system having a lower block triangular matrix, with coincident diagonal blocks, using a block forward substitution algorithm.

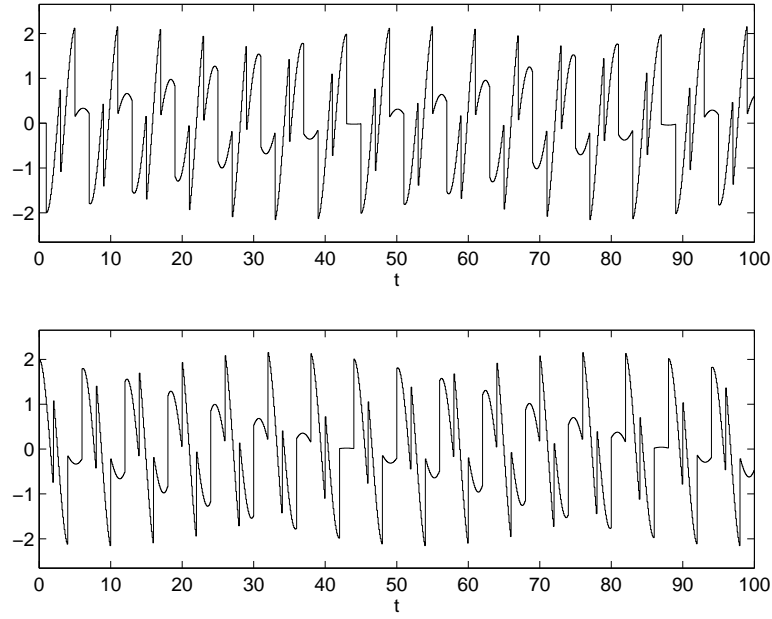


Fig. 2.7: Numerical stability of the approximate solution of the second test problem for large times obtained with linear shape functions.

## 2.2 Neumann problem

Similar considerations as those developed in the section 2.1 can be done for the wave problem with Neumann boundary condition:

$$(P_{\mathcal{N}}^e) \cup (P_{\mathcal{N}}) \begin{cases} u_{tt}(x,t) - u_{xx}(x,t) = 0 & x \in \mathbb{R} \setminus \{0, L\}, \quad t \in (0, T) \\ u(x,0) = u_t(x,0) = 0 & x \in \mathbb{R} \setminus \{0, L\}, \\ \frac{\partial u}{\partial \mathbf{n}}(x,t) = g_{\mathcal{N}}(x,t) & (x,t) \in \Sigma = \{0, L\} \times [0, T]. \end{cases} \quad (2.21)$$

In this case the solution  $u(x,t)$  can be expressed through the double layer representation (N3a) with the unknown retarded potential  $\phi$ :

$$u(x,t) = (\mathcal{K}\phi)(x,t) = \sum_{y=0, L, -\infty}^{+\infty} \int \frac{\partial}{\partial \mathbf{n}_y} G(x-y, t-\tau) \phi(y, \tau) d\tau \quad (2.22)$$

where  $G(\cdot, \cdot)$  is given by (2.2).

After a straightforward calculation the more explicit formula is

$$u(x,t) = \frac{1}{2} \frac{x}{|x|} \phi^0(t - |x|) - \frac{1}{2} \frac{x-L}{|x-L|} \phi^L(t - |x|),$$

from which

$$[u](0,t) := u^-(0,t) - u^+(0,t) = \phi^0(t), \quad [u](L,t) := u^-(L,t) - u^+(L,t) = \phi^L(t).$$

By deriving formula (2.22), taking the limits as  $x \rightarrow 0$  and  $x \rightarrow L$  and using the Neumann data  $\partial_n u(x,t) = g_{\mathcal{N}}(x,t)$ , the boundary equations for the unknown potential  $\phi$  at the endpoints of the interval  $(0,L)$  are:

$$D\phi := \partial_n K\phi = g_{\mathcal{N}}, \quad (2.23)$$

that is

$$(D\phi)(0,t) = \frac{1}{2} [\phi_t^0(t) - \phi_t^L(t-L)] = g_{\mathcal{N}}^0(t)$$

$$(D\phi)(L,t) = -\frac{1}{2} [\phi_t^0(t-L) - \phi_t^L(t)] = g_{\mathcal{N}}^L(t).$$

In order to derive a weak formulation of the equation (2.23), the starting point is again the energy identity, that for the Neumann boundary condition assumes the form

$$\mathcal{E}(T) = \int_0^T \frac{\partial u}{\partial n} \cdot [u]_t dt = \int_0^T D\phi \cdot \phi_t dt.$$

Thus, having defined the bilinear form

$$\tilde{a}_{\mathcal{E}} : H_{\{0\}}^1(\Sigma) \times H_{\{0\}}^1(\Sigma) \rightarrow \mathbb{R}, \quad \tilde{a}_{\mathcal{E}}(\phi, \psi) := \langle D\phi, \psi_t \rangle_{L^2(\Sigma)}, \quad (2.24)$$

the coerciveness of  $\tilde{a}_{\mathcal{E}}(\cdot, \cdot)$  follows at once from the observation that

$$\tilde{a}_{\mathcal{E}}(\phi, \phi) = \int_0^T A\tilde{\phi}_t \cdot \tilde{\phi}_t dt$$

where

$$\tilde{\phi}(t) = (\phi^0(t), -\phi^L(t))^{\top},$$

and  $A$  is the operator defined in (2.11). Then from theorem 19 it follows that

**Theorem 20** *For every  $T > 0$ , there exists a positive constant  $c(T)$  such that*

$$\tilde{a}_{\mathcal{E}}(\phi, \phi) \geq c(T) |\phi_t|_{L^2(\Sigma)}^2, \quad \phi \in H_{\{0\}}^1(\Sigma).$$

*The constant  $c(T)$  is bounded from below as in (2.16).*

Since Dirichlet or Neumann boundary conditions are similar for what concerns the analysis of the energetic weak formulations related to the corresponding BIEs I do not give here numerical examples for one dimensional Neumann problems. These will be presented in section 3.2 in the more significative context of two dimensional problems.

### 2.3 Mixed Boundary Value Problems

The one dimensional wave equation can be revised with suitable modifications as a model for elastodynamics in one dimension. In literature there are several numerical results related to this kind of problem ([24, 26, 25, 8]) to which compare. Therefore it becomes relevant to deep investigate in this subsection the elastodynamic problem ( $P_{EI}$ ) that describes the propagation of displacement field  $u(x,t)$  and traction field  $p(x,t)$  along a weightless rod of finite length  $L$  and section area  $A$ , with no external forces acting on it, when an initial configuration different from that one of statical equilibrium is imposed, under small displacements hypothesis.

$$(P_{EI}) \begin{cases} u_{xx}(x,t) - \frac{1}{c^2} u_{tt}(x,t) = 0 & x \in (0,L), t \in (0,T) \\ u(x,0) = u_t(x,0) = 0 & x \in (0,L) \\ u(0,t) = \bar{u}(t) & t \in [0,T] \\ p(L,t) := EA \frac{\partial u}{\partial n}(L,t) = \bar{p}(t) & t \in [0,T] \end{cases} \quad (2.25)$$

where  $c = \sqrt{E/\rho}$  is the assigned scalar wave velocity with  $E$  and  $\rho$  denoting Young's modulus and mass density of the material, respectively.

The rod under consideration can be represented by a structured 3D body, with a dimension much larger than the remaining ones: the length  $L$  along the  $x$ -direction. For this reason its geometry is describable by a line, the axial line of the rod, which passes through the barycenters of all transversal sections, while displacements and tractions are referred to the axial coordinates of the bar. The homogeneous linear-elastic material constituting the rod follows Hooke's law and no flexural moment is considered.

In the one dimensional case, having defined the traction as  $p(x,t) := EA \partial_n u(x,t)$  depending on a unitary (outward) normal vector with respect to the transversal section of the rod, the problem with mixed boundary conditions ( $P_{\mathcal{D},\mathcal{N}}$ ), as introduced in page 2, can be seen as an elastodynamic problem ( $P_{EI}$ ) with constant parameter  $c = A = E = 1$  and all the considerations made about ( $P_{\mathcal{D},\mathcal{N}}$ ) in chapter 1 can be easily extended to ( $P_{EI}$ ).

In order to obtain a boundary integral formulation of the problem (2.25), we have to use Love's representation formula (the analogue of the representation formula (1.7) for ( $P_{\mathcal{D},\mathcal{N}}$ )), which depends on the fundamental solution of the wave hyperbolic equation in (2.25). This fundamental solution corresponds to the displacements field generated in an unbounded rod by an impulsive load applied in a point  $\xi$  at the time instant  $\tau$ , i.e. it is the solution of the differential problem

$$u_{xx}(x,t) - \frac{1}{c^2} u_{tt}(x,t) = -\frac{1}{EA} \delta(x-\xi) \delta(t-\tau), \quad x \in \mathbb{R}, t > 0, \quad (2.26)$$

where  $\delta$  is Dirac distribution, and reads, having set  $r = |x - \xi|$ :

$$G_{uu}(x, \xi; t - \tau) = \frac{c}{2EA} H(t - \tau) H(c(t - \tau) - r), \quad (2.27)$$

where  $H(t)$  is the Heaviside step function which assures the causality of the wave. The function (2.27) is known in literature as the first Kelvin solution for the wave problem applied to the rod.

Multiplying the partial differential equation in (2.25) by  $EA G_{uu}(x, \xi; t - \tau)$ , integrating in space and time and using the integration by part technique, one obtains the following Love's representation formula for the solution of (2.25), for  $x \in (0, L)$  and  $t \in (0, T)$ :

$$u(x, t) = \sum_{\xi=0, L} G_{uu}(x, \xi; t) * p(\xi, t) - \sum_{\xi=0, L} G_{up}(x, \xi; t) * u(\xi, t), \quad (2.28)$$

where the asterisk denotes the time convolution product and  $G_{up}(x, \xi; t)$  is the so called Gebbia first fundamental solution, given by:

$$G_{up}(x, \xi; t - \tau) = EA \frac{\partial G_{uu}}{\partial n_{\xi}}(x, \xi; t - \tau) = \frac{c}{2} H(t - \tau) \frac{\partial H}{\partial \xi}(c(t - \tau) - r) n_{1, \xi}. \quad (2.29)$$

At this stage, it is clear that in order to recover the solution of (2.25) there is the need to know the time history for traction in the first end-point and for displacement in the second end-point of the rod, i.e.  $p(0, t)$  and  $u(L, t)$  respectively. After the limiting procedure in (2.28), for  $x$  tending to the end-points of the rod, the first BIE has the form:

$$u(x, t) = \sum_{\xi=0, L} G_{uu}(x, \xi; t) * p(\xi, t) - \sum_{\xi=0, L} G_{up}(x, \xi; t) * u(\xi, t), \quad x \in \{0, L\}, t \in (0, T). \quad (2.30)$$

Then, remembering the definition of  $p(x, t)$ , from (2.30) one can obtain a second BIE, of the form:

$$p(x, t) = \sum_{\xi=0, L} G_{pu}(x, \xi; t) * p(\xi, t) - \sum_{\xi=0, L} G_{pp}(x, \xi; t) * u(\xi, t), \quad x \in \{0, L\}, t \in (0, T). \quad (2.31)$$

In the BIE (2.31) there is the second Kelvin fundamental solution:

$$G_{pu}(x, \xi; t - \tau) = EA \frac{\partial G_{uu}}{\partial n_x}(x, \xi; t - \tau) = \frac{c}{2} H(t - \tau) \frac{\partial H}{\partial x}(c(t - \tau) - r) n_{1, x}, \quad (2.32)$$

which represents the stress field generated by an impulsive load applied to the rod, and the derivative of Gebbia fundamental solution, i.e.:

$$G_{pp}(x, \xi; t - \tau) = EA \frac{\partial G_{up}}{\partial n_x}(x, \xi; t - \tau) = \frac{EA c}{2} H(t - \tau) \frac{\partial H}{\partial x \partial \xi}(c(t - \tau) - r) n_{1, \xi} n_{1, x}. \quad (2.33)$$

Of course, derivatives in (2.29), (2.32) and (2.33) have to be understood in a distributional sense.

Using equations (2.30), (2.31) in  $x = 0$  and  $x = L$ , respectively, the explicit expression of the kernels  $G_{uu}$ ,  $G_{up}$ ,  $G_{pu}$ ,  $G_{pp}$  and the boundary data, one obtains, after an

integration by parts involving the kernel  $G_{pp}$  and some straightforward calculations, the following integro-differential equation system for  $t \in (0, T)$ :

$$\begin{cases} \frac{c}{EA} \int_0^t p(0, \tau) d\tau + H(t - \frac{L}{c}) u(L, t - \frac{L}{c}) = f_u(t) \\ -H(t - \frac{L}{c}) p(0, t - \frac{L}{c}) + \frac{EA}{c} u_t(L, t) = f_p(t) \end{cases} \quad (2.34)$$

having set:

$$f_u(t) = \bar{u}(t) - \frac{c}{EA} H(t - \frac{L}{c}) \int_0^{t - \frac{L}{c}} \bar{p}(\tau) d\tau, \quad f_p(t) = \frac{EA}{c} H(t - \frac{L}{c}) \bar{u}_t(t - \frac{L}{c}) + \bar{p}(t). \quad (2.35)$$

In (2.34) the unknowns are the time history of traction in  $x = 0$  and of displacement in  $x = L$ , i.e. the two time functions  $p(0, t)$  and  $u(L, t)$ .

Now, let me introduce the following operators:

$$(Vg)(t) = \frac{c}{EA} \int_0^t g(\tau) d\tau, \quad (Dg)(t) = \frac{EA}{c} g_t(t), \quad (2.36)$$

and the anticipated and retarded shift operators:

$$(S_+g)(t) := H(T - t - \frac{L}{c}) g(t + \frac{L}{c}), \quad (S_-g)(t) := H(t - \frac{L}{c}) g(t - \frac{L}{c}). \quad (2.37)$$

Using these operators, the system (2.34) can be rewritten in compact form as:

$$\begin{bmatrix} V & S_- \\ -S_- & D \end{bmatrix} \begin{bmatrix} p^0(t) \\ u^L(t) \end{bmatrix} = \begin{bmatrix} f_u(t) \\ f_p(t) \end{bmatrix}, \quad t \in (0, T), \quad (2.38)$$

where  $p^0(t)$ ,  $u^L(t)$  represent the unknown time functions  $p(0, t)$  and  $u(L, t)$ , respectively.

### 2.3.1 Energetic weak problem related to the BIEs

Also in this case a weak formulation derives from the consideration of the positive energy for the hyperbolic wave problem (2.25) at the final time instant  $T$  inside the rod that can be expressed as:

$$\mathcal{E}_{(0,L)}(T) := \frac{1}{2} \int_0^L \left[ \left( \frac{1}{c} u_t(x,T) \right)^2 + \left( u_x(x,T) \right)^2 \right] dx = \frac{1}{EA} \int_0^T \sum_{x=0,L} u_t(x,t) p(x,t) dt \geq 0. \quad (2.39)$$

Since the first equation in (2.34) comes from (2.30), we have to differentiate it with respect to time before projecting onto the space  $L^2(0,T)$ , while the second equation, coming from (2.31), has to be projected onto the space of time derivatives of functions belonging to  $H_{\{0\}}^1(0,T)$ . Hence the auxiliary problem deduced from (2.34) is

$$\begin{cases} \frac{c}{EA} p(0,t) + H(t - \frac{L}{c}) u_t(L, t - \frac{L}{c}) = f_{u,t}(t) \\ -H(t - \frac{L}{c}) p(0, t - \frac{L}{c}) + \frac{EA}{c} u_t(L,t) = f_p(t) \end{cases} \quad (2.40)$$

Then, remembering the definitions (2.36) and (2.37) and having set  $W = L^2(0,T) \times H_{\{0\}}^1(0,T)^2$ ,  $\tilde{W} = H_{\{0\}}^1(0,T) \times L^2(0,T)$ , define the bilinear form:

$$a_{\mathcal{E}}(\cdot, \cdot) := \left\langle \begin{bmatrix} V_t & S_{-t} \\ -S_{-} & D \end{bmatrix} \cdot, \cdot \right\rangle : W \times W \longrightarrow \mathbb{R}, \quad (2.41)$$

obtaining the following energetic weak formulation of the problem (2.38):

given  $(f_u \ f_p)^\top \in \tilde{W}$ , find  $(p^0 \ u^L)^\top \in W$  such that

$$a_{\mathcal{E}} \left( \begin{pmatrix} p^0 \\ u^L \end{pmatrix}, \begin{pmatrix} \Psi \\ \varphi_t \end{pmatrix} \right) = \left\langle \begin{pmatrix} f_{u,t} \\ f_p \end{pmatrix}, \begin{pmatrix} \Psi \\ \varphi_t \end{pmatrix} \right\rangle, \quad \forall (\Psi \ \varphi)^\top \in W. \quad (2.42)$$

The bilinear form  $a_{\mathcal{E}}(\cdot, \cdot)$  is continuous and coercive on  $W \times W$ , thus assuring existence and uniqueness of the weak solution.

In order to derive these theoretical results, the attention has to be concentrated on the operator  $\mathcal{A}$  defined by:

$$\mathcal{A} : L^2(0,T) \times L^2(0,T) \rightarrow L^2(0,T) \times L^2(0,T), \quad \mathcal{A} := \begin{bmatrix} \alpha I & S_{-} \\ -S_{-} & \frac{1}{\alpha} I \end{bmatrix}, \quad (2.43)$$

where  $\alpha = c/EA > 0$  and  $I$  is the identity operator. Recalling the definitions of operators  $V$ ,  $D$  and  $S_{-}$ , with a straightforward calculations:

$$a_{\mathcal{E}} \left( \begin{pmatrix} p \\ u \end{pmatrix}, \begin{pmatrix} q \\ v_t \end{pmatrix} \right) = \left\langle \begin{pmatrix} \alpha p + S_{-} u_t \\ -S_{-} p + \frac{1}{\alpha} u_t \end{pmatrix}, \begin{pmatrix} q \\ v_t \end{pmatrix} \right\rangle = \langle \mathcal{A} \begin{pmatrix} p \\ u_t \end{pmatrix}, \begin{pmatrix} q \\ v_t \end{pmatrix} \rangle. \quad (2.44)$$

Now, introduce two new operators: the adjoint and the symmetric part of the operator  $\mathcal{A}$ , i.e. respectively

---

<sup>2</sup>  $H_{\{0\}}^1(0,T)$  is the space of functions belonging to  $H^1(0,T)$  and vanishing for  $t = 0$ .



$$\mathcal{A}^* := \begin{bmatrix} \alpha I & -S_+ \\ S_+ & \frac{1}{\alpha} I \end{bmatrix}, \quad \mathcal{A}_s := \frac{\mathcal{A} + \mathcal{A}^*}{2} = \begin{bmatrix} \alpha I & \frac{1}{2}[S_- - S_+] \\ \frac{1}{2}[-S_- + S_+] & \frac{1}{\alpha} I \end{bmatrix}. \quad (2.45)$$

From definitions (2.43) and (2.45), it follows:

$$\langle \mathcal{A} \begin{pmatrix} P \\ u_t \end{pmatrix}, \begin{pmatrix} P \\ u_t \end{pmatrix} \rangle = \langle \mathcal{A}_s \begin{pmatrix} P \\ u_t \end{pmatrix}, \begin{pmatrix} P \\ u_t \end{pmatrix} \rangle, \quad \forall (p \ u)^\top \in W. \quad (2.46)$$

**Proposition 1** *The operator  $\mathcal{A}_s : L^2(0, T) \times L^2(0, T) \rightarrow L^2(0, T) \times L^2(0, T)$  is a continuous, bijective and self-adjoint positive operator. Moreover*

$$\langle \mathcal{A}_s \begin{pmatrix} P \\ u_t \end{pmatrix}, \begin{pmatrix} P \\ u_t \end{pmatrix} \rangle \geq \frac{1}{\|\mathcal{A}_s^{-1}\|} \|\begin{pmatrix} P \\ u_t \end{pmatrix}\|_2^2. \quad (2.47)$$

*Proof.* From definitions (2.45) it follows directly that the operator  $\mathcal{A}_s$  is continuous and self-adjoint, therefore it suffices to prove that it is injective and surjective. For what concerns the first point from (2.44) and (2.46), on has:

$$\begin{aligned} \langle \mathcal{A}_s \begin{pmatrix} P \\ u_t \end{pmatrix}, \begin{pmatrix} P \\ u_t \end{pmatrix} \rangle &= \langle \mathcal{A} \begin{pmatrix} P \\ u_t \end{pmatrix}, \begin{pmatrix} P \\ u_t \end{pmatrix} \rangle \\ &= \alpha \int_0^T p^2(t) dt + \frac{1}{\alpha} \int_0^T u_t^2(t) dt + \int_{L/c}^T p(t) u_t(t - \frac{L}{c}) dt - \int_{L/c}^T u_t(t) p(t - \frac{L}{c}) dt. \end{aligned} \quad (2.48)$$

Considering the integrand functions in the last two integrals, it holds:

$$\begin{aligned} p(t) u_t(t - \frac{L}{c}) &= \frac{1}{2} [\sqrt{\alpha} p(t) + \frac{1}{\sqrt{\alpha}} u_t(t - \frac{L}{c})]^2 - \frac{1}{2} \alpha p^2(t) - \frac{1}{2\alpha} u_t^2(t - \frac{L}{c}) \\ -u_t(t) p(t - \frac{L}{c}) &= \frac{1}{2} [-\sqrt{\alpha} p(t - \frac{L}{c}) + \frac{1}{\sqrt{\alpha}} u_t(t)]^2 - \frac{1}{2} \alpha p^2(t - \frac{L}{c}) - \frac{1}{2\alpha} u_t^2(t) \end{aligned}$$

and replacing in (2.48):

$$\begin{aligned} \langle \mathcal{A}_s \begin{pmatrix} P \\ u_t \end{pmatrix}, \begin{pmatrix} P \\ u_t \end{pmatrix} \rangle &= \\ &= \frac{\alpha}{2} \int_0^{L/c} p^2(t) dt + \frac{\alpha}{2} \int_{T-L/c}^T p^2(t) dt + \frac{1}{2\alpha} \int_0^{L/c} u_t^2(t) dt + \frac{1}{2\alpha} \int_{T-L/c}^T u_t^2(t) dt + \\ &+ \frac{1}{2} \int_{L/c}^T [\sqrt{\alpha} p(t) + \frac{1}{\sqrt{\alpha}} u_t(t - \frac{L}{c})]^2 dt + \frac{1}{2} \int_{L/c}^T [-\sqrt{\alpha} p(t - \frac{L}{c}) + \frac{1}{\sqrt{\alpha}} u_t(t)]^2 dt \geq 0, \end{aligned}$$

because sum of positive terms. Now, suppose  $\langle \mathcal{A}_s \begin{pmatrix} P \\ u_t \end{pmatrix}, \begin{pmatrix} P \\ u_t \end{pmatrix} \rangle = 0$ . Then it happens that every integrand function in the previous equality identically vanishes. In



Matrix  $\mathcal{M}_s$  is symmetric and positive definite, hence the surjective property (invertibility) of operator  $\mathcal{A}_s$  is proved.

More precisely, the spectrum of this matrix is constituted by  $M/2$  distinct eigenvalues, each with double algebraic multiplicity, for  $\alpha = 1$  given by:

$$\lambda_k = 1 - \cos\left(\frac{\pi k}{\frac{M}{2} + 1}\right), \quad k = 1, \dots, \frac{M}{2}, \quad (2.53)$$

or, in the general case  $\alpha > 0$ ,  $\alpha \neq 1$ , having set  $\beta = \min(\alpha, 1/\alpha)$  and  $\gamma = \max(\alpha, 1/\alpha)$ , with an asymptotic behavior for  $\beta \rightarrow 0$ , of the type:

$$\begin{cases} \frac{\beta}{2} [1 - \cos \zeta_k] - \left(\frac{\beta}{2}\right)^3 [1 - \cos 2\zeta_k] + \mathcal{O}\left(\left(\frac{\beta}{2}\right)^5\right), & k = 1, \dots, \frac{M}{4}; \\ \gamma + \frac{\beta}{2} [1 - \cos \chi_k] + \left(\frac{\beta}{2}\right)^3 [1 - \cos 2\chi_k] + \mathcal{O}\left(\left(\frac{\beta}{2}\right)^5\right), & k = \frac{M}{4} + 1, \dots, \frac{M}{2}; \end{cases} \quad (2.54)$$

where:

$$\zeta_k = \frac{2\pi k}{\frac{M}{2} + 1}, \quad \chi_k = \frac{(2(k - \frac{M}{4}) - 1)\pi}{\frac{M}{2} + 1}.$$

Therefore, for the least eigenvalue ( $k = 1$ ), which represents  $1/\|\mathcal{A}_s^{-1}\|$  it holds:

$$\lambda_1(\mathcal{A}_s) \simeq \frac{\beta}{2\delta_{1\alpha}} \frac{\pi^2}{\left(\frac{M}{2} + 1\right)^2} = \mathcal{O}\left(\frac{1}{M^2}\right), \quad M \rightarrow \infty, \quad (2.55)$$

where  $\delta_{1\alpha}$  is the Kronecker symbol.

At last, inequality (2.47) is a standard result of functional analysis.

At this stage we can prove the following conclusive result:

**Theorem 21** *The real bilinear form  $a_{\mathcal{E}}(\cdot, \cdot)$  of the energetic weak formulation is continuous and coercive on  $W \times W$ .*

*Proof.* Observe that from (2.44) it will be sufficient to prove the continuity and coerciveness of the bilinear form  $a_{\mathcal{E}}(\cdot, \cdot)$  for functions  $(p \ u_t)^\top$  in  $L^2(0, T) \times L^2(0, T)$ , since  $\|u\|_{H_{\{0\}}^1(0, T)}$  and  $\|u_t\|_{L^2(0, T)}$  are equivalent norms, owing to the homogeneous initial condition in our hyperbolic problem (2.25).

For what concerns continuity:

$$\begin{aligned}
|a_{\mathcal{E}}\left(\begin{pmatrix} p \\ u \end{pmatrix}, \begin{pmatrix} q \\ v \end{pmatrix}\right)| &= |\langle \mathcal{A}\left(\begin{pmatrix} p \\ u \end{pmatrix}, \begin{pmatrix} q \\ v \end{pmatrix}\right) \rangle| \\
&= \left| \int_0^T [\alpha q(t)p(t) + \frac{1}{\alpha} v_t(t) u_t(t)] dt + \int_{L/c}^T [q(t) u_t(t - \frac{L}{c}) - v_t(t) p(t - \frac{L}{c})] dt \right| \\
&\leq \int_0^T \left| \begin{pmatrix} \alpha p(t) \\ \frac{1}{\alpha} u_t(t) \end{pmatrix} \cdot \begin{pmatrix} q(t) \\ v_t(t) \end{pmatrix} \right| dt + \int_{L/c}^T \left| \begin{pmatrix} u_t(t - \frac{L}{c}) \\ -p(t - \frac{L}{c}) \end{pmatrix} \cdot \begin{pmatrix} q(t) \\ v_t(t) \end{pmatrix} \right| dt \\
&\leq \int_0^T \left\| \begin{pmatrix} \alpha p(t) \\ \frac{1}{\alpha} u_t(t) \end{pmatrix} \right\|_2 \left\| \begin{pmatrix} q(t) \\ v_t(t) \end{pmatrix} \right\|_2 dt + \int_{L/c}^T \left\| \begin{pmatrix} u_t(t - \frac{L}{c}) \\ -p(t - \frac{L}{c}) \end{pmatrix} \right\|_2 \left\| \begin{pmatrix} q(t) \\ v_t(t) \end{pmatrix} \right\|_2 dt
\end{aligned}$$

and using the Cauchy-Schwarz inequality finally:

$$\begin{aligned}
&\leq \left\| \begin{pmatrix} \alpha p \\ \frac{1}{\alpha} u_t \end{pmatrix} \right\|_{L^2(0,T)} \left\| \begin{pmatrix} q \\ v_t \end{pmatrix} \right\|_{L^2(0,T)} + \left\| \begin{pmatrix} p \\ u_t \end{pmatrix} \right\|_{L^2(L/c,T)} \left\| \begin{pmatrix} q \\ v_t \end{pmatrix} \right\|_{L^2(L/c,T)} \\
&\leq [\max(\alpha, \frac{1}{\alpha}) + 1] \left\| \begin{pmatrix} p \\ u_t \end{pmatrix} \right\|_{L^2(0,T)} \left\| \begin{pmatrix} q \\ v_t \end{pmatrix} \right\|_{L^2(0,T)}.
\end{aligned}$$

The proof of the coerciveness of the bilinear form  $a_{\mathcal{E}}(\cdot, \cdot)$  follows easily from (2.44), (2.46) and inequality (2.47). In fact, we have:

$$a_{\mathcal{E}}\left(\begin{pmatrix} p \\ u \end{pmatrix}, \begin{pmatrix} p \\ u \end{pmatrix}\right) = \langle \mathcal{A}_s\left(\begin{pmatrix} p \\ u \end{pmatrix}, \begin{pmatrix} p \\ u \end{pmatrix}\right) \rangle \geq \frac{1}{\|\mathcal{A}_s^{-1}\|} \left\| \begin{pmatrix} p \\ u \end{pmatrix} \right\|_2^2, \quad (2.56)$$

and for the coerciveness constant of the energetic bilinear form, remembering that  $M = \frac{2c}{L} T$  and (2.55), it holds

$$\frac{1}{\|\mathcal{A}_s^{-1}\|} = \lambda_1(\mathcal{A}_s) = \mathcal{O}(T^{-2}), \quad T \rightarrow +\infty.$$

### 2.3.2 Numerical results

This kind of problem is a good occasion to compare this energetic weak formulation with the one introduced by Bamberger and Ha Duong and reassumed in section 1.2. Following the procedure explained in ([10, 11]) we can deduce the continuous and coercive bilinear form:

$$a_{\sigma}(\cdot, \cdot) = \left\langle \begin{bmatrix} V_t & S_{-t} \\ -S_{-} & D \end{bmatrix} \cdot, \cdot \right\rangle_{\sigma} : W \times W \rightarrow \mathbb{R} \quad (2.57)$$

where the scalar product is defined as:

$$\langle f, g \rangle_\sigma := \int_{-\infty}^{+\infty} e^{-2\sigma t} f(t) g(t) dt \quad (2.58)$$

with  $\sigma$  a real strictly positive parameter that has to be fixed. Hence, the weak formulation associate to (2.38) is:

given  $(f_u \ f_p)^\top \in \tilde{W}$ , find  $(p^0 \ u^L)^\top \in W$  such that

$$a_\sigma \left( \begin{pmatrix} p^0 \\ u^L \end{pmatrix}, \begin{pmatrix} \Psi \\ \Phi_t \end{pmatrix} \right) = \left\langle \begin{pmatrix} f_{u,t} \\ f_p \end{pmatrix}, \begin{pmatrix} \Psi \\ \Phi_t \end{pmatrix} \right\rangle_\sigma, \quad \forall (\Psi \ \Phi)^\top \in W. \quad (2.59)$$

From now on, problem (2.59) will be referred to as  $\sigma$  weak formulation of the wave problem (2.38).

As already established in section 2.1.2, together with a uniform decomposition of the time interval  $[0, T]$  we can introduce the standard finite element spaces

$$X_{-1, \Delta t} := \{ \Psi_{\Delta t}(t) \in L^2(0, T) : \Psi_{\Delta t}|_{[t_k, t_{k+1}]} \in \mathcal{P}_{d_k}, d_k \geq 0, k = 0, \dots, N_{\Delta t} - 1 \}.$$

and

$$X_{0, \Delta t} := \{ \Phi_{\Delta t}(t) \in C^0(0, T) : \Phi_{\Delta t}|_{[t_k, t_{k+1}]} \in \mathcal{P}_{d_{k+1}}, d_{k+1} \geq 0, k = 0, \dots, N_{\Delta t} - 1 \}.$$

Then, considering the finite dimensional space  $W_{\Delta t} = X_{-1, \Delta t} \times X_{0, \Delta t}$ , we can write down the discrete form of weak problem (2.42):

given  $(f_u \ f_p)^\top \in \tilde{W}$ , find  $(p_{\Delta t}^0 \ u_{\Delta t}^L)^\top \in W_{\Delta t}$  such that

$$a_{\mathcal{E}} \left( \begin{pmatrix} p_{\Delta t}^0 \\ u_{\Delta t}^L \end{pmatrix}, \begin{pmatrix} \Psi_{\Delta t} \\ \Phi_{\Delta t, t} \end{pmatrix} \right) = \left\langle \begin{pmatrix} f_{u,t} \\ f_p \end{pmatrix}, \begin{pmatrix} \Psi_{\Delta t} \\ \Phi_{\Delta t, t} \end{pmatrix} \right\rangle, \quad \forall (\Psi_{\Delta t} \ \Phi_{\Delta t})^\top \in W_{\Delta t}, \quad (2.60)$$

Denoting with  $\{\psi_k\}$  a basis for  $X_{-1, \Delta t}$  and with  $\{\varphi_k\}$  a basis for  $X_{0, \Delta t}$ , the unknown functions  $p_{\Delta t}^0(t), u_{\Delta t}^L(t)$  can be expressed as:

$$p_{\Delta t}^0(t) = \sum_k p_k^0 \psi_k(t), \quad u_{\Delta t}^L(t) = \sum_k u_k^L \varphi_k(t) \quad (2.61)$$

and problem (2.60) can be equivalently written as a linear system:

$$\mathbb{E}_{\mathcal{E}} \alpha_{\mathcal{E}} = \mathbf{b}_{\mathcal{E}}. \quad (2.62)$$

The matrix  $\mathbb{E}_{\mathcal{E}}$  has a  $2 \times 2$  block structure, whose elements are of the form:

$$\begin{aligned}
(\mathbb{E}_{\mathcal{E}}^{11})_{kj} &= \frac{c}{EA} \int_0^T \psi_k(t) \psi_j(t) dt, & (\mathbb{E}_{\mathcal{E}}^{12})_{kj} &= \int_{\frac{L}{c}}^T \psi_k(t) \varphi_{jt}(t - \frac{L}{c}) dt, \\
(\mathbb{E}_{\mathcal{E}}^{21})_{kj} &= - \int_{\frac{L}{c}}^T \varphi_{kt}(t) \psi_j(t - \frac{L}{c}) dt, & (\mathbb{E}_{\mathcal{E}}^{22})_{kj} &= \frac{EA}{c} \int_0^T \varphi_{kt}(t) \varphi_{jt}(t) dt.
\end{aligned}$$

The discretization of weak problem (2.59) can be equivalently written as a linear system, too:

$$\mathbb{E}_{\sigma} \alpha_{\sigma} = \mathbf{b}_{\sigma}, \quad (2.63)$$

where the elements of the four blocks of matrix  $\mathbb{E}_{\sigma}$  are of the form:

$$\begin{aligned}
(\mathbb{E}_{\sigma}^{11})_{kj} &= \frac{c}{EA} \int_0^T e^{-2\sigma t} \psi_k(t) \psi_j(t) dt, & (\mathbb{E}_{\sigma}^{12})_{kj} &= \int_{\frac{L}{c}}^T e^{-2\sigma t} \psi_k(t) \varphi_{jt}(t - \frac{L}{c}) dt, \\
(\mathbb{E}_{\sigma}^{21})_{kj} &= - \int_{\frac{L}{c}}^T e^{-2\sigma t} \varphi_{kt}(t) \psi_j(t - \frac{L}{c}) dt, & (\mathbb{E}_{\sigma}^{22})_{kj} &= \frac{EA}{c} \int_0^T e^{-2\sigma t} \varphi_{kt}(t) \varphi_{jt}(t) dt.
\end{aligned}$$

Observe that these elements depend on a real strictly positive parameter  $\sigma$  that has to be fixed and greatly influences the condition number of matrix  $\mathbb{E}_{\sigma}$ .

**Remark.** Matrices  $\mathbb{E}_{\mathcal{E}}$  and  $\mathbb{E}_{\sigma}$  are not symmetric; in fact the corresponding bilinear forms  $a_{\mathcal{E}}(\cdot, \cdot)$  and  $a_{\sigma}(\cdot, \cdot)$  are not symmetric and the related weak formulations can't be written as equivalent variational problems. Anyway, owing to the coerciveness of  $a_{\mathcal{E}}(\cdot, \cdot)$  and  $a_{\sigma}(\cdot, \cdot)$ , their diagonal blocks are positive definite.

- As test problem, taken from [24], consider a rod of unitary length  $L = 1$ , fixed in  $x = 0$  and subjected to a uniform traction at the other end-point. Hence, we introduce the following boundary conditions:  $u(0, t) = 0$ ,  $p(L, t) = H(t)$ . The wave velocity is set  $c = 1$ ; further  $A = 1$ ,  $E = 1$ . The observation time interval is  $(0, 20)$ . For the discretization, two time steps have been considered: the first,  $\Delta t = 0.1$ , is such that the time  $L/c$  required by the elastic wave to cover the distance between the two end-points of the rod is a multiple of it; the second,  $\Delta t = 0.08$ , has not this property. Traction in  $x = 0$  are approximated by constant shape functions and displacements in  $x = L$  by linear shape functions. In Figure 2.8 there is the numerical solution obtained with  $\Delta t = 0.1$ , starting from the energetic weak formulation. The same graph has been obtained with the  $\sigma$  weak formulation. The approximate solution overlaps the analytical one and it is in perfect agreement with that reported in [24], obtained with a collocation technique using the first BIE (2.30) alone. In Figures 2.9 the sparse structure of matrices  $\mathbb{E}_{\mathcal{E}}$  and  $\mathbb{E}_{\sigma}$  are reported. For what concerns their spectral condition number we have:  $\mu_2(\mathbb{E}_{\mathcal{E}}) = 6.82 \cdot 10^2$  and in table 2.1

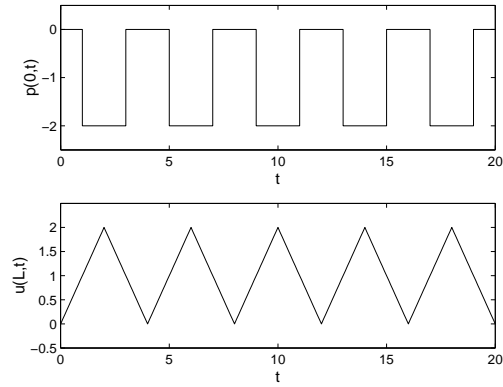


Fig. 2.8: Numerical solution obtained with  $\Delta t = 0.1$  using constant shape functions to approximate  $p(0,t)$  and linear shape functions to approximate  $u(L,t)$ .

the spectral condition number of  $\mathbb{E}_\sigma$  for different values of the parameter  $\sigma$ , for two different time steps. As one can see, the condition number of  $\mathbb{E}_\sigma$  rapidly increases even for small values of  $\sigma$ , however the solution is still stable. In Figure 2.10 there

$\sigma$	0	0.2	0.4	$\Delta t$
$\mu_2(\mathbb{E}_\sigma)$	$6.82E+02$	$3.30E+05$	$8.40E+08$	0.1
$\mu_2(\mathbb{E}_\sigma)$	$1.04E+03$	$4.91E+05$	$1.31E+09$	0.08

Table 2.1: Spectral condition number of matrix  $\mathbb{E}_\sigma$ , for different values of  $\sigma$  and  $\Delta t$ .

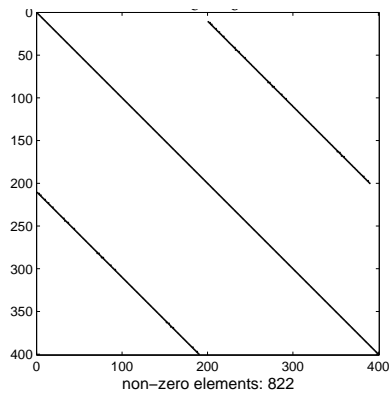


Fig. 2.9: The highly sparse structure of matrices  $\mathbb{E}_\sigma$  and  $\mathbb{E}_\sigma$ .

is the numerical solution obtained with  $\Delta t = 0.08$ , starting from energetic weak

formulation, compared with the analytical one. Also in this case the approximate solution is in perfect agreement with that reported in [24].

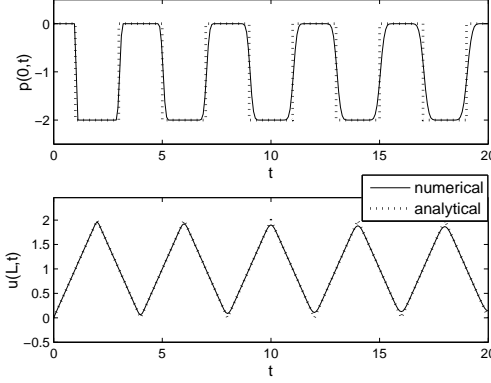


Fig. 2.10: Comparison between the analytical solution and its numerical approximation obtained using the energetic weak formulation with constant shape functions to approximate  $p(0,t)$ , linear shape functions to approximate  $u(L,t)$  and time-discretization parameter  $\Delta t = 0.08$ .

- The theoretical analysis of given energetic weak formulation remains the same considering slightly different differential model problems, such as

$$\begin{cases} u_{xx}(x,t) - \frac{1}{c^2}u_{tt}(x,t) = \bar{g}(x,t) & x \in (0,L), t \in (0,T), \\ u(x,0) = u_t(x,0) = 0 & x \in (0,L), \\ u(0,t) = 0 & t \in (0,T), \\ p(L,t) = 0 & t \in (0,T), \end{cases} \quad (2.64)$$

where right-hand side in the wave equation is non-trivial and initial and mixed boundary conditions are homogeneous, or

$$\begin{cases} u_{xx}(x,t) - \frac{1}{c^2}u_{tt}(x,t) = 0 & x \in (0,L), t \in (0,T), \\ u(x,0) = u_0(x) & x \in (0,L), \\ u_t(x,0) = v_0(x) & x \in (0,L), \\ u(0,t) = 0 & t \in (0,T), \\ p(L,t) = 0 & t \in (0,T), \end{cases} \quad (2.65)$$

where initial conditions are non-trivial in a rod with fixed and free endpoints, respectively, with no external forces. Note that initial conditions have to be compatible with the homogeneous boundary data, hence they have to satisfy the properties:



$$u_0(0) = v_0(0) = 0, \quad \frac{du_0}{dx}(L) = \frac{dv_0}{dx}(L) = 0.$$

In the above cases, the energetic bilinear form  $a_{\mathcal{E}}(\cdot, \cdot)$  does not change, while the right-hand side in (2.42) can be deduced from the following functions depending on the given data:

$$f_u(t) = \frac{c}{EA} \int_0^L \int_0^{t-\frac{\xi}{c}} \bar{g}(\xi, \tau) d\tau d\xi, \quad f_p(t) = - \int_0^L \bar{g}(\xi, t - \frac{L-\xi}{c}) d\xi \quad (2.66)$$

for problem (2.64) and

$$f_u(t) = -\frac{1}{cA} \int_0^{ct} v_0(\xi) d\xi - \frac{1}{A} u_0(ct), \quad f_p(t) = \frac{E}{c} v_0(L-ct) - E \frac{du_0}{dx}(L-ct) \quad (2.67)$$

for problem (2.65).

In figure 2.11 there is the numerical solution of the problem (2.64) with  $\bar{g}(x, t) = H(t)$  related to the previous rod, obtained with energetic weak formulation and using  $\Delta t = 0.1$  as discretization time step, and the evaluated displacements in  $x = \frac{L}{4}, \frac{L}{2}, \frac{3L}{4}, L$  are presented. The approximated solutions overlap the analytical ones, deducible from:

$$u(x, t) = \frac{1}{2} \sum_{k=0}^{+\infty} (-1)^k [H(t-x-2kL)(t-x-2kL)^2 + H(t+x-2(k+1)L)(t+x-2(k+1)L)^2] - \frac{t^2}{2}.$$

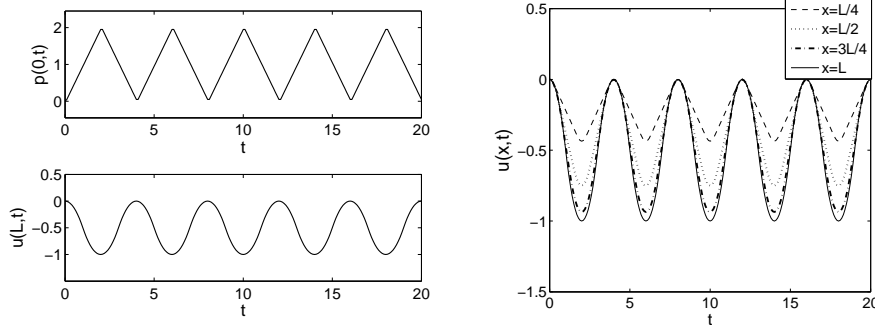


Fig. 2.11: Numerical solution of problem (2.64) and evaluated displacements in different points of the rod, obtained using linear shape functions to approximate in time.

At last, in figure 2.12 there is the numerical solution of problem (2.65) with  $u_0(x) = x(x-L)^2, v_0(x) = 0$ , obtained for the previous rod with energetic weak formulation, using  $\Delta t = 0.1$  as discretization time step. Also in this case the approximated displacement and traction overlap the corresponding analytical solutions

deducible from:

$$u(x, t) = \sum_{k=1}^{+\infty} \alpha_k \cos\left(\frac{(2k-1)\pi c}{2L} t\right) v_k(x),$$

with

$$v_k(x) = \sqrt{\frac{2}{L}} \sin\left(\frac{(2k-1)\pi}{2L} x\right), \quad \alpha_k = \int_0^L u_0(x) v_k(x) dx.$$

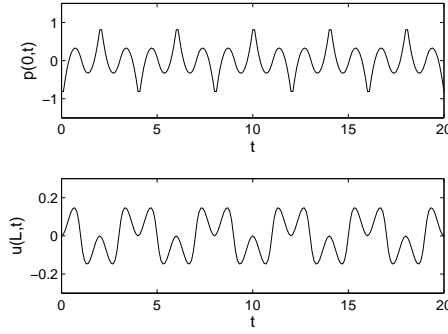


Fig. 2.12: Numerical solution of problem (2.65), obtained with the energetic weak formulation and using linear shape functions to approximate in time.

- The energetic weak formulation has been applied in the analysis of layered media ([2, 4]). Corresponding numerical results are not reported here for brevity.

## Chapter 3

### The two dimensional wave problem

In this section I will consider two dimensional wave propagation problems reformulated in terms of boundary integral equations, extending the energetic space-time weak formulation with some theoretical analysis. At last, various numerical simulations will be presented and discussed, showing the stability of the space-time Galerkin boundary element method applied to the energetic weak problem.

#### 3.1 Exterior Dirichlet problem

Consider the Dirichlet problem formulated over a domain exterior to an open arc  $\Gamma \subset \mathbb{R}^2$ :

$$(P_{\mathcal{D}}^e) \begin{cases} u_{tt}(\mathbf{x}, t) - \Delta u(\mathbf{x}, t) = 0 & \mathbf{x} \in \mathbb{R}^2 \setminus \Gamma, t \in (0, T), \\ u(\mathbf{x}, 0) = u_t(\mathbf{x}, 0) = 0 & \mathbf{x} \in \mathbb{R}^2 \setminus \Gamma, \\ u(\mathbf{x}, t) = g_{\mathcal{D}}(\mathbf{x}, t) & (\mathbf{x}, t) \in \Sigma = \Gamma \times [0, T] \end{cases} \quad (3.1)$$

In this case the boundary datum  $g_{\mathcal{D}}(\mathbf{x}, t)$  represents the value of the excitation field over  $\Gamma$ . As seen for one dimensional problems, consider the single-layer representation (D2c) of the solution of (3.1):

$$u(\mathbf{x}, t) = \int_{\Gamma} \int_0^t G(r; t - \tau) \varphi(\xi, \tau) d\tau d\xi_{\Gamma} = (\mathcal{V}\varphi)(\mathbf{x}, t), \quad \mathbf{x} \in \mathbb{R}^2 \setminus \Gamma, t \in (0, T), \quad (3.2)$$

with  $r = \|\mathbf{r}\|_2 = \|\mathbf{x} - \xi\|_2$ ,  $\varphi = \left[ \frac{\partial u}{\partial \mathbf{n}} \right]$  the jump of the normal derivative of  $u$  along  $\Gamma$  and  $G$  the fundamental solution given in (1.3). After having derived the related space-time BIE (see (D2c) introduced in page 6)

$$g_{\mathcal{D}}(\mathbf{x}, t) = \int_{\Gamma} \int_0^t G(r, t - \tau) \varphi(\xi, \tau) d\tau d\xi_{\Gamma} = V\varphi(\mathbf{x}, t), \quad \mathbf{x} \in \Gamma, t \in (0, T). \quad (3.3)$$

the energetic weak formulation of problem (3.3) is defined as in (2.18), with

$$a_{\mathcal{E}}(\varphi, \psi) = \langle (V\varphi)_t, \psi \rangle_{L^2(\Sigma)} = \int_{\Gamma} \int_0^T (V\varphi)_t(\mathbf{x}, t) \psi(\mathbf{x}, t) dt d\mathbf{x}_{\Gamma}, \quad (3.4)$$

where  $\psi$  is a suitable test function, belonging to the same functional space of  $\varphi$ . With an integration by parts and (3.1)

$$a_{\mathcal{E}}(\varphi, \psi) = \int_{\Gamma} (V\varphi)(\mathbf{x}, T) \psi(\mathbf{x}, T) d\mathbf{x}_{\Gamma} - \int_{\Gamma} \int_0^T (V\varphi)(\mathbf{x}, t) \psi_t(\mathbf{x}, t) dt d\mathbf{x}_{\Gamma}. \quad (3.5)$$

In order to apply the Fourier transform to the analysis of the bilinear form (3.4), assume that the obstacle  $\Gamma$  is flat, that is  $\Gamma = \{(x, 0) : x \in [0, L]\} \subset \mathbb{R}$ . Then, for a given regular function  $\varphi$  having support in  $\Sigma$ , the function  $u$  in (3.2) can be reinterpreted as the solution of the jump problem:

$$\begin{cases} u_{tt} - u_{xx} - u_{yy} = 0 & (x, y) \in \mathbb{R}^2 \setminus \Gamma, t > 0, \\ \left[ \frac{\partial u}{\partial y} \right] (x, 0, t) = \varphi(x, t) & 0 \leq x \leq L, t > 0, \\ [u](x, 0, t) = 0 & 0 \leq x \leq L, t > 0, \\ u(x, y, 0) = u_t(x, y, 0) = 0 & (x, y) \in \mathbb{R}^2 \end{cases} \quad (3.6)$$

For any  $f \in L^2(\Sigma)$ , define the Fourier transform with respect to a single variable, either  $x$  or  $t$ , as follows

$$\begin{aligned} \hat{f}(\xi, t) &:= \mathcal{F}_x(f)(\xi, t) = \frac{1}{\sqrt{2\pi}} \int_{-\infty}^{+\infty} e^{-ix\xi} f(x, t) dx, \\ \hat{f}(x, \omega) &:= \mathcal{F}_t(f)(x, \omega) = \frac{1}{\sqrt{2\pi}} \int_{-\infty}^{+\infty} e^{-it\omega} f(x, t) dt \end{aligned}$$

while

$$\tilde{f}(\xi, \omega) := \mathcal{F}(f)(\xi, \omega) = \frac{1}{2\pi} \int_{-\infty}^{+\infty} \int_{-\infty}^{+\infty} e^{-i(t\omega + \xi x)} f(x, t) dt dx \quad (3.7)$$

will denote the Fourier transform with respect to both variables. As it is well-known by the Paley-Wiener theorem 7,  $\tilde{f}(\omega, \xi)$  is an entire analytical function of exponential type.

Assume for the moment that  $\varphi \in C_0^\infty(\Sigma)$  and perform the transformation of the operator  $\varphi \mapsto (V\varphi)_t$  into a multiplication operator in the frequency variables. Having set

$$\hat{u}(\xi, y, t) := \frac{1}{\sqrt{2\pi}} \int_{-\infty}^{+\infty} e^{-ix\xi} u(x, y, t) dx, \quad y \neq 0, t > 0,$$

we obtain the following homogeneous Cauchy problem with a jump condition for  $\hat{u}_y$  in  $y = 0$ , for the Klein-Gordon equation with mass  $\xi^2$ :

$$\hat{u}_{tt} - \hat{u}_{yy} - \xi^2 \hat{u} = 0 \quad y \neq 0, \quad t > 0, \quad (3.8)$$

$$\left[ \frac{\partial \hat{u}}{\partial y} \right] (\xi, 0, t) = \hat{\phi}(\xi, t) \quad t > 0, \quad (3.9)$$

$$[\hat{u}] (\xi, 0, t) = 0 \quad t > 0, \quad (3.10)$$

$$\hat{u}(\xi, y, 0) = \hat{u}_t(\xi, y, 0) = 0 \quad y \neq 0. \quad (3.11)$$

In order to represent  $\hat{u}$  as a single layer integral, use the expression of the fundamental solution of the Klein-Gordon equation which is given by (see [22])

$$\widehat{G}(\xi, y, t) = \frac{1}{2} H[t - |y|] J_0(|\xi| \sqrt{t^2 - y^2}) \quad (3.12)$$

where  $J_0$  represents the Bessel function of order 0. Then

$$\hat{u}(\xi, y, t) = \frac{1}{2} \int_0^{t-|y|} J_0(|\xi| \sqrt{(t-\tau)^2 - y^2}) \hat{\phi}(\xi, \tau) d\tau, \quad \xi \in \mathbb{R}, y \neq 0, t > 0, \quad (3.13)$$

and by taking the limit  $y \rightarrow 0$ ,

$$\hat{u}(\xi, 0, t) = \frac{1}{2} \int_0^t J_0(|\xi|(t-\tau)) \hat{\phi}(\xi, \tau) d\tau, \quad \xi \in \mathbb{R}, t > 0. \quad (3.14)$$

Since

$$\hat{u}_t = \frac{\partial}{\partial t} \mathcal{F}_x[u] = \mathcal{F}_x[u_t] = \mathcal{F}_x[(V\phi)_t],$$

$J_0(0) = 1$  and  $J_0'(t) = -J_1(t)$ , deriving in (3.14) with respect to  $t$ ,

$$\mathcal{F}_x[(V\phi)_t] = \hat{u}_t(\xi, 0, t) = \frac{1}{2} \hat{\phi}(\xi, t) - \frac{|\xi|}{2} \int_0^t J_1(|\xi|(t-\tau)) \hat{\phi}(\xi, \tau) d\tau. \quad (3.15)$$

We need the following result (see [21]) on the Fourier transform of  $H[t]J_1(t)$ :

$$\mathcal{G}(\omega) := \sqrt{2\pi} \mathcal{F}[H[t]J_1(t)](\omega) = 1 + \frac{i\omega \chi_{\{|\omega| < 1\}}}{\sqrt{1-\omega^2}} - \frac{|\omega| \chi_{\{|\omega| > 1\}}}{\sqrt{\omega^2-1}},$$

where  $\chi_{\mathcal{L}}$  is the characteristic function of the set  $\mathcal{L}$ . Therefore

$$\sqrt{2\pi} \mathcal{F}_t[H[t]J_1(|\xi|t)](\omega) = \frac{1}{|\xi|} \mathcal{G}\left(\frac{\omega}{|\xi|}\right) = \frac{1}{|\xi|} \left[1 + \frac{i\omega \chi_{\{|\omega| < |\xi|\}}}{\sqrt{|\xi|^2 - \omega^2}} - \frac{|\omega| \chi_{\{|\omega| > |\xi|\}}}{\sqrt{\omega^2 - |\xi|^2}}\right].$$

Finally, from (3.15), the desired expression of the Fourier transform of  $(V\varphi)_t$ , when  $\varphi \in C_0^\infty(\Sigma)$  is:

$$\begin{aligned} \mathcal{F}[(V\varphi)_t](\xi, \omega) &= \frac{1}{2} \tilde{\varphi}(\xi, \omega) - \frac{1}{2} \mathcal{G}\left(\frac{\omega}{|\xi|}\right) \tilde{\varphi}(\xi, \omega) \\ &= \frac{1}{2} \frac{|\omega| \chi_{\{|\omega| > |\xi|\}}}{\sqrt{\omega^2 - |\xi|^2}} \tilde{\varphi}(\xi, \omega) - \frac{1}{2} \frac{i\omega \chi_{\{|\omega| < |\xi|\}}}{\sqrt{|\xi|^2 - \omega^2}} \tilde{\varphi}(\xi, \omega). \end{aligned} \quad (3.16)$$

Owing to the Parseval identity, for  $\psi, \varphi \in C_0^\infty(\Sigma)$ , the following representation of the bilinear form is obtained

$$\begin{aligned} a_{\mathcal{E}}(\varphi, \psi) &= \int_{-\infty}^{+\infty} \int_{-\infty}^{+\infty} (V\varphi)_t(x, t) \psi(x, t) dt dx = \\ &= \frac{1}{2} \int_{-\infty}^{+\infty} d\xi \int_{|\omega| > |\xi|} \frac{|\omega|}{\sqrt{\omega^2 - \xi^2}} \tilde{\varphi}(\xi, \omega) \overline{\tilde{\psi}(\xi, \omega)} d\omega \\ &\quad - \frac{i}{2} \int_{-\infty}^{+\infty} d\xi \int_{|\omega| < |\xi|} \frac{\omega}{\sqrt{\xi^2 - \omega^2}} \tilde{\varphi}(\xi, \omega) \overline{\tilde{\psi}(\xi, \omega)} d\omega. \end{aligned} \quad (3.17)$$

Of course, when the support of the function  $\psi$  lies in  $\Sigma$ , the double integral on the left-hand side of (3.17) is restricted to  $\Sigma$ . In particular, for  $\psi = \varphi$ , from the property  $\mathcal{E}(T, \varphi) = \Re(a_{\mathcal{E}}(\varphi, \varphi))$ , or remembering that for real valued functions  $\tilde{\varphi}(\xi, -\omega) = \overline{\tilde{\varphi}(\xi, \omega)}$ , one has

**Proposition 2** *For any  $\varphi \in C_0^\infty(\Sigma)$ , the energy at time  $T$  of the solution  $u$  to the problem (3.6), is given by the following formula*

$$\mathcal{E}(T, \varphi) = a_{\mathcal{E}}(\varphi, \varphi) = \int_{\Sigma} (V\varphi)_t(x, t) \varphi(x, t) dt dx = \frac{1}{2} \int_{-\infty}^{+\infty} d\xi \int_{|\omega| > |\xi|} \frac{|\omega| |\tilde{\varphi}(\xi, \omega)|^2}{\sqrt{\omega^2 - \xi^2}} d\omega. \quad (3.18)$$

Let  $\mathcal{S}(a_{\mathcal{E}}) \subset L^2(\Sigma)$  be the set of functions  $\varphi, \psi$  such that  $|a_{\mathcal{E}}(\varphi, \psi)| < +\infty$ . In order to characterize  $\mathcal{S}(a_{\mathcal{E}})$ , assume for the moment that  $\varphi, \psi$  are complex-valued functions. In this case, also the imaginary part of  $a_{\mathcal{E}}(\varphi, \varphi)$  does not vanish, thus

$$a_{\mathcal{E}}(\varphi, \varphi) = \frac{1}{2} \int_{-\infty}^{+\infty} d\xi \int_{|\omega| > |\xi|} \frac{|\omega| |\tilde{\varphi}(\xi, \omega)|^2}{\sqrt{\xi^2 - \omega^2}} d\omega - \frac{i}{2} \int_{-\infty}^{+\infty} d\xi \int_{|\omega| < |\xi|} \frac{\omega |\tilde{\varphi}(\xi, \omega)|^2}{\sqrt{\omega^2 - \xi^2}} d\omega. \quad (3.19)$$

It follows that

$$\mathcal{S}(a_\varepsilon) = \left\{ \varphi \in L^2(\Sigma) : \int_{\mathbb{R}^2} \frac{|\omega| |\tilde{\varphi}(\xi, \omega)|^2}{\sqrt{|\xi^2 - \omega^2|}} d\omega d\xi < +\infty \right\}.$$

Now we can state the following

**Proposition 3** *The space  $L^2((0, T); H^{1/4}(\Gamma))$ , that is the closure of  $C_0^\infty(\Sigma)$  with respect to the norm*

$$\|\varphi\|_{L^2((0, T); H^{1/4}(\Gamma))}^2 = \int_{-\infty}^{+\infty} \int_{-\infty}^{+\infty} (1 + |\xi|)^{1/2} |\tilde{\varphi}(\xi, \omega)|^2 d\xi d\omega,$$

is contained in  $\mathcal{S}(a_\varepsilon)$ . Moreover there exists a positive constant  $C$  such that, for every  $\varphi, \psi \in L^2((0, T); H^{1/4}(\Gamma))$ ,

$$a_\varepsilon(\varphi, \psi) \leq C(1 + T) \|\varphi\|_{L^2((0, T); H^{1/4}(\Gamma))} \|\psi\|_{L^2((0, T); H^{1/4}(\Gamma))}$$

*Proof.* Obviously

$$\int_{\mathbb{R}^2} \frac{|\omega| |\tilde{\varphi}(\xi, \omega)|^2}{\sqrt{|\xi^2 - \omega^2|}} d\omega d\xi = \int_{\{|\omega| > |\xi|\}} \frac{|\omega| |\tilde{\varphi}(\xi, \omega)|^2}{\sqrt{\omega^2 - \xi^2}} d\omega d\xi + \int_{\{|\omega| < |\xi|\}} \frac{|\omega| |\tilde{\varphi}(\xi, \omega)|^2}{\sqrt{\xi^2 - \omega^2}} d\omega d\xi. \quad (3.20)$$

Estimating the first addendum, one has

$$\begin{aligned} & \int_{-\infty}^{+\infty} d\xi \int_{|\omega| > |\xi|} \frac{|\omega| |\tilde{\varphi}(\xi, \omega)|^2}{\sqrt{\omega^2 - \xi^2}} d\omega = \\ & \int_{-\infty}^{+\infty} d\xi \int_{|\xi| < |\omega| < |\xi| + 1} \frac{|\omega| |\tilde{\varphi}(\xi, \omega)|^2}{\sqrt{\omega^2 - \xi^2}} d\omega + \int_{-\infty}^{+\infty} d\xi \int_{|\omega| > |\xi| + 1} \frac{|\omega| |\tilde{\varphi}(\xi, \omega)|^2}{\sqrt{\omega^2 - \xi^2}} d\omega =: I_1^a + I_2^a. \end{aligned}$$

From the definition of  $\tilde{\varphi}$  and thanks to Cauchy-Schwarz inequality, one get

$$|\tilde{\varphi}(\xi, \omega)|^2 \leq \frac{T}{2\pi} \int_0^T |\hat{\varphi}(\xi, t)|^2 dt.$$

Therefore, by a simple integration and thanks to the Parseval identity, one has

$$\begin{aligned} I_1^a & \leq \frac{T}{2\pi} \int_{-\infty}^{+\infty} \left( \int_0^T |\hat{\varphi}(\xi, t)|^2 dt \right) d\xi \int_{|\xi| < |\omega| < |\xi| + 1} \frac{|\omega|}{\sqrt{\omega^2 - \xi^2}} d\omega \\ & = \frac{T}{\pi} \int_{-\infty}^{+\infty} \left( \int_0^T |\hat{\varphi}(\xi, t)|^2 dt \right) \sqrt{2|\xi| + 1} d\xi \leq \frac{\sqrt{2}T}{\pi} \|\varphi\|_{L^2((0, T); H^{1/4}(\Gamma))}^2. \end{aligned}$$

On the other hand, from the inequality

$$\frac{|\omega|}{\sqrt{\omega^2 - \xi^2}} \leq \sqrt{|\xi| + 1} \quad (|\omega| > |\xi| + 1),$$

one has the estimate

$$I_2^a \leq \int_{-\infty}^{+\infty} \int_{|\omega| > |\xi| + 1} \sqrt{|\xi| + 1} |\tilde{\varphi}(\xi, \omega)|^2 d\omega d\xi \leq \|\varphi\|_{L^2((0,T); H^{1/4}(\Gamma))}^2.$$

The estimate for the second term in (3.20) is quite similar. Also in this case the integral can be splitted as follows:

$$\begin{aligned} & \int_{\{|\xi| > |\omega|\}} \frac{|\omega| |\tilde{\varphi}(\xi, \omega)|^2}{\sqrt{\xi^2 - \omega^2}} d\xi d\omega = \\ & \int_{|\xi| > 1} d\xi \int_{|\omega| < |\xi| - 1} \frac{|\omega| |\tilde{\varphi}(\xi, \omega)|^2}{\sqrt{\xi^2 - \omega^2}} d\xi d\omega + \int_{-\infty}^{+\infty} \int_{|\xi| - 1 < |\omega| < |\xi|} \frac{|\omega| |\tilde{\varphi}(\xi, \omega)|^2}{\sqrt{\xi^2 - \omega^2}} d\xi d\omega =: I_1^b + I_2^b. \end{aligned}$$

By an argument similar to the previous one, one get

$$I_1^b \leq \int_{|\xi| > 1} d\xi \int_{|\omega| < |\xi| - 1} \frac{(|\xi| - 1) |\tilde{\varphi}(\xi, \omega)|^2}{\sqrt{2|\xi| - 1}} d\omega \leq \|\varphi\|_{L^2((0,T); H^{1/4}(\Gamma))}^2.$$

On the other hand

$$\begin{aligned} I_2^b & \leq \frac{T}{2\pi} \int_{-\infty}^{+\infty} \left( \int_0^T |\hat{\varphi}(\xi, t)|^2 dt \right) d\xi \int_{|\xi| - 1 < |\omega| < |\xi|} \frac{|\omega|}{\sqrt{\xi^2 - \omega^2}} d\omega = \\ & = \frac{T}{\pi} \int_{-\infty}^{+\infty} \mu(|\xi|) \left( \int_0^T |\hat{\varphi}(\xi, t)|^2 dt \right) d\xi, \end{aligned}$$

where  $\mu(|\xi|) = |\xi|$  for  $|\xi| < 1$  and  $\mu(|\xi|) = \sqrt{2|\xi| + 1}$  for  $|\xi| > 1$ . Thus

$$I_1^b \leq \frac{\sqrt{2}T}{\pi} \|\varphi\|_{L^2((0,T); H^{1/4}(\Gamma))}^2.$$

Now I will try to answer to the question of the coerciveness of the energy functional. Two simple considerations can be drawn by the fact that the domain of integration in formula (3.18) is the cone  $\mathcal{C} := \{(\xi, \omega) : |\omega| > |\xi|\}$ . The first one is that the energy is a strictly positive functional. This follows immediately from the fact that  $\tilde{\varphi}$  is an entire analytic function, therefore it cannot vanish in  $\mathcal{C}$  unless it vanishes on the whole  $\mathbb{R}^2$ . The second and more relevant consideration is that most of the



information regarding oscillations in the space variable is not taken into account by the energy. This crucial remark is made more precise by the following theorem which states that the quadratic form  $a_{\mathcal{E}}(\varphi, \varphi)$  cannot be coercive with respect to any Sobolev norm.

**Theorem 22** *There exists a sequence  $(\varphi_n)_{n \in \mathbb{N}}$  of non vanishing functions in  $C_0^\infty(\Sigma)$ , such that, for any  $s \in \mathbb{R}$*

$$\lim_{n \rightarrow \infty} \frac{a_{\mathcal{E}}(\varphi_n, \varphi_n)}{\|\varphi_n\|_s^2} = 0, \quad (3.21)$$

where  $\|\cdot\|_s^2$  stands for the norm in  $H^s(\mathbb{R}^2)$ .

*Proof.* It suffices to show (3.21) for negative Sobolev exponents. The definition of the sequence  $(\varphi_n)_{n \in \mathbb{N}}$  is very simple: let  $\varphi \in C_0^\infty(\Sigma)$  be a non vanishing function. We set

$$\varphi_n(x, t) = \cos(nx)\varphi(x, t). \quad (3.22)$$

It will be shown that

- (i)  $\forall k \in \mathbb{N}^+ \quad a_{\mathcal{E}}(\varphi_n, \varphi_n) = O\left(\frac{1}{n^{2k}}\right)$  for  $n \rightarrow +\infty$ ,
- (ii)  $\forall s \geq 0 \exists c > 0$  such that  $\|\varphi_n\|_{-s}^2 \geq \frac{c}{n^{2s}}$ .

It is clear that (i) and (ii) yield (3.21). From the definition of  $\varphi_n$ , one has

$$\tilde{\varphi}_n(\xi, \omega) = \frac{1}{2}\tilde{\varphi}(\xi - n, \omega) + \frac{1}{2}\tilde{\varphi}(\xi + n, \omega),$$

then

$$|\tilde{\varphi}_n(\xi, \omega)|^2 \leq \frac{1}{2}|\tilde{\varphi}(\xi - n, \omega)|^2 + \frac{1}{2}|\tilde{\varphi}(\xi + n, \omega)|^2.$$

From (3.18), it follows that

$$\begin{aligned} a_{\mathcal{E}}(\varphi_n, \varphi_n) &= \frac{1}{2} \int_{-\infty}^{+\infty} d\xi \int_{|\omega| > |\xi|} \frac{|\omega| |\tilde{\varphi}_n(\xi, \omega)|^2}{\sqrt{\omega^2 - \xi^2}} d\omega \\ &\leq \frac{1}{4} \int_{-\infty}^{+\infty} d\xi \int_{|\omega| > |\xi|} \frac{|\omega| |\tilde{\varphi}(\xi - n, \omega)|^2}{\sqrt{\omega^2 - \xi^2}} d\omega + \frac{1}{4} \int_{-\infty}^{+\infty} d\xi \int_{|\omega| > |\xi|} \frac{|\omega| |\tilde{\varphi}(\xi + n, \omega)|^2}{\sqrt{\omega^2 - \xi^2}} d\omega. \end{aligned}$$

Estimate the second term in (3.23), the estimate of the first one being very similar. By a simple change of variable, one get

$$\int_{-\infty}^{+\infty} d\xi \int_{|\omega| > |\xi|} \frac{|\omega| |\tilde{\varphi}(\xi + n, \omega)|^2}{\sqrt{\omega^2 - \xi^2}} d\omega = \int_{-\infty}^{+\infty} d\xi \int_{|\omega| > |\xi - n|} \frac{|\omega| |\tilde{\varphi}(\xi, \omega)|^2}{\sqrt{\omega^2 - (\xi - n)^2}} d\omega. \quad (3.23)$$

Since  $\varphi \in \mathcal{C}_0^\infty(\mathbb{R}^2)$ , its Fourier transform  $\tilde{\varphi}$  is rapidly decreasing. Therefore for every  $k \in \mathbb{N}^+$  there exists  $C_k > 0$  such that

$$|\tilde{\varphi}(\xi, \omega)|^2 \leq \frac{C_k}{(1 + \omega^2 + \xi^2)^{k+2}}.$$

Note that if  $(\xi, \omega) \in \mathcal{C}_n := \{(\xi, \omega) : |\omega| > |\xi - n|\}$  then  $\omega^2 + \xi^2 \geq \frac{n^2}{2}$ ; it follows that for every  $k \in \mathbb{N}^+$  there exists  $C_k > 0$  such that

$$|\tilde{\varphi}(\xi, \omega)|^2 \leq \frac{C_k}{n^{2k} [1 + \omega^2 + \xi^2]^2} \quad \forall (\xi, \omega) \in \mathcal{C}_n.$$

From this last inequality and owing to (3.23), one has

$$\int_{\mathcal{C}_n} \frac{|\omega| |\tilde{\varphi}(\xi, \omega)|^2}{\sqrt{\omega^2 - (\xi - n)^2}} d\omega d\xi \leq \frac{C_k}{n^{2k}} \int_{\mathcal{C}_n} \frac{|\omega|}{\sqrt{\omega^2 - (\xi - n)^2}} \frac{1}{[1 + \omega^2 + \xi^2]^2} d\omega d\xi. \quad (3.24)$$

This concludes the proof of (i) since, as it is not difficult to show, the last integral in (3.24) is finite.

Turn to the property (ii). Having set  $B = \{\omega^2 + \xi^2 \leq 1\}$ , by a simple change of variable, one obtains

$$\begin{aligned} \|\varphi_n\|_{-s}^2 &= \int_{-\infty}^{\infty} \int_{-\infty}^{\infty} \frac{|\tilde{\varphi}_n(\xi, \omega)|^2}{[1 + \omega^2 + \xi^2]^s} d\omega d\xi = \frac{1}{4} \int_{-\infty}^{\infty} \int_{-\infty}^{\infty} \frac{|\tilde{\varphi}(\xi - n, \omega) + \tilde{\varphi}(\xi + n, \omega)|^2}{[1 + \omega^2 + \xi^2]^s} d\omega d\xi \\ &\geq \frac{1}{4} \int_{\{\omega^2 + (\xi - n)^2 \leq 1\}} \frac{|\tilde{\varphi}(\xi - n, \omega) + \tilde{\varphi}(\xi + n, \omega)|^2}{[1 + \omega^2 + \xi^2]^s} d\omega d\xi \\ &= \frac{1}{4} \int_B \frac{|\tilde{\varphi}(\xi, \omega) + \tilde{\varphi}(\xi + 2n, \omega)|^2}{[1 + \omega^2 + (\xi + n)^2]^s} d\omega d\xi \\ &\geq \frac{1}{4(n-1)^{2s}} \int_B |\tilde{\varphi}(\xi, \omega) + \tilde{\varphi}(\xi + 2n, \omega)|^2 d\omega d\xi. \end{aligned} \quad (3.25)$$

Remark that

$$\begin{aligned} |\tilde{\varphi}(\xi, \omega) + \tilde{\varphi}(\xi + 2n, \omega)|^2 &= |\tilde{\varphi}(\xi, \omega)|^2 + |\tilde{\varphi}(\xi + 2n, \omega)|^2 + 2\Re[\tilde{\varphi}(\xi, \omega)\overline{\tilde{\varphi}(\xi + 2n, \omega)}] \\ &\geq |\tilde{\varphi}(\xi, \omega)|^2 - 2|\tilde{\varphi}(\xi, \omega)||\tilde{\varphi}(\xi + 2n, \omega)| \\ &\geq \frac{1}{2}|\tilde{\varphi}(\xi, \omega)|^2 - 2|\tilde{\varphi}(\xi + 2n, \omega)|. \end{aligned}$$

Since for every  $h > 0$  there exists  $C_h > 0$  such that

$$|\tilde{\varphi}(\xi + 2n, \omega)| \leq \frac{C_h}{[1 + (\xi + 2n)^2]^h} \leq \frac{C_h}{n^{2h}} \quad (|\xi| \leq 1),$$

it follows that

$$\int_B |\tilde{\varphi}_n(\xi + 2n, \omega)|^2 d\omega d\xi \rightarrow 0 \quad \text{for } n \rightarrow +\infty.$$

Thus, for  $n$  sufficiently large,

$$\int_B |\tilde{\varphi}(\xi, \omega) + \tilde{\varphi}(\xi + 2n, \omega)|^2 d\omega d\xi \geq \frac{1}{4} \int_B |\tilde{\varphi}(\xi, \omega)|^2 d\omega d\xi. \quad (3.26)$$

Owing to (3.25) and (3.26), one can conclude that there exists  $C > 0$  such that

$$\|\varphi_n\|_{-s}^2 \geq \frac{C}{n^{2s}},$$

which proves **(ii)**.

The main consequence of theorem 22 is that in order to obtain satisfactory *a priori* bounds on the energetic Galerkin approximated solutions of problem (3.3), the information coming from the quadratic form  $a_{\mathcal{E}}(\varphi, \varphi)$  has to be complemented with some other arising from alternative arguments. In this respect, I present two possible strategies:

- 1) to obtain a constraint on the oscillations in the space variable of the approximating solutions. In fact, as shown below, under a suitable constraint, the energetic bilinear form is coercive with respect to the  $L^2(\Sigma)$  norm.
- 2) to fill the gap in the frequency space in formula (3.18), considering the energetic bilinear form modified by an additional term which takes into account also the skew-symmetric part of the operator  $\varphi \mapsto (V\varphi)_t$ . I shall briefly discuss this point at the end of this subsection.

In order to investigate the first point, fix  $P > 0$  and consider the following maximum problem:

$$\lambda_0 = \max \left\{ \int_{-P}^P |\hat{f}(\omega)|^2 d\omega : f \in L^2(0, T), \int_0^T |f(t)|^2 dt = 1 \right\}.$$

It is not difficult to see that  $\lambda_0 = \lambda_0(PT) < 1$ ,  $\lambda_0(\rho)$  is an increasing function and that  $\lim_{\rho \rightarrow 0^+} \lambda_0(\rho) = 0$ ,  $\lim_{\rho \rightarrow +\infty} \lambda_0(\rho) = 1$ . The number  $\lambda_0(PT)$  is the first eigenvalue of the so called time-band limited operator which has been deeply studied in the sixties by Slepian, Landau and Pollack (see e.g. [50]). Fix  $\xi$  and set  $P = |\xi|$ ,  $f = \hat{\varphi}(\xi, \cdot)$ . One gets

$$\begin{aligned} \int_{|\omega| > |\xi|} |\tilde{\varphi}(\xi, \omega)|^2 d\omega &= \int_{-\infty}^{\infty} |\tilde{\varphi}(\xi, \omega)|^2 d\omega - \int_{-\xi}^{|\xi|} |\tilde{\varphi}(\xi, \omega)|^2 d\omega \\ &\geq (1 - \lambda_0(|\xi|T)) \int_{-\infty}^{\infty} |\tilde{\varphi}(\xi, \omega)|^2 d\omega. \end{aligned} \quad (3.27)$$

Since  $|\omega| > \sqrt{\omega^2 - \xi^2}$  for  $|\omega| > |\xi|$ , one obviously has from (3.18),

$$a_{\mathcal{E}}(\varphi, \varphi) \geq \frac{1}{2} \int_{-\infty}^{+\infty} d\xi \int_{|\omega| > |\xi|} |\tilde{\varphi}(\xi, \omega)|^2 d\omega, \quad (3.28)$$

thus, integrating with respect to  $\xi$  in (3.28) and owing to (3.27),

$$a_{\mathcal{E}}(\varphi, \varphi) \geq \frac{1}{2} \int_{-\infty}^{+\infty} d\xi \int_{-\infty}^{+\infty} (1 - \lambda_0(|\xi|T)) |\tilde{\varphi}(\xi, \omega)|^2 d\omega.$$

Unfortunately, when  $\rho \rightarrow +\infty$ , the function  $1 - \lambda_0(\rho)$  tends to zero exponentially. More precisely, Fuchs in [27] has shown that

$$1 - \lambda_0(\rho) \sim 4 \sqrt{\frac{\pi}{2}} \sqrt{\rho} e^{-\rho}, \quad \rho \rightarrow +\infty.$$

Therefore, by the properties of  $\lambda_0(\rho)$ , there exists a constant  $C > 0$  such that

$$1 - \lambda_0(\rho) \geq C \sqrt{1 + \rho} e^{-\rho} \quad (\rho > 0). \quad (3.29)$$

As a consequence, the following very poor coerciveness estimate holds

$$a_{\mathcal{E}}(\varphi, \varphi) \geq C \int_{-\infty}^{+\infty} d\xi \int_{-\infty}^{+\infty} \sqrt{1 + |\xi|T} e^{-|\xi|T} |\tilde{\varphi}(\xi, \omega)|^2 d\omega.$$

Now, what can we say if the frequencies of the function  $\varphi$  are not spread over the whole  $\mathbb{R}^2$  and, for instance,  $\tilde{\varphi}$  has “mass” concentrated on the strip  $|\xi| \leq R$ , for some  $R > 0$ ?

I try to give a quantitative answer to this question in the following way. Fix  $R > 0$  and consider the following closed set in  $L^2(\Sigma)$ :

$$K_R := \left\{ \tilde{\varphi} \in L^2(\Sigma) : \int_{-\infty}^{+\infty} d\xi \int_{|\xi| \leq R} |\tilde{\varphi}(\xi, \omega)|^2 d\omega \geq \frac{1}{2} \int_{-\infty}^{+\infty} d\xi \int_{-\infty}^{+\infty} |\tilde{\varphi}(\xi, \omega)|^2 d\omega \right\}.$$

From (3.27), (3.28), and the above mentioned properties of  $\lambda_0$ , one get

$$\begin{aligned} a_{\mathcal{E}}(\varphi, \varphi) &\geq \int_{-R}^R d\xi \int_{|\omega| > |\xi|} |\tilde{\varphi}(\xi, \omega)|^2 d\omega \geq \int_{-R}^R (1 - \lambda_0(|\xi|T)) d\xi \int_{-\infty}^{+\infty} |\tilde{\varphi}(\xi, \omega)|^2 d\omega \\ &\geq (1 - \lambda_0(RT)) \int_{-R}^R d\xi \int_{-\infty}^{+\infty} |\tilde{\varphi}(\xi, \omega)|^2 d\omega. \end{aligned} \quad (3.30)$$

Thus, owing to (3.29) and Parseval identity, the following theorem has just been proved

**Theorem 23** For every  $\varphi \in K_R \cap \mathcal{S}(a_{\mathcal{E}})$ ,

$$a_{\mathcal{E}}(\varphi, \varphi) \geq \frac{C}{2} \sqrt{1+RT} e^{-RT} \|\varphi\|_{L^2(\Sigma)}^2. \quad (3.31)$$

To summarize: if the approximating solutions  $\varphi_h$  satisfy the constraint  $\varphi_h \in K_R$  for some  $R > 0$ , from the inequality (3.31) one gets a stability estimate in  $L^2(\Sigma)$ .

As an application of this argument, fix an integer  $n \geq 1$ , set  $\Delta x = L/n$  and consider the functions

$$\varphi(x, t) = \sum_{k=0}^{n-1} f_k(t) \psi_k(x)$$

where  $\psi_k(x) = H[(k+1)\Delta x - x] - H[k\Delta x - x]$  and  $f_k(t) \in L^2(0, T)$ ,  $k = 0, \dots, n-1$ . Denote by  $\mathcal{S}_n$  the (infinite dimensional) space of such functions and remark that  $\mathcal{S}_n \subset L^2((0, T), H^{1/4}(\Gamma)) \subset \mathcal{S}(a_{\mathcal{E}})$ .

**Lemma 3.1.**  $\mathcal{S}_n \subset K_R$ , provided  $R \geq \frac{8L}{\pi \Delta x^2}$ .

*Proof.* By computing the Fourier transform of  $\varphi \in \mathcal{S}_n$ ,

$$\tilde{\varphi}(\xi, \omega) = \sqrt{\frac{2}{\pi}} e^{-i\frac{\Delta x \xi}{2}} \frac{\sin\left(\frac{\Delta x \xi}{2}\right)}{\xi} \sum_{k=0}^{n-1} e^{-ik\Delta x \xi} \hat{f}_k(\omega),$$

thus

$$|\tilde{\varphi}(\xi, \omega)|^2 = \frac{2}{\pi} \frac{\sin^2\left(\frac{\Delta x \xi}{2}\right)}{\xi^2} \left| \sum_{k=0}^{n-1} e^{-ik\Delta x \xi} \hat{f}_k(\omega) \right|^2 \leq \frac{2n}{\pi} \frac{\sin^2\left(\frac{\Delta x \xi}{2}\right)}{\xi^2} \sum_{k=0}^{n-1} |\hat{f}_k(\omega)|^2.$$

Since, for  $\varphi \in \mathcal{S}_n$ ,  $\|\varphi\|_{L^2(\Sigma)}^2 = \Delta x \sum_{k=0}^{n-1} \int_0^T |f_k(t)|^2 dt = \Delta x \sum_{k=0}^{n-1} \int_{-\infty}^{+\infty} |\hat{f}_k(\omega)|^2 d\omega$ ,

$$\int_{-\infty}^{+\infty} d\xi \int_{|\xi|>R} |\tilde{\varphi}(\xi, \omega)|^2 d\omega \leq \frac{2n}{\pi \Delta x} \left( \int_{|\xi|>R} \frac{\sin^2\left(\frac{\Delta x \xi}{2}\right)}{\xi^2} d\xi \right) \|\varphi\|_{L^2(\Sigma)}^2.$$

The conclusion follows by the elementary inequality

$$\int_{|\xi|>R} \frac{\sin^2\left(\frac{\Delta x \xi}{2}\right)}{\xi^2} d\xi \leq \frac{2}{R}.$$

Putting together the estimate (3.31) and Lemma 3.1 it follows that

**Proposition 4** Every  $\varphi \in \mathcal{S}_n$  satisfies inequality (3.31) with  $R = \frac{8L}{\pi \Delta x^2}$ .

The theoretical value of the coerciveness constant in (3.31) is very small but it should be probably improved by a subtler analysis.

Finally, I sketch a few considerations on the second strategy (point 2) above). In general terms, there is the following situation: let  $A$  be a linear operator (bounded or not) on a Hilbert space; consider the equation

$$A\varphi = A_s\varphi + A_{ss}\varphi = g, \quad (3.32)$$

where  $A_s$  and  $A_{ss}$  stand for the symmetric and the skew-symmetric part of  $A$ . Multiply by  $\varphi$  in (3.32), then

$$a(\varphi, \varphi) = \langle A\varphi, \varphi \rangle = \langle A_s\varphi, \varphi \rangle + \langle A_{ss}\varphi, \varphi \rangle = \langle g, \varphi \rangle.$$

Now, if the quadratic form  $a(\varphi, \varphi)$  enjoys some reasonable coerciveness property, one applies the usual arguments to prove the convergence of the Galerkin approximants, and eventually is allowed to neglect the skew-symmetric component of the operator. Unfortunately, this is not the case for the BIE treated in this paper. Thus we need an idea on how to resume information from the skew-symmetric part of the operator.

A possibility could be that of choosing a suitable unitary operator  $J$  and considering an auxiliary bilinear form  $\bar{a}(\varphi, \psi) = \langle A\varphi, J\psi \rangle$ , in order to modify the weak formulation of the problem introducing  $b(\varphi, \psi) = a(\varphi, \psi) + \bar{a}(\varphi, \psi)$ . In our case, a natural choice is provided by the Hilbert transform  $\mathcal{H}$  with respect to the time variable. For our purposes, it is convenient to define the Hilbert transform as a Fourier multiplier:

$$\mathcal{H} : L^2(\mathbb{R}^2) \longrightarrow L^2(\mathbb{R}^2), \quad \mathcal{F}[\mathcal{H}](\xi, \omega) := i \operatorname{sign}(\omega) \tilde{\varphi}(\xi, \omega).$$

As it is well-known, one has

$$\mathcal{H}^{-1} = \mathcal{H}^* = -\mathcal{H}; \quad \|\mathcal{H}\varphi\|_{H^s(\mathbb{R}^2)} = \|\varphi\|_{H^s(\mathbb{R}^2)}, \quad \text{with } s \in \mathbb{R}. \quad (3.33)$$

Moreover, as a consequence of formula (3.17), one has, for  $\varphi \in C_0^\infty(\mathbb{R}^2)$ ,

$$\bar{a}(\varphi, \varphi) = \int_0^{+\infty} \int_0^L (V\varphi)_t(x, t) (\mathcal{H}\varphi)(x, t) dx dt = -\frac{1}{2} \int_{-\infty}^{+\infty} d\xi \int_{|\omega| < |\xi|} \frac{|\omega| |\tilde{\varphi}(\xi, \omega)|^2}{\sqrt{\xi^2 - \omega^2}} d\omega. \quad (3.34)$$

From (3.17) and (3.19) we can conclude that, in our case, the modified quadratic form would read

$$\begin{aligned}
b(\varphi, \varphi) &:= \int_0^{+\infty} \int_0^L (V\varphi)_t(x, t) (\varphi(x, t) - (\mathcal{H}\varphi)(x, t)) \, dx dt \\
&= \frac{1}{2} \int_{-\infty}^{+\infty} d\xi \int_{-\infty}^{+\infty} \frac{|\omega| |\tilde{\varphi}(\xi, \omega)|^2}{\sqrt{|\xi^2 - \omega^2|}} \, d\omega.
\end{aligned} \tag{3.35}$$

Regarding the coerciveness of the quadratic form  $b(\varphi, \varphi)$ , it holds, for instance

$$2b(\varphi, \varphi) \geq \int_{-\infty}^{+\infty} \int_{-\infty}^{+\infty} v(|\omega|, |\xi|) |\tilde{\varphi}(\xi, \omega)|^2 \, d\xi d\omega, \quad v(|\omega|, |\xi|) := \frac{|\omega| \wedge |\xi|}{|\xi|}.$$

Starting from here, the coerciveness with respect to  $L^2((0, T); H^{-1/2}(\Gamma))$  norm can be obtained. In fact, for every  $0 < r \leq 1$ , evidently one has  $v(|\omega|, |\xi|) > r/(|\xi| + 1)$  for  $|\omega| > r$ ; hence

$$2b(\varphi, \varphi) \geq r \int_{-\infty}^{+\infty} \int_{|\omega| > r} \frac{|\tilde{\varphi}(\xi, \omega)|^2}{|\xi| + 1} \, d\xi d\omega. \tag{3.36}$$

On the other side, remembering inequalities on band limited functions, one has, for every  $\xi \in \mathbb{R}$ ,

$$\int_{|\omega| > r} |\tilde{\varphi}(\xi, \omega)|^2 \, d\omega \geq (1 - \lambda_0(rT)) \int_{-\infty}^{+\infty} |\tilde{\varphi}(\xi, \omega)|^2 \, d\omega;$$

in particular choosing  $r = 1 \wedge (1/T)$ , and applying (3.36),

$$2b(\varphi, \varphi) \geq [1 \wedge (1/T)] (1 - \lambda_0(1)) \int_{-\infty}^{+\infty} \int_{-\infty}^{+\infty} \frac{|\tilde{\varphi}(\xi, \omega)|^2}{|\xi| + 1} \, d\xi d\omega.$$

Hence, to conclude it follows that

**Theorem 24** *There exists a positive constant  $C$  such that, for every  $\varphi \in C_0^\infty(\Sigma)$*

$$b(\varphi, \varphi) \geq \frac{C}{1+T} \|\varphi\|_{L^2((0, T); H^{-1/2}(\Gamma))}^2. \tag{3.37}$$

Note that, unless  $\varphi \equiv 0$ , it is impossible to have both  $\varphi$  and  $\mathcal{H}\varphi$  supported on the finite time interval  $[0, T]$ . However, thanks to (3.33), one can define, denoting by  $\mathcal{I}$  the identity operator, the new bilinear form:

$$b(\varphi, \psi) = \langle (\mathcal{I} + \mathcal{H})(V\varphi)_t, \psi \rangle_{L^2(\mathbb{R}^2)},$$

from which, one can derive, for test functions supported in  $\Sigma$ , the modified energetic weak formulation of the problem (3.3)

$$\langle (\mathcal{I} + \mathcal{H})(V\varphi)_t, \Psi \rangle_{L^2(\Sigma)} = \langle (\mathcal{I} + \mathcal{H})g_{\mathcal{D}t}, \Psi \rangle_{L^2(\Sigma)} .$$

The hope is that, starting from these suggestions, one can achieve a relevant progress towards a complete theory for the convergence of the energetic Galerkin BEM applied to the BIE (3.3).

**Remark.** In the past years and in different contexts, several authors [29, 36, 43] have dealt with the properties of the Neumann pseudo-differential operator

$$V : \left[ \frac{\partial u}{\partial n} \right] \mapsto u, \quad (x, t) \in \Gamma \times (0, +\infty), \quad (3.38)$$

related to the wave equation in the case of a flat boundary  $\Gamma$ . Due to an obvious division problem in the symbol of the operator, any analysis has been done by recurring to a Fourier-Laplace transform with non vanishing imaginary part  $\sigma$  in the phase variable  $\tau + i\sigma$ . In particular in reference [29], devoted to the transient BIE for the acoustic equation, Ha Duong performs a detailed analysis of the symbol and obtains, under the restriction  $\sigma \geq \sigma_0 > 0$ , optimal results in terms of regularity and stability of the associated bilinear form. As shown in the same paper, this turns out to be equivalent to a coerciveness property of the functional

$$\int_0^T \mathcal{E}(s, u) ds.$$

On the other side, it should be noted that, as far as we know, in any numerical implementation of energy related Galerkin methods for the transient wave equation, the parameter  $\sigma$  has always been set equal to 0.

So, at now, we can refer to [29, 30] for the analysis of the operator (3.38) and to [3] for the just reported properties of the associated quadratic form  $\mathcal{E}(T, u)$  (the energy at a fixed time  $T$ ) in the Dirichlet case; note that the main difference between this work and the cited Ha Duong papers is that here  $\sigma = 0$  and that, even in this case, it is possible to obtain some stability results, as stated in theorems 23 and 24.

### 3.1.1 Numerical results

The following numerical results are obtained applying the standard Galerkin BEM discretization with time step  $\Delta t$  and space step  $\Delta x$  to the energetic weak formulation as it will be explained in chapter 4.

- As first two dimensional test problems consider (3.1) with  $\Gamma = \{(x, 0), x \in [0, 1]\}$  and Dirichlet boundary datum



$$g_{\mathcal{D}}(x,t) = H[t - kx]f(t - kx), \quad \text{where} \quad f(z) = \begin{cases} \sin^2\left(\frac{\omega z}{2}\right) & \text{if } 0 \leq z \leq \frac{\pi}{\omega} \\ 1 & \text{if } z \geq \frac{\pi}{\omega} \end{cases} \quad (3.39)$$

with  $\omega = 8\pi$ ,  $k = \cos \theta$  and  $\theta \in (0, \pi)$ . For this problem the decomposition of  $\Gamma$  is uniform and constituted by 40 nodes ( $\Delta x = 0.025$ ) and a subdivision of the time interval  $[0, 2]$  operated by 160 instants ( $\Delta t = 0.0125$ ). In figure 3.1 there is the numerical solution of BIE (3.3), that in the sequel will be indicated with  $\varphi(x, t)$ , obtained in some points of  $\Gamma$  for different values of the angle  $\theta$  and considering spatial constant shape and test functions. When  $\theta = \pi/2$ , the excitation field is uniform on  $\Gamma$  at initial time, hence symmetric points of  $\Gamma$  behave in the same way; further, note that points  $x = 1/4$ ,  $x = 3/4$  and  $x = 1/2$  are excited till the time instant  $\pi/\omega = 1/8$ , but while the first two are influenced at  $t = 1/4$  by the wave coming from the endpoints of  $\Gamma$  and travelling with unitary velocity, the midpoint of  $\Gamma$  is influenced at  $t = 1/2$ . When  $\theta = \pi/4$ , the excitation field is not uniform on  $\Gamma$  at initial time; hence, differently from the previous case, symmetric points of  $\Gamma$  do not behave in the same way at the beginning of the simulation.

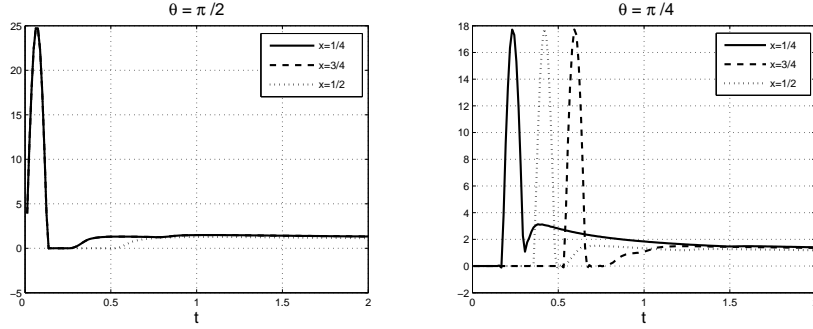


Fig. 3.1: Density  $\varphi(x, t)$  in some points of  $\Gamma$  for different values of  $\theta$  approximated, in space and in time, by constant shape functions.

- Now, on the same domain of the previous test problem, the Dirichlet datum applied is the one shown in figure 3.2, and the observation time interval is  $[0, 10]$ . The uniform temporal and spatial discretization steps are  $\Delta t = 0.1$  and  $\Delta x = 0.0125$  respectively and I adopted spatial constant shape and test functions. In figure 3.3 it is shown the time history of the density  $\varphi$  obtained in the point  $x = \frac{1}{2}$ . As one can note, it has the same form of the derivative of the boundary datum and hence it vanishes for long times. In figure 3.4 there is represented a section of the solution  $u(x, y, t)$  of the problem (3.1), in the same point  $x = \frac{1}{2}$ , for  $t \in [0, 10]$ : as one can observe, the wave travelling away from the boundary  $\Gamma$  assumes the same structure of the Dirichlet boundary datum but with diminishing intensity. Figure 3.5 shows the time dependent behavior of the solution  $u(\mathbf{x}, t)$  outside  $\Gamma$ .

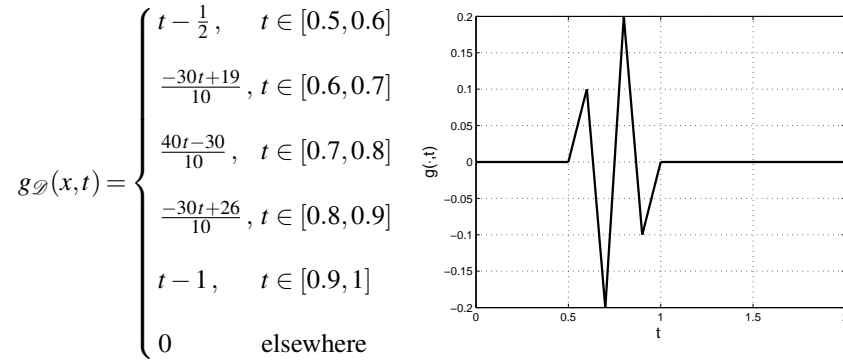


Fig. 3.2: Dirichlet boundary condition.

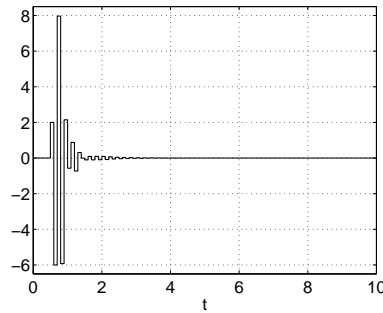


Fig. 3.3: Density  $\varphi(\frac{1}{2}, t)$  obtained for  $\Delta t = 0.1$  and  $\Delta x = 0.0125$  approximated, in space and in time, by constant shape functions.

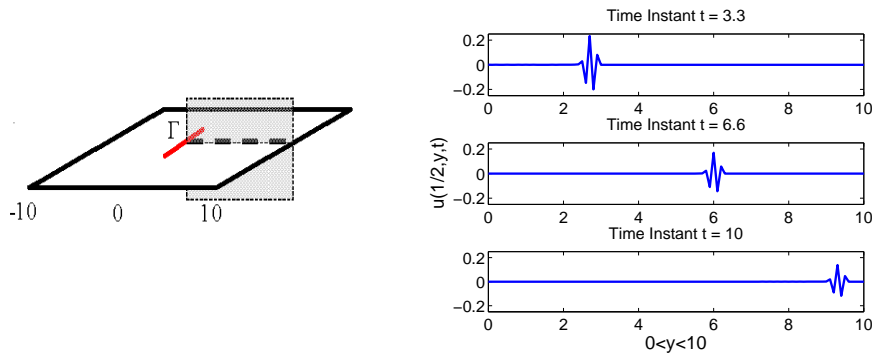


Fig. 3.4: Section of the solution  $u(x, y, t)$  in  $x = \frac{1}{2}$  in some time instants.

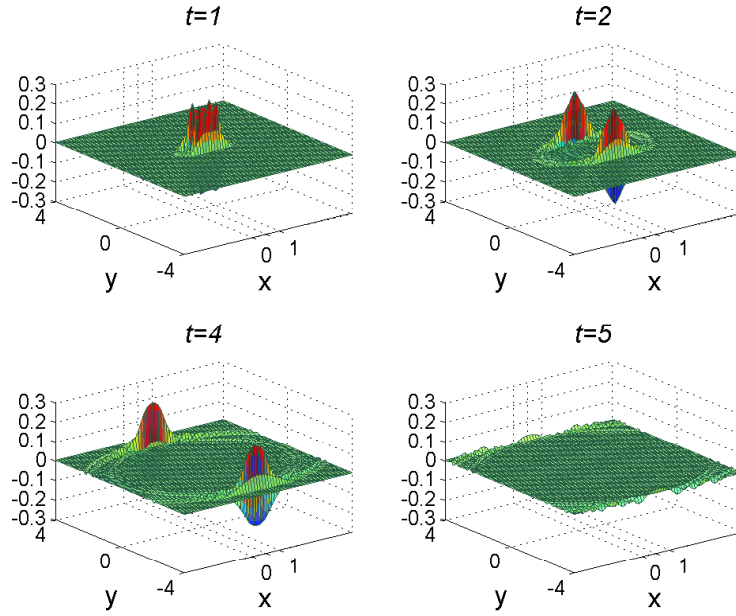


Fig. 3.5: Solution  $u(\mathbf{x}, t)$  outside  $\Gamma$  in some time instants.

- Further, let us consider problem (3.1) assigned on the semi-circular arc

$$\Gamma = \{ \mathbf{x} \in \mathbb{R}^2 : \mathbf{x} = (\cos \alpha, \sin \alpha), \alpha \in [0, \pi] \},$$

depending on the clockwise angle  $\alpha$ , and with Dirichlet boundary datum

$$g_{\mathcal{D}}(\alpha, t) = H[t] f(t) \cos \alpha,$$

where  $f$  has been already given in (3.39) with  $\omega = 8\pi$ . The observation time interval is  $[0, 10]$ . The uniform temporal discretization step is  $\Delta t = 0.1$  and  $\Gamma$  is uniformly approximated by 40 straight boundary elements where constant shape and test functions have been adopted. In figure 3.6, there is the approximate solution  $\varphi(\alpha, 10)$  at the final instant of analysis. Since the Dirichlet datum becomes independent of time, the transient solution on  $\Gamma$  tends to the stationary one  $\varphi_{\infty}(\alpha)$ , which is the solution of the BIE related to the following problem:

$$\begin{cases} -\Delta u_{\infty} = 0 & \text{in } \mathbb{R}^2 \setminus \Gamma, & u(\mathbf{x}) = O(1) & \text{for } \|\mathbf{x}\|_2 \rightarrow \infty \\ u_{\infty} = \cos \alpha & \text{on } \Gamma \end{cases}. \quad (3.40)$$

Also  $\varphi_\infty(\alpha)$  has been reported in figure 3.6 and, as one can observe, the two curves overlap. In figure 3.7 the graph of  $\|\varphi(\cdot, t) - \varphi_\infty(\cdot)\|_{L^1(\Gamma)}$ , which is a function of time, emphasizes this phenomenon.

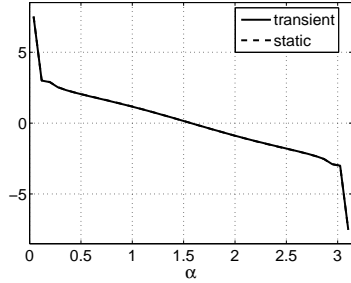


Fig. 3.6: Densities  $\varphi(\alpha, 10)$ , obtained on  $\Gamma$  at final time  $T = 10$ , and  $\varphi_\infty(\alpha)$ .

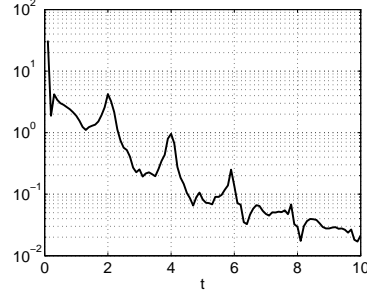


Fig. 3.7: Graph of the time function  $\|\varphi(\cdot, t) - \varphi_\infty(\cdot)\|_{L^1(\Gamma)}$ .

**Remark.** In figure 3.8, we show the typical behavior of the minimum eigenvalue of the symmetric part of matrices  $\mathbb{E}$ , which is related to the coercivity constant of the energetic bilinear form, for fixed  $\Delta x$  and vanishing  $\Delta t$ ; the graphs are presented for Dirichlet problems outside rectilinear obstacles of length  $L = 0.2$ ,  $L = 0.4$  respectively, having fixed  $\Delta x = 0.1$  for the spatial discretization and space-time piece-wise constant shape and test functions; in these cases, the final observation time is  $T = 1$ . The obtained curves are in agreement with theoretical result stated in Proposition 4.

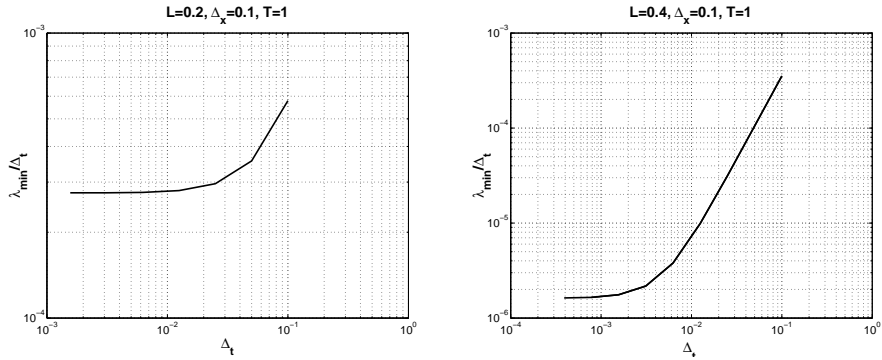


Fig. 3.8: Typical behavior of the minimum eigenvalue of  $\mathbb{E}$  symmetric part.

### 3.2 Exterior Neumann problem

Consider the scattering problem by a crack  $\Gamma$  represented through an open arc in an unbounded elastic isotropic medium that occupies  $\mathbb{R}^2 \setminus \Gamma$ . Let  $\Gamma^-$  and  $\Gamma^+$  denote the lower and upper faces of the crack and  $\mathbf{n}$  the normal unit vector to  $\Gamma$ , oriented from  $\Gamma^-$  to  $\Gamma^+$ . As usual, the total displacement field can be represented as the sum of the incident field (the wave propagating without the crack) and the scattered field. In a three-dimensional elastic isotropic medium, there are three plane waves propagating in a fixed direction: the P wave, the SH wave and the SV wave. The two-dimensional antiplane problem corresponds to an incident SH wave, when all quantities are independent of the third component  $z$  (in particular, the crack must be invariant with respect to  $z$ ).

The scattered wave satisfies the following Neumann problem for the wave operator (without loss of generality consider a dimensionless problem which can be obtained after an appropriate scaling of the units):

$$(P_{\mathcal{N}}^e) \begin{cases} u_{tt}(\mathbf{x}, t) - \Delta u(\mathbf{x}, t) = 0 & \mathbf{x} \in \mathbb{R}^2 \setminus \Gamma, \quad t \in (0, T) \\ u(\mathbf{x}, 0) = u_t(\mathbf{x}, 0) = 0 & \mathbf{x} \in \mathbb{R}^2 \setminus \Gamma \\ \frac{\partial u}{\partial \mathbf{n}}(\mathbf{x}, t) = g_{\mathcal{N}}(\mathbf{x}, t) & (\mathbf{x}, t) \in \Sigma = \Gamma \times [0, T] \end{cases} \quad (3.41)$$

In (3.41) the unknown function  $u$  stands for the third component of the displacement field and  $g_{\mathcal{N}}$  is the datum, which is the opposite of the normal derivative of the incident wave along  $\Gamma$ , i.e.  $g_{\mathcal{N}} = -\frac{\partial u^i}{\partial \mathbf{n}}$ .

Consider the double-layer representation of the solution of (3.41):

$$u(\mathbf{x}, t) = \int_{\Gamma} \int_0^t \frac{\partial}{\partial \mathbf{n}_{\xi}} G(r, t - \tau) \phi(\xi, \tau) d\tau d\xi_{\Gamma} = \mathcal{H}\phi(\mathbf{x}, t), \quad \mathbf{x} \in \mathbb{R}^2 \setminus \Gamma, \quad t \in (0, T) \quad (3.42)$$

where  $G$  is given in (1.3) and  $\phi = [u]$  is the jump of  $u$  along  $\Gamma$ . After having derived the hypersingular space-time BIE (N2d) already introduced in page 6

$$g_{\mathcal{N}}(\mathbf{x}, t) = \int_{\Gamma} \int_0^t \frac{\partial^2}{\partial \mathbf{n}_{\mathbf{x}} \partial \mathbf{n}_{\xi}} G(r, t - \tau) \phi(\xi, \tau) d\tau d\xi_{\Gamma} = D\phi(\mathbf{x}, t), \quad \mathbf{x} \in \Gamma, \quad t \in (0, T) \quad (3.43)$$

the energetic weak problem related to (3.43) will be of the form:

$$\tilde{a}_{\mathcal{E}}(\phi, \eta) = \langle g_{\mathcal{N}}, \eta_t \rangle_{L^2(\Sigma)}$$

where

$$\tilde{a}_{\mathcal{E}}(\phi, \eta) := \langle D\phi, \eta_t \rangle_{L^2(\Sigma)} = \int_{\Gamma} \int_0^T (D\phi)(\mathbf{x}, t) \eta_t(\mathbf{x}, t) dt d\mathbf{x}_{\Gamma}$$

and  $\eta$  is a suitable test function belonging to the same functional space of  $\phi$ . The hypersingular integral operator  $D$  can be equivalently expressed in the following way:

$$\begin{aligned} D\phi(\mathbf{x}, t) &= \int_{\Gamma} \frac{\partial^2 r}{\partial \mathbf{n}_{\mathbf{x}} \partial \mathbf{n}_{\xi}} \int_0^t G(r, t - \tau) \left[ \phi_{\tau}(\xi, \tau) + \frac{\phi(\xi, \tau)}{(t - \tau + r)} \right] d\tau d\xi_{\Gamma} \\ &+ \int_{\Gamma} \frac{\partial r}{\partial \mathbf{n}_{\mathbf{x}}} \frac{\partial r}{\partial \mathbf{n}_{\xi}} \int_0^t G(r, t - \tau) \left[ \phi_{\tau\tau}(\xi, \tau) + 2 \frac{\phi_{\tau}(\xi, \tau)}{(t - \tau + r)} + 3 \frac{\phi(\xi, \tau)}{(t - \tau + r)^2} \right] d\tau d\xi_{\Gamma}. \end{aligned} \quad (3.44)$$

### 3.2.1 Numerical results

The following numerical results are obtained applying the standard Galerkin BEM discretization with time step  $\Delta t$  and space step  $\Delta x$  to the energetic weak formulation, as it will be explained in chapter 4.

- For the first numerical example related to the two dimensional Neumann exterior problem (3.41), consider  $\Gamma = \{(x, 0) : x \in [0, 1]\}$ . The incident wave  $u^I(\mathbf{x}, t)$  is a plane wave propagating in direction  $\mathbf{k} = (\cos \theta, \sin \theta)$  with unitary amplitude:

$$u^I(\mathbf{x}, t) = f(t - \mathbf{k} \cdot \mathbf{x}). \quad (3.45)$$

Hence, the Neumann datum on  $\Gamma$  is:

$$g_{\mathcal{N}}(x, t) = - \frac{\partial}{\partial \mathbf{n}_{\mathbf{x}}} f(t - \mathbf{k} \cdot \mathbf{x}) \Big|_{\Gamma}. \quad (3.46)$$

The shown results have been obtained for two different functions, chosen for the known asymptotic behavior of the solution, which allows to validate the approximate solution, in the sequel indicated with  $\phi(x, t)$ .

*Plane harmonic wave.* Consider a wave which becomes harmonic after a fixed time (see [12]):

$$f(t) = \begin{cases} 0 & \text{if } t < 0, \\ \frac{1}{2}(1 - \cos \omega t) & \text{if } 0 \leq t \leq \frac{\pi}{\omega}, \\ \sin\left(\frac{\omega t}{2}\right) & \text{if } t \geq \frac{\pi}{\omega}, \end{cases} \quad (3.47)$$

where  $\omega$  represents the frequency. In this case the solution has to become harmonic too, with the same period as the incident wave, i.e.  $P = 2\pi/\tilde{\omega}$ , where  $\tilde{\omega} = \omega/2$ . The fixed circular frequency  $\omega = 8\pi$  is such that the wave length  $\lambda = 2\pi/\omega$  is equal to a quarter the crack length.

The decomposition of the crack  $\Gamma$  is made of 20 uniform subintervals ( $\Delta x = 0.05$ ) and the observation time interval  $[0, 10]$  is decomposed in 400 equal parts ( $\Delta t = 0.025$ ). For this numerical simulation spatial linear shape and test functions have been chosen.

In figure 3.9 there is the time harmonic behavior for  $\theta = \frac{\pi}{2}$  of the crack opening displacement (COD)  $\phi$  at  $x = 0.4$ , obtained starting from the energetic weak formulation. Note that the solution becomes immediately not trivial since the incident wave strikes the whole crack simultaneously. In figure 3.10 the approximated COD at instants 2, 4, 5, 10 are presented: the four curves overlap each other since the period is  $P = 0.5$ .

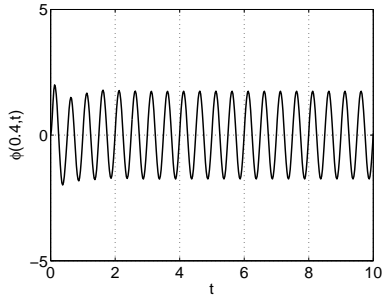


Fig. 3.9: Density  $\phi(0.4, t)$  approximated by linear shape functions for  $\theta = \pi/2$ .

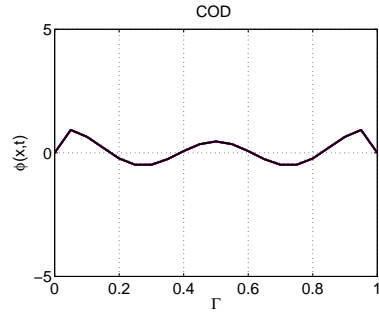


Fig. 3.10: COD at  $t = 2, 4, 5, 10$  approximated by linear shape functions for  $\theta = \pi/2$ .

In figure 3.11 there is the time harmonic behavior for  $\theta = \frac{\pi}{3}$  of the crack opening displacement  $\phi$  at  $x = 0.4$ . Note that the COD is zero till the time instant  $t^* = \cos(\theta)x = x/2$ , since the incident wave, differently from the previous case, doesn't invest the whole crack simultaneously.

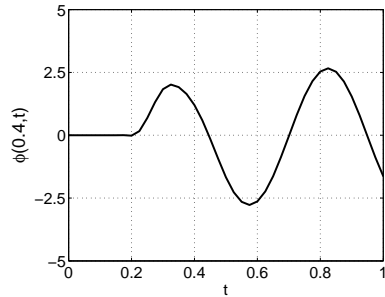
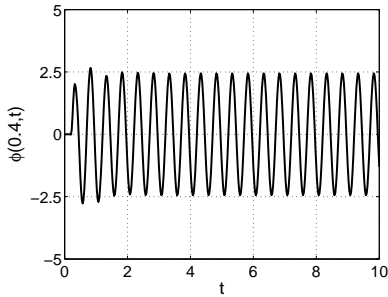


Fig. 3.11: Density  $\phi(x, t)$  approximated, in space and in time, by linear shape functions calculated in  $x = 0.4$  for  $\theta = \pi/3$ , with a zoom.

In order to verify that the period of  $\phi$  coincides with the period of the incident wave, in figure 3.12 the approximate solution  $\phi$  on  $\Gamma$  is plotted in time instants separated by multiples of the time period.

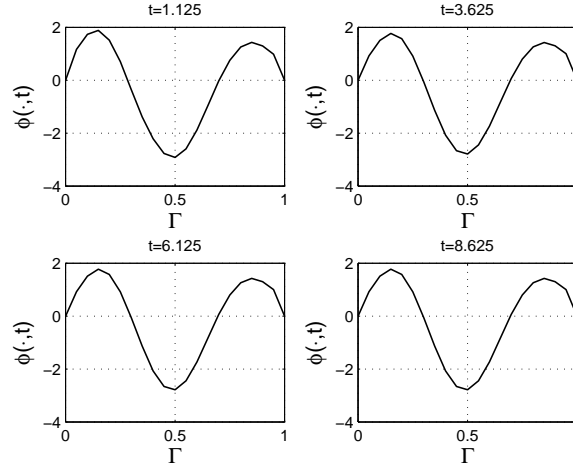


Fig. 3.12: Solution  $\phi(x,t)$  approximated, in space and in time, by linear shape functions, is here displayed in different time instants separated by  $5P$ .

*Plane linear wave.* Always in [12], a Neumann boundary condition comes from this choice of  $f$ :

$$f(t) = tH[t].$$

In this case, the Neumann datum (3.46) tends to the constant value  $g_\theta = \sin \theta$  when  $t$  tends to infinity. The solution  $u$  tends to the solution of the static problem

$$\begin{cases} -\Delta u_\infty = 0 & \text{in } \mathbb{R}^2 \setminus \Gamma, & u(\mathbf{x}) = O(\|\mathbf{x}\|_2^{-1}) & \text{for } \|\mathbf{x}\|_2 \rightarrow \infty \\ \frac{\partial u_\infty}{\partial \mathbf{n}} = g_\theta & \text{on } \Gamma \end{cases} \quad (3.48)$$

and the associated jump  $\phi_\theta^\infty(x) = [u_\infty]$  across  $\Gamma$  can be computed explicitly:

$$\phi_\theta^\infty(x) = \sin \theta \sqrt{x(1-x)}.$$

Hence, the solution  $\phi(x,t)$  can be compared with the static solution  $\phi_\theta^\infty(x)$ . The crack  $\Gamma$  is decomposed in 20 subintervals ( $\Delta x = 0.05$ ), the final observation time is  $T = 10$ , the time step is  $\Delta t = 0.025$  and spatial linear shape and test functions have been adopted. Also in this case, the numerical solution obtained for large times and reported in figure 3.13 for  $\theta = \frac{\pi}{3}$  is in perfect agreement with the corresponding one reported in [12]. Note that points of  $\Gamma$ , symmetric with respect to



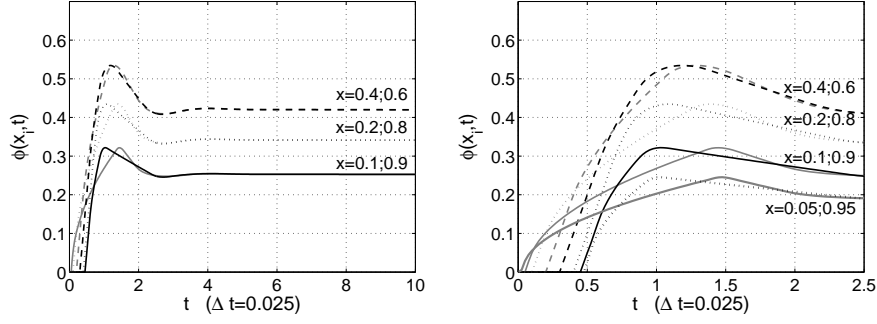


Fig. 3.13: Density  $\phi(x, t)$  approximated, in space and in time, by linear shape functions, is here evaluated in some points of  $\Gamma$  for  $\theta = \pi/3$ .

$x = 0.5$  behaves in different ways at the beginning of the simulation, since the incident wave does not strike simultaneously the crack; then they assume a symmetric behavior for sufficiently large times. Finally, to verify that the whole numerical solution  $\phi(x, t)$  stabilizes itself, in figure 3.14 there is the COD on  $\Gamma$  in different time instants  $t \geq 4$ . Numerical results are in agreement with those reported in [12], but differently from what is said in that paper, they seem to be independent of the ratio  $\frac{\Delta t}{\Delta x}$  as can be seen in figure 3.15.

In figure 3.16, analogous numerical results are obtained for  $\theta = \frac{\pi}{4}$ , and in figure 3.17 the approximate COD for  $T = 4, 5, 10$  are plotted together with the analytical solution of the corresponding static problem: the four curves overlap each other.

At last, to complete numerical simulations, there are some results involving the total displacement field  $u(\mathbf{x}, t)$  obtained by the superposition of the incident wave  $u^I(\mathbf{x}, t)$  and the reflected and diffracted waves caused by the presence of a crack  $\Gamma \subset \mathbb{R}^2$ . The temporal profile of the incident wave, that strikes the crack and from which the Neumann datum on  $\Gamma$  is deduced, is shown in figure 3.18 and it's similar to that one considered in [48] and [32].

- In the first simulation the crack  $\Gamma = \{(x, 0), x \in [-1, 1]\}$  is struck perpendicularly by the incident wave. The observation time interval is  $[0, 4]$ . For the discretization,  $\Gamma$  is subdivided in 40 uniform elements ( $\Delta x = 0.05$ ), the time step is  $\Delta t = 0.1$  and spatial linear shape and test functions have been adopted.

Figure 3.19 shows the total recovered displacement in a square around the crack for different time instants. These results illustrate how the plane wave reaches the crack and how the diffraction caused at the edges of the crack degenerates the wavefront. The effect of the diffraction on the upper half of the square creates a shadow. On the other hand, diffraction can be observed on the lower half of the square, too. Note that at the beginning of the simulation, the reflected wave on the upper half of the square cancel out with the incident wave. As time increases, the wavefront recovers and the scattering effect caused by the crack on the plane wave diminishes.

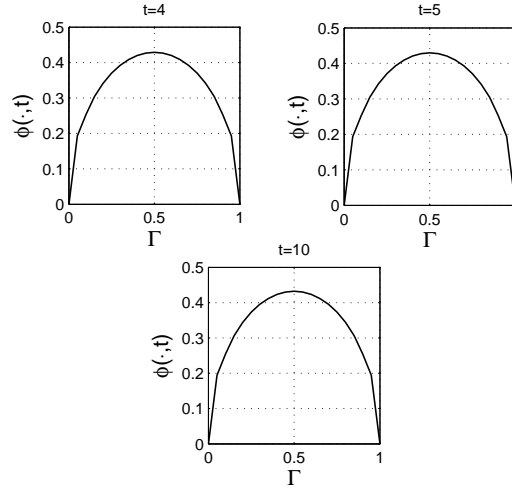


Fig. 3.14: Solution  $\phi(x, t)$  approximated, in space and in time, by linear shape functions, is displayed in different time instants.

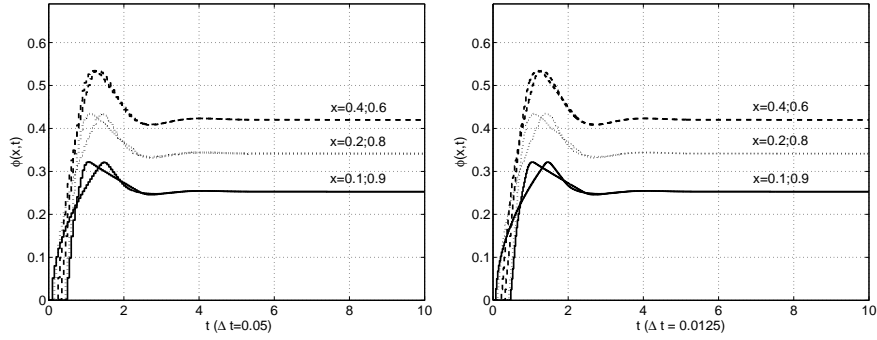


Fig. 3.15: Density  $\phi(x, t)$  for  $\theta = \pi/3$  approximated, in space and in time, by linear shape functions, with different time parameters of discretization.

- In the second simulation the obstacle is the semi-circular arc

$$\Gamma = \{ \mathbf{x} \in \mathbb{R}^2 : \mathbf{x} = (\cos \alpha, \sin \alpha), \alpha \in [0, \pi] \},$$

depending on the clockwise angle  $\alpha$ , struck by the plane wave with an incident angle of amplitude  $\frac{\pi}{3}$ . The observation time interval is  $[0, 4]$ . The uniform temporal discretization step is  $\Delta t = 0.1$  and  $\Gamma$  is uniformly approximated by 40 straight boundary elements where spatial linear shape and test functions have been adopted. In figure 3.20 there is shown the total recovered displacement in a square around the crack for different time instants. We are able to identify at  $t = 0.1$  the incident wave,

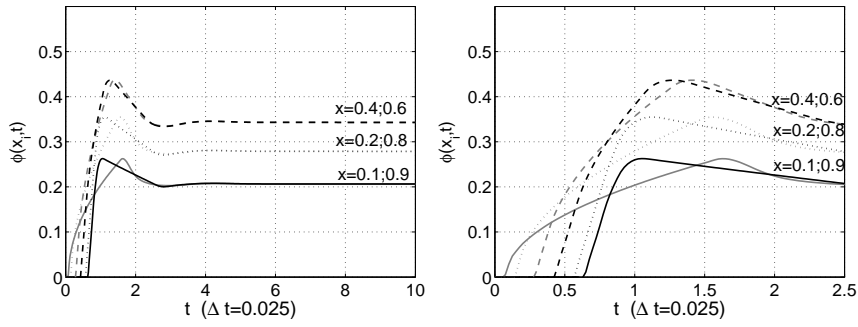


Fig. 3.16: Density  $\phi(x,t)$  approximated, in space and in time, by linear shape functions, is evaluated in some points of  $\Gamma$  for  $\theta = \pi/4$ .

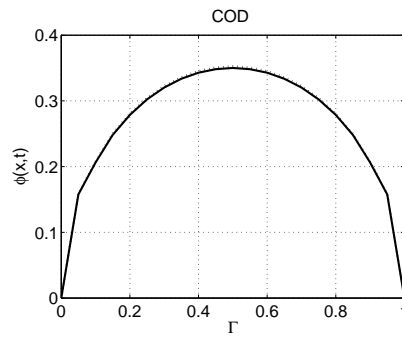


Fig. 3.17: COD at  $t = 4, 5, 10$  compared with static solution for  $\theta = \pi/4$ .

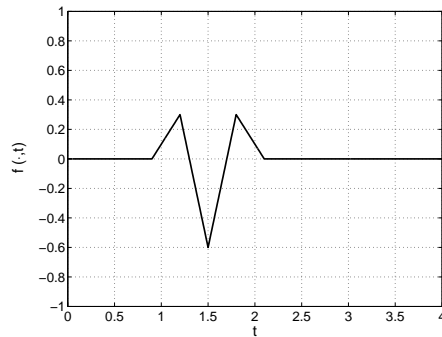


Fig. 3.18: Temporal profile of the incident wave in the last two examples.

at  $t = 1.0$  the reflected wave, at  $t = 1.6$  the first circular diffracted wave generated at the left edge of the crack, at  $t = 2.5$  the first diffracted wave generated at the right edge of the crack.

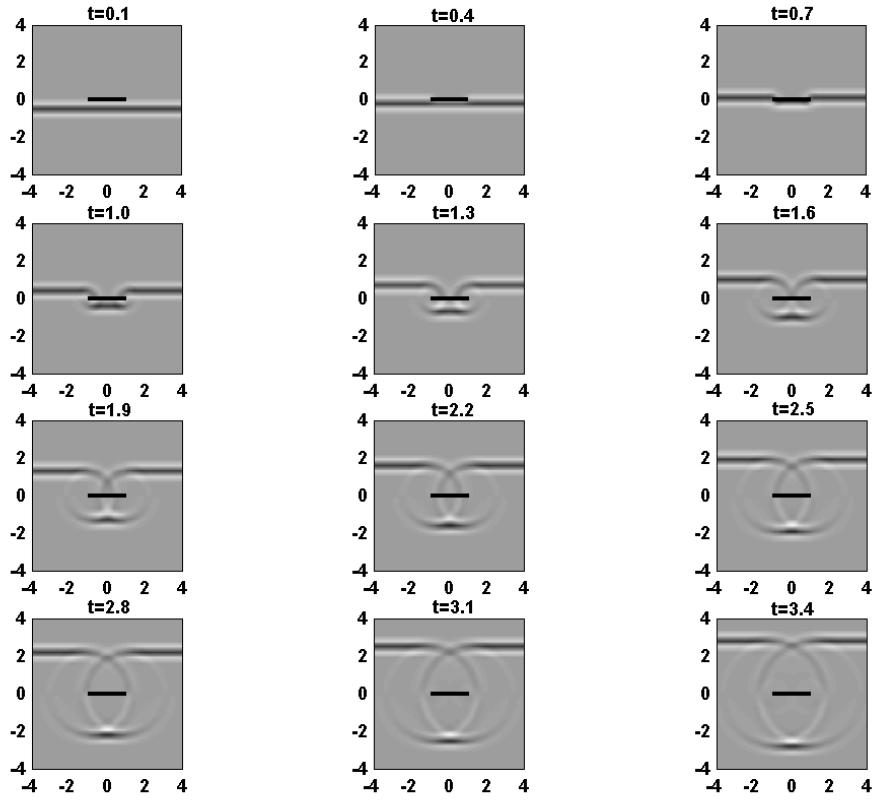


Fig. 3.19: Total recovered displacement  $u(\mathbf{x}, t)$  around the straight crack.

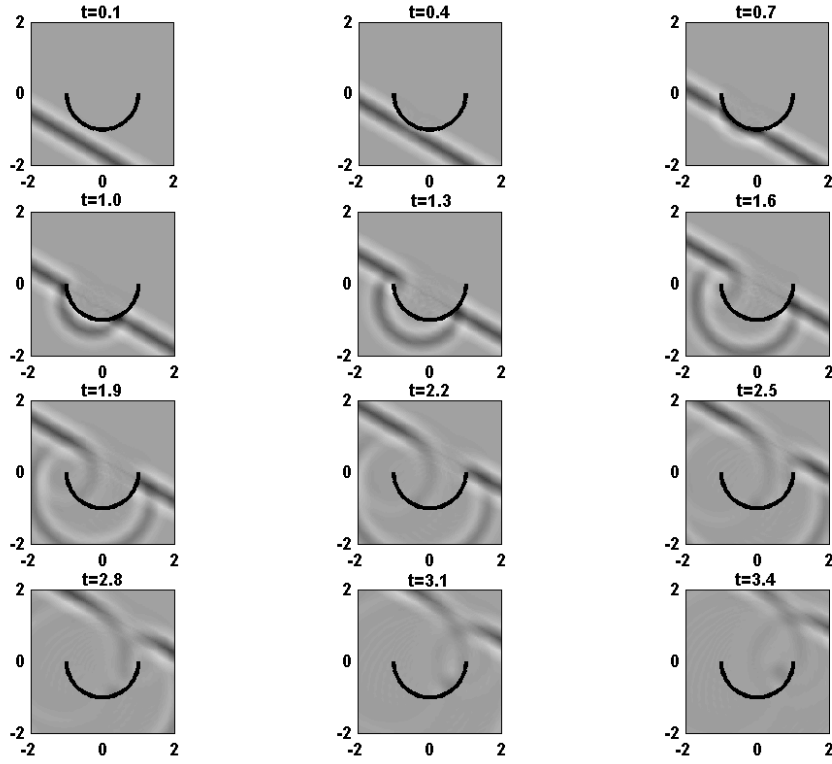


Fig. 3.20: Total recovered displacement  $u(\mathbf{x}, t)$  around the semicircular crack.

### 3.3 Mixed Boundary Value Problems

Consider a mixed boundary value problem  $(P_{\mathcal{D}, \mathcal{N}})$  for the wave equation in a domain  $\Omega \subset \mathbb{R}^2$  with boundary  $\Gamma$

$$(P_{\mathcal{D}, \mathcal{N}}) \begin{cases} u_{tt}(\mathbf{x}, t) - \Delta u(\mathbf{x}, t) = 0 & \mathbf{x} \in \Omega, t \in (0, T) \\ u(\mathbf{x}, 0) = u_t(\mathbf{x}, 0) = 0 & \mathbf{x} \in \Omega \\ u(\mathbf{x}, t) = g_{\mathcal{D}}(\mathbf{x}, t) & (\mathbf{x}, t) \in \Sigma_{\mathcal{D}} = \Gamma_{\mathcal{D}} \times [0, T] \\ \frac{\partial u}{\partial \mathbf{n}}(\mathbf{x}, t) = g_{\mathcal{N}}(\mathbf{x}, t) & (\mathbf{x}, t) \in \Sigma_{\mathcal{N}} = \Gamma_{\mathcal{N}} \times [0, T] \end{cases}$$

The boundary integral representation of its solution is:  $\forall (\mathbf{x}, t) \in \Omega \times (0, T)$

$$u(\mathbf{x}, t) = \int_{\Gamma} \int_0^t \left[ G(r, t, \tau) \frac{\partial u}{\partial \mathbf{n}_{\xi}}(\xi, \tau) - \frac{\partial G}{\partial \mathbf{n}_{\xi}}(r, t, \tau) u(\xi, \tau) \right] d\tau d\xi_{\Gamma}. \quad (3.49)$$

and, as explained in section 1.1 at page 7 the system of space-time BIE (M1) is

$$\begin{cases} \frac{1}{2}u(\mathbf{x},t) = \int_{\Gamma_0}^t \int G(r,t,\tau) \frac{\partial u}{\partial \mathbf{n}_\xi}(\xi,\tau) d\tau d\xi_\Gamma - \int_{\Gamma_0}^t \int \frac{\partial G}{\partial \mathbf{n}_\xi}(r,t,\tau) u(\xi,\tau) d\tau d\xi_\Gamma, \\ -\frac{1}{2} \frac{\partial u}{\partial \mathbf{n}_\mathbf{x}}(\mathbf{x},t) = -\int_{\Gamma_0}^t \int \frac{\partial G}{\partial \mathbf{n}_\mathbf{x}}(r,t,\tau) \frac{\partial u}{\partial \mathbf{n}_\xi}(\xi,\tau) d\tau d\xi_\Gamma + \int_{\Gamma_0}^t \int \frac{\partial^2 G}{\partial \mathbf{n}_\mathbf{x} \partial \mathbf{n}_\xi}(r,t,\tau) u(\xi,\tau) d\tau d\xi_\Gamma, \end{cases} \quad (3.50)$$

compactly written, applying the boundary conditions,

$$\begin{bmatrix} V_{\mathcal{D}} & -K_{\mathcal{N}} \\ -K'_{\mathcal{D}} & D_{\mathcal{N}} \end{bmatrix} \begin{bmatrix} \partial_{\mathbf{n}} u \\ u \end{bmatrix} = \begin{bmatrix} -V_{\mathcal{N}} & \frac{1}{2}I + K_{\mathcal{D}} \\ -\frac{1}{2}I + K'_{\mathcal{N}} & -D_{\mathcal{D}} \end{bmatrix} \begin{bmatrix} g_{\mathcal{N}} \\ g_{\mathcal{D}} \end{bmatrix}, \quad \begin{matrix} (\mathbf{x},t) \in \Sigma_{\mathcal{D}} \\ (\mathbf{x},t) \in \Sigma_{\mathcal{N}} \end{matrix}, \quad (3.51)$$

where the boundary integral operator subscripts  $\beta = \mathcal{D}, \mathcal{N}$  define their restriction to  $\Sigma_\beta$ . Then, the energetic weak formulation of the system (3.51) is defined (see [2, 3]) as described at page 30 for the one dimensional case

$$\begin{cases} \langle (V_{\mathcal{D}} \partial_{\mathbf{n}} u)_t, \psi \rangle_{L^2(\Sigma_{\mathcal{D}})} - \langle (K_{\mathcal{N}} u)_t, \psi \rangle_{L^2(\Sigma_{\mathcal{D}})} = \langle f_{\mathcal{D},t}, \psi \rangle_{L^2(\Sigma_{\mathcal{D}})} \\ - \langle K'_{\mathcal{D}} \partial_{\mathbf{n}} u, \eta_t \rangle_{L^2(\Sigma_{\mathcal{N}})} + \langle D_{\mathcal{N}} u, \eta_t \rangle_{L^2(\Sigma_{\mathcal{N}})} = \langle f_{\mathcal{N}}, \eta_t \rangle_{L^2(\Sigma_{\mathcal{N}})} \end{cases}, \quad (3.52)$$

where  $f_{\mathcal{D},t} = -(V_{\mathcal{N}} g_{\mathcal{N}})_t + ((\frac{1}{2}I + K_{\mathcal{D}}) g_{\mathcal{D}})_t$ ,  $f_{\mathcal{N}} = (-\frac{1}{2}I + K'_{\mathcal{N}}) g_{\mathcal{N}} - D_{\mathcal{D}} g_{\mathcal{D}}$  and  $\psi, \eta$  are suitable test functions, belonging to the same functional space of  $\partial_{\mathbf{n}} u, u$ , respectively. Note that the operator  $K'$  is the adjoint of the Cauchy singular operator  $K$ , which can be expressed as

$$(Ku)(\mathbf{x},t) = \int_{\Gamma} \frac{\partial r}{\partial \mathbf{n}_\xi} \int_0^t G(r,t,\tau) \left[ u_t(\xi,\tau) + \frac{u(\xi,\tau)}{(t-\tau+r)} \right] d\tau d\xi_\Gamma, \quad (3.53)$$

while the hypersingular integral operator  $D$  is that one shown in (3.44).

### 3.3.1 Numerical results

Results below have been obtained applying the standard Galerkin approximation with time step parameter  $\Delta t$  and space step parameter  $\Delta x$  as explained in chapter 4.

- At first I have considered a standard benchmark (see for instance [26] and [52]) involving a strip  $\Omega$  of height  $L = 1$ , unbounded in horizontal direction, fixed in the inferior part where the Dirichlet boundary datum  $g_{\mathcal{D}} = 0$  is assigned, and subject to a uniform traction  $g_{\mathcal{N}} = H[t]$  in its superior part, as shown in figure 3.21. A finite portion of the strip is taken into account, in such a way that vertical dimension of the resulting rectangle is five times the other one. On the ‘‘cut’’ sides of the do-

main the equilibrium condition  $g_{,\mathcal{N}} = 0$  has been assigned. This is the scalar version of a traditional elastodynamic problem, so, in this particular case, I will talk about “traction” and I will use the letter  $p$  when I refer to the quantity  $\partial_{\mathbf{n}}u$  to uniform my notation with the standard elastodynamic one.

In order to apply energetic Galerkin BEM,  $\Gamma$  is discretized with uniform mesh with 24 elements ( $\Delta x = l = 0.125$ ) and, in spatial variable, constant shape functions for the approximation of  $p$  and linear shape functions for the approximation of  $u$  have been used. The time interval of analysis  $[0, 8]$  has been discretized with different time steps.

In figure 3.22 there is the recovered numerical solution obtained with  $\Delta t = 0.0875$ . In particular for this ratio  $\beta := \frac{\Delta t}{\Delta x} = 0.7$ , time history of traction in the point  $A$ ,  $p(A, t)$ , is shown on the left, together with the corresponding analytical solution, while displacements in the points  $B, C, D$ , respectively  $u(B, t), u(C, t), u(D, t)$  are shown on the right: here the three curves overlap with their respective analytical solutions. Note that the oscillations in the graph of  $p(A, t)$  are due to the difficulty of approximating the jump discontinuities of the analytical solution; anyway, the obtained numerical solution is substantially better with respect to those found in literature, which present much more instabilities (see e.g. [26]).

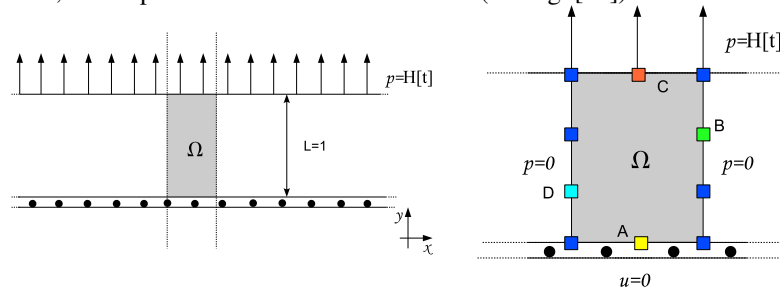


Fig. 3.21: Domain and mixed boundary conditions for the first test problem.

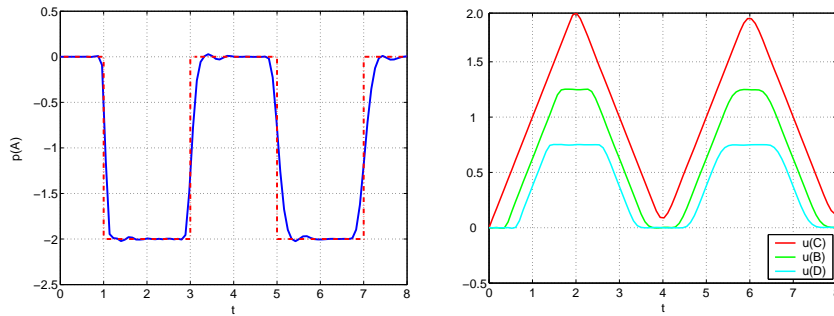


Fig. 3.22: Numerical solution for  $p$  and  $u$  of the first test problem.  $p$  has been approximated by constant shape functions both in time and space.  $u$  has been approximated by linear shape functions in space and by “ramp” functions in time (see (4.2)).

In the following sequence of figures 3.23, I show the stability of these results also changing the ratio  $\beta$  as in [52], that is decreasing to rather small time parameters  $\Delta t$ .

Due to the substantial invariance of the displacement plots, here I have reproduced only the graphics of traction  $p$  in  $x = A$ .

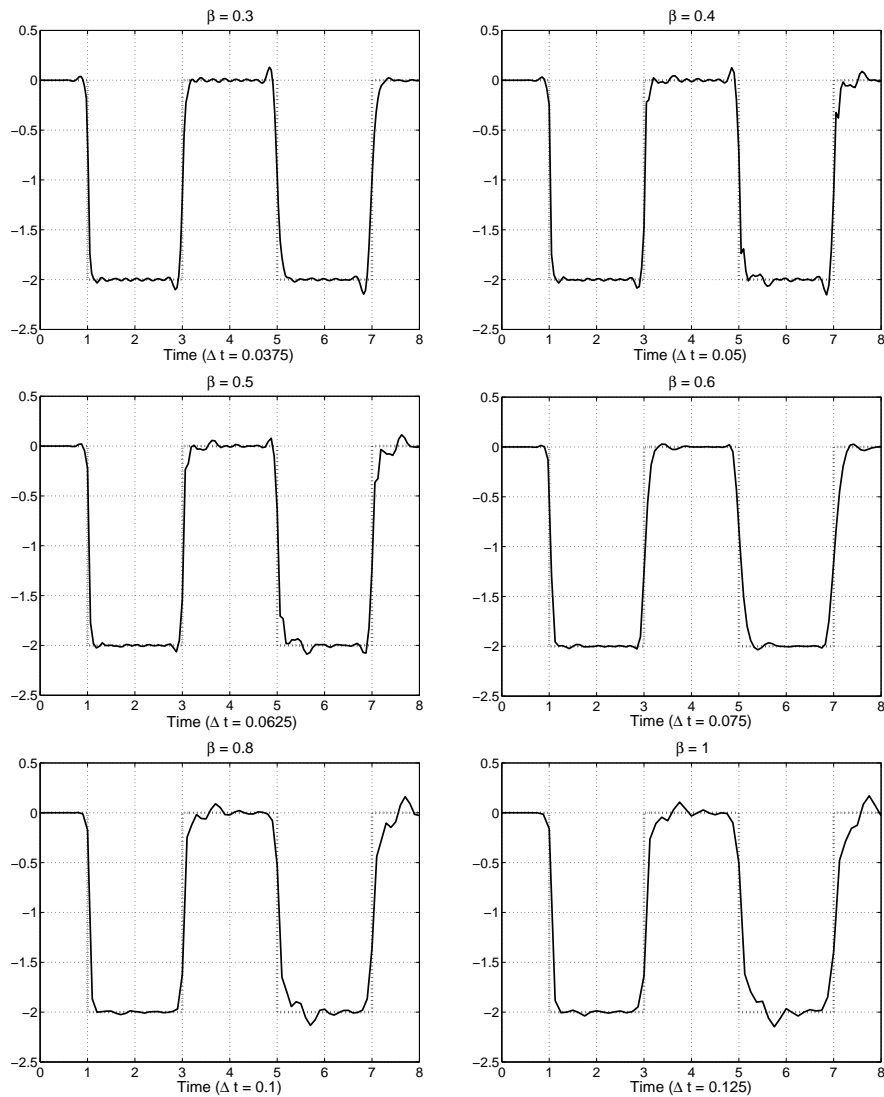


Fig. 3.23: Numerical solution  $p(A, t)$  approximated by constant shape functions both in time and space, varying  $\Delta t$ .

Then, even for  $\beta = 1.0$ , that seems to be one of the worst ratios, we can observe in figure 3.24 that the solution behavior for long time is stable and that it can be also improved refining the mesh of discretization as shown in figure 3.25.



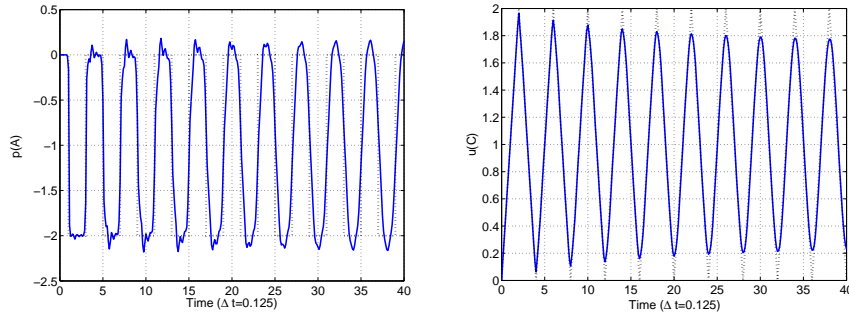


Fig. 3.24: Numerical solution for  $p$  and  $u$  obtained for the ratio  $\beta = 1.0$  with  $\Delta x = \Delta t = 0.125$ .  $p$  has been approximated by constant shape functions both in time and space.  $u$  has been approximated by linear shape functions in space and by “ramp” functions in time (see (4.2)).

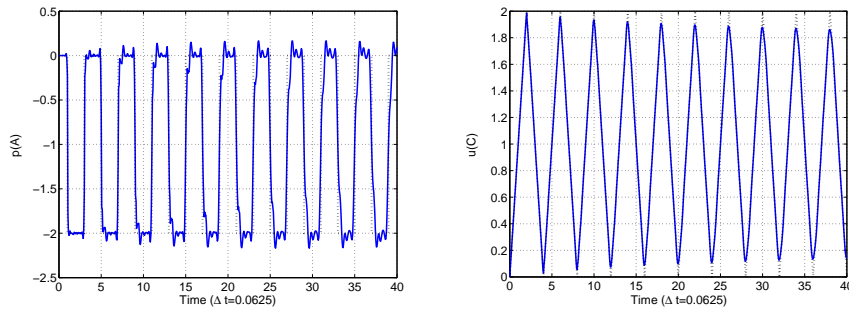


Fig. 3.25: Numerical solution for  $p$  and  $u$  obtained for the ratio  $\beta = 1.0$  with  $\Delta x = \Delta t = 0.0625$ .  $p$  has been approximated by constant shape functions both in time and space.  $u$  has been approximated by linear shape functions in space and by “ramp” functions in time (see (4.2)).

- As second simulation, I have considered a unitary disk, whose upper semi-circular boundary is subject to the Neumann boundary datum  $g_{\mathcal{N}} = H[t]$ , while its lower semi-circular boundary is fixed. Domain and mixed boundary conditions are shown in figure 3.26 on the left.

For the discretization phase, the boundary  $\Gamma$  has been approximated introducing a uniform mesh with 24 straight elements and, in spatial variable, constant shape functions for the approximation of  $p$  and linear shape functions for the approximation of  $u$  have been used. The time interval of analysis  $[0, 10]$  has been discretized with different uniform time meshes. In figure 3.27 the approximate solution obtained with the energetic approach, fixing  $\Delta t = 0.2$ , is presented. In particular, on the left the time history  $p(E, t)$ ,  $p(F, t)$  of  $p$  on the elements  $E, F$  is shown and one can note that while the element  $E$  near the Neumann boundary is immediately affected by the wave, the solution on the element  $F$  is trivial till the time instant  $\bar{t} \simeq 1.5$ . On the right the time history of the solution  $u$  at nodes  $A, B, C, D$  is shown: of course, the nearer these nodes are to  $\Gamma_{\mathcal{D}}$ , which is fixed, the lower is the value of the corresponding solution.

- For the last test problem, the same domain of the previous simulation has been taken into consideration but subject to pure Neumann boundary conditions  $g_{\mathcal{N}} = H[t]$  (see figure 3.26 on the right). For the discretization phase, the boundary  $\Gamma$  has been approximated introducing a decomposition in 24 straight elements, equipped with linear shape functions. The time interval of analysis  $[0, 12\pi]$  (that is much longer than anyone I found in articles such as [1] or [52]) has been discretized with  $\Delta t = \pi/10$ . In figure 3.28, on the left, the time history of the approximate solution  $u(A, t)$  in the point A of the mesh, obtained with the energetic approach, is presented for this interior problem. For the sake of completeness, the approximate solution  $u(A, t)$  of the exterior wave propagation problem ( $P_{\mathcal{D}, \mathcal{N}}^e$ ), defined in  $\Omega^e = \mathbb{R}^2 \setminus \Gamma$  with the same Neumann boundary conditions, obtained with the same discretization parameters, is shown on the right. This latter is in perfect agreement with that one reported in [1].

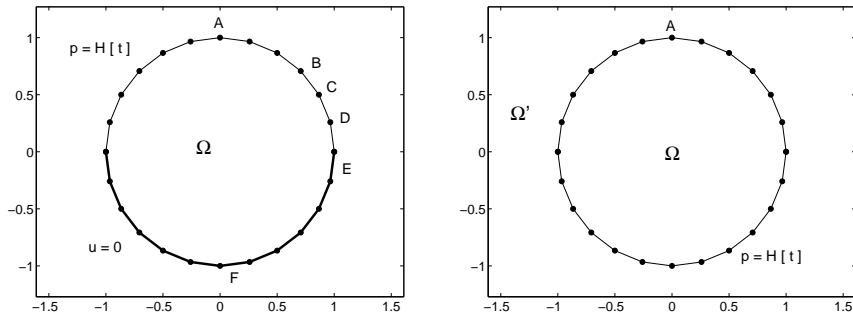


Fig. 3.26: Domains and boundary conditions of the second (left) and of the third (right) simulation.

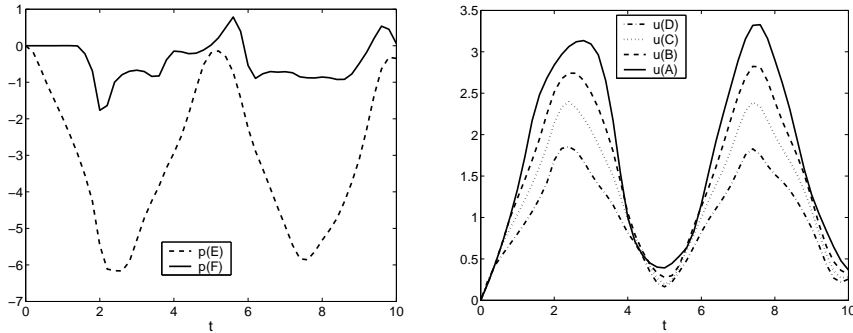


Fig. 3.27: Numerical solution of the second simulation.  $p$  has been approximated by constant shape functions both in time and space.  $u$  has been approximated by linear shape functions in space and by “ramp” functions in time (see (4.2)).

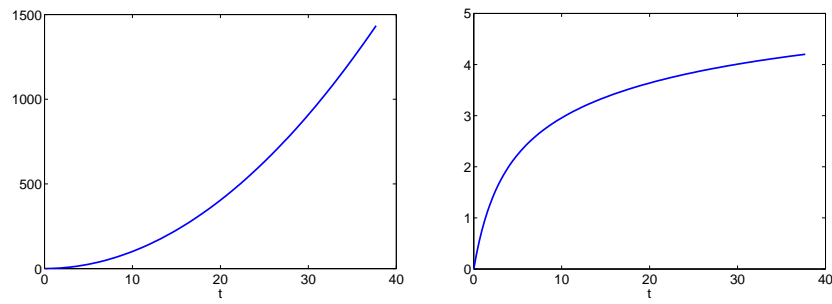


Fig. 3.28: Solutions  $u$  of the interior (left) and exterior (right) problem on the unitary circle with Neumann boundary conditions approximated by linear shape functions in space and by “ramp” functions in time (see (4.2)).



## Chapter 4

# Discretization

In this chapter I will describe the numerical techniques used to obtain the energetic Galerkin approximated solution starting, as a model problem, from an interior wave propagation problem with vanishing initial and mixed boundary conditions reformulated in terms of the boundary integral equations with retarded potential (3.51), as described in section 3.3. In this equation one finds all the kernels involved in the problems treated till now in this thesis. The integral problem is set in the weak form based on the energy identity. The related energetic Galerkin boundary element method used in the discretization phase both in space and in time, after a double integration in time variables, has to deal with weakly singular, singular and hyper-singular double integrals in space variables. Efficient quadrature schemes for the numerical evaluation of these integrals are here proposed.

The stability of the obtained numerical results, illustrated in section 3.3.1, emphasize the efficiency of the numerical schemes involved in this approximation process.

### 4.1 Galerkin BEM discretization

Start considering the mixed boundary value problem  $(P_{\mathcal{D},\mathcal{N}})$  for the wave equation and its energetic weak formulation 3.52 just introduced in section 3.3 at page 68.

For time discretization a uniform decomposition of the time interval  $[0, T]$  have been considered with time step  $\Delta t = T/N_{\Delta t}, N_{\Delta t} \in \mathbb{N}^+$ , generated by the  $N_{\Delta t} + 1$  instants

$$t_k = k \Delta t, \quad k = 0, \dots, N_{\Delta t},$$

and temporally piecewise constant shape functions for the approximation of  $\partial_{\mathbf{n}}u$  and piecewise linear shape functions for the approximation of  $u$ , although higher degree shape functions can be used. Note that, for this particular choice, temporal shape functions, for  $k = 0, \dots, N_{\Delta t} - 1$ , will be defined as

$$v_k^{\mathcal{D}}(t) = H[t - t_k] - H[t - t_{k+1}] \quad (4.1)$$

for the approximation of  $\partial_{\mathbf{n}}u$ , or as

$$v_k^{\mathcal{N}}(t) = R(t - t_k) - R(t - t_{k+1}), \quad (4.2)$$

for the approximation of  $u$ , where  $R(t - t_k) = \frac{t - t_k}{\Delta t} H[t - t_k]$  is the ramp function. For the space discretization, I have employed a Galerkin boundary element method. The boundary mesh on  $\Gamma_{\mathcal{D}}$  is constituted by  $M_{\mathcal{D}}$  straight elements  $\{e_1^{\mathcal{D}}, \dots, e_{M_{\mathcal{D}}}^{\mathcal{D}}\}$ , with  $e_i^{\mathcal{D}} \cap e_j^{\mathcal{D}} = \emptyset$  if  $i \neq j$  and such that  $\bigcup_{i=1}^{M_{\mathcal{D}}} e_i^{\mathcal{D}} = \bar{\Gamma}_{\mathcal{D}}$ ,  $2l_i^{\mathcal{D}} := \text{length}(e_i^{\mathcal{D}})$ ,  $l^{\mathcal{D}} = \max_i \{2l_i^{\mathcal{D}}\}$ . The same is done for the Neumann part of the boundary  $\Gamma_{\mathcal{N}}$  with obvious change of notation. Let  $l = \max\{l^{\mathcal{D}}, l^{\mathcal{N}}\}$ . The functional background compels one to choose spatially shape functions belonging to  $L^2(\Gamma_{\mathcal{D}})$  for the approximation of  $\partial_{\mathbf{n}}u$  and to  $H^1(\Gamma_{\mathcal{N}})$  for the approximation of  $u$ . Therefore, having defined  $\mathcal{P}_{d_i}$  the space of algebraic polynomials of degree  $d_i$ , consider, respectively, the space of piecewise polynomial functions

$$X_{-1,l} := \{w^{\mathcal{D}}(\mathbf{x}) \in L^2(\Gamma_{\mathcal{D}}) : w|_{e_i^{\mathcal{D}}} \in \mathcal{P}_{d_i}, \forall e_i^{\mathcal{D}} \subset \Gamma_{\mathcal{D}}\}; \quad (4.3)$$

and the space of continuous piecewise polynomial functions

$$X_{0,l} := \{w^{\mathcal{N}}(\mathbf{x}) \in C^0(\Gamma_{\mathcal{N}}) : w|_{e_j^{\mathcal{N}}} \in \mathcal{P}_{d_j}, \forall e_j^{\mathcal{N}} \subset \Gamma_{\mathcal{N}}\}. \quad (4.4)$$

Hence, denoted with  $M_{\mathcal{D}}, M_{\mathcal{N}}$  the number of unknowns on  $\Gamma_{\mathcal{D}}$  and  $\Gamma_{\mathcal{N}}$ , respectively, and having introduced the standard piece-wise polynomial boundary element basis functions  $w_j^{\mathcal{D}}(\mathbf{x})$ ,  $j = 1, \dots, M_{\mathcal{D}}$ , in  $X_{-1,l}$  and  $w_j^{\mathcal{N}}(\mathbf{x})$ ,  $j = 1, \dots, M_{\mathcal{N}}$  in  $X_{0,l}$ , the solutions of the problem at hand will be approximated as follows:

$$\frac{\partial u}{\partial \mathbf{n}}(\mathbf{x}, t) \approx \sum_{k=0}^{N_{\Delta t}-1} \sum_{j=1}^{M_{\mathcal{D}}} \alpha_{\mathcal{D},j}^{(k)} w_j^{\mathcal{D}}(\mathbf{x}) v_k^{\mathcal{D}}(t) \quad \text{and} \quad u(\mathbf{x}, t) \approx \sum_{k=0}^{N_{\Delta t}-1} \sum_{j=1}^{M_{\mathcal{N}}} \alpha_{\mathcal{N},j}^{(k)} w_j^{\mathcal{N}}(\mathbf{x}) v_k^{\mathcal{N}}(t). \quad (4.5)$$

The Galerkin BEM discretization coming from energetic weak formulation produces the linear system

$$\mathbb{E} \alpha = \mathbf{b}, \quad (4.6)$$

where matrix  $\mathbb{E}$  has a block lower triangular Toeplitz structure, since its elements depend on the difference  $t_h - t_k$  and in particular they vanish if  $t_h \leq t_k$ . Each block has dimension  $M := M_{\mathcal{D}} + M_{\mathcal{N}}$ . Indicating with  $\mathbb{E}^{(\ell)}$  the block obtained when  $t_h - t_k = (\ell + 1)\Delta t$ ,  $\ell = 0, \dots, N_{\Delta t} - 1$ , the linear system can be written as

$$\begin{pmatrix} \mathbb{E}^{(0)} & 0 & 0 & \dots & 0 \\ \mathbb{E}^{(1)} & \mathbb{E}^{(0)} & 0 & \dots & 0 \\ \mathbb{E}^{(2)} & \mathbb{E}^{(1)} & \mathbb{E}^{(0)} & \dots & 0 \\ \dots & \dots & \dots & \dots & 0 \\ \mathbb{E}^{(N_{\Delta t}-1)} & \mathbb{E}^{(N_{\Delta t}-2)} & \dots & \mathbb{E}^{(1)} & \mathbb{E}^{(0)} \end{pmatrix} \begin{pmatrix} \alpha^{(0)} \\ \alpha^{(1)} \\ \alpha^{(2)} \\ \vdots \\ \alpha^{(N_{\Delta t}-1)} \end{pmatrix} = \begin{pmatrix} \mathbf{b}^{(0)} \\ \mathbf{b}^{(1)} \\ \mathbf{b}^{(2)} \\ \vdots \\ \mathbf{b}^{(N_{\Delta t}-1)} \end{pmatrix} \quad (4.7)$$

where

$$\boldsymbol{\alpha}^{(\ell)} = \left( \boldsymbol{\alpha}_j^{(\ell)} \right) \quad \text{and} \quad \mathbf{b}^{(\ell)} = \left( b_j^{(\ell)} \right), \quad \text{with} \quad \ell = 0, \dots, N_{\Delta t} - 1; \quad j = 1, \dots, M. \quad (4.8)$$

Note that each block has a  $2 \times 2$  block sub-structure of the type

$$\mathbb{E}^{(\ell)} = \begin{bmatrix} \mathbb{E}_{\mathcal{D}\mathcal{D}}^{(\ell)} & \mathbb{E}_{\mathcal{D}\mathcal{N}}^{(\ell)} \\ \mathbb{E}_{\mathcal{N}\mathcal{D}}^{(\ell)} & \mathbb{E}_{\mathcal{N}\mathcal{N}}^{(\ell)} \end{bmatrix} \quad (4.9)$$

where diagonal sub-blocks have dimensions  $M_{\mathcal{D}}$ ,  $M_{\mathcal{N}}$ , respectively and

$$\boldsymbol{\alpha}^{(\ell)} = \left( \boldsymbol{\alpha}_{\mathcal{D}1}^{(\ell)}, \dots, \boldsymbol{\alpha}_{\mathcal{D}M_{\mathcal{D}}}^{(\ell)}, \boldsymbol{\alpha}_{\mathcal{N}1}^{(\ell)}, \dots, \boldsymbol{\alpha}_{\mathcal{N}M_{\mathcal{N}}}^{(\ell)} \right)^{\top}.$$

In the case of a Dirichlet problem, the block  $\mathbb{E}^{(\ell)}$  written in (4.9) is equal to  $\mathbb{E}_{\mathcal{D}\mathcal{D}}^{(\ell)}$  only. In the case of a Neumann problem, the block  $\mathbb{E}^{(\ell)}$  written in (4.9) is equal to  $\mathbb{E}_{\mathcal{N}\mathcal{N}}^{(\ell)}$  only.

**Proposition 5** *If  $v_k^{\mathcal{D}}$  and  $v_k^{\mathcal{N}}$  are chosen as in (4.1) and (4.2) respectively, it holds  $\mathbb{E}_{\mathcal{D}\mathcal{N}}^{(\ell)} = (\mathbb{E}_{\mathcal{N}\mathcal{D}}^{(\ell)})^{\top}$ .*

*Proof.* Here the proof for the two dimensional case:

$$\begin{aligned} [\mathbb{E}_{\mathcal{D}\mathcal{N}}^{(\ell)}]_{ij} &= \int_0^T \int_{\Gamma_{\mathcal{D}}} w_i^{\mathcal{D}}(\mathbf{x}) v_k^{\mathcal{D}}(t) (K_t [w_j^{\mathcal{N}} v_h^{\mathcal{N}}])(\mathbf{x}, t) d\mathbf{x}_{\Gamma_{\mathcal{D}}} dt = \\ &= \int_0^T \int_{\Gamma_{\mathcal{D}}} w_i^{\mathcal{D}}(\mathbf{x}) v_k^{\mathcal{D}}(t) \int_0^t \int_{\Gamma_{\mathcal{N}}} \left[ \frac{\partial r}{\partial \mathbf{n}_{\xi}} \frac{1}{2\pi} \frac{H[t-\tau-r]}{[(t-\tau)^2-r^2]^{1/2}} \left( [w_j^{\mathcal{N}}(\xi) v_h^{\mathcal{N}}(\tau)]_{\tau} + \frac{w_j^{\mathcal{N}}(\xi) v_h^{\mathcal{N}}(\tau)}{(t-\tau+r)} \right) \right]_{t} \\ &\quad d\xi_{\Gamma_{\mathcal{N}}} d\tau d\mathbf{x}_{\Gamma_{\mathcal{D}}} dt = \\ &= \frac{1}{2\pi} \int_0^T \int_{\Gamma_{\mathcal{D}}} w_i^{\mathcal{D}}(\mathbf{x}) v_k^{\mathcal{D}}(t) \int_0^t \int_{\Gamma_{\mathcal{N}}} \frac{\partial r}{\partial \mathbf{n}_{\xi}} \\ &\quad \left\{ - \left[ \frac{H[t-\tau-r]}{[(t-\tau)-r]^{1/2}} \right]_{\tau} \frac{1}{[(t-\tau)+r]^{1/2}} \left( [w_j^{\mathcal{N}}(\xi) v_h^{\mathcal{N}}(\tau)]_{\tau} + \frac{w_j^{\mathcal{N}}(\xi) v_h^{\mathcal{N}}(\tau)}{(t-\tau+r)} \right) \right\} + \\ &\quad + \frac{H[t-\tau-r]}{[(t-\tau)-r]^{1/2}} \left[ \frac{1}{[(t-\tau)+r]^{1/2}} \left( [w_j^{\mathcal{N}}(\xi) v_h^{\mathcal{N}}(\tau)]_{\tau} + \frac{w_j^{\mathcal{N}}(\xi) v_h^{\mathcal{N}}(\tau)}{(t-\tau+r)} \right) \right]_{\tau} \right\} \\ &\quad d\xi_{\Gamma_{\mathcal{N}}} d\tau d\mathbf{x}_{\Gamma_{\mathcal{D}}} dt = \end{aligned}$$

integrating internally by parts in time the first addend and taking into account that when  $\tau = t$  it vanishes (because the argument of the Heaviside function is negative) and  $v_h^{\mathcal{N}}(0) = 0$

$$\begin{aligned}
&= \frac{1}{2\pi} \int_0^T \int_{\Gamma_{\mathcal{D}}} w_i^{\mathcal{D}}(\mathbf{x}) v_k^{\mathcal{D}}(t) \int_0^t \int_{\Gamma_{\mathcal{N}}} \frac{\partial r}{\partial \mathbf{n}_{\xi}} \\
&\quad \left\{ \frac{H[t - \tau - r]}{[(t - \tau) - r]^{1/2}} \left[ \frac{1}{[(t - \tau) + r]^{1/2}} \left( [w_j^{\mathcal{N}}(\xi) v_h^{\mathcal{N}}(\tau)]_{\tau} + \frac{w_j^{\mathcal{N}}(\xi) v_h^{\mathcal{N}}(\tau)}{(t - \tau + r)} \right) \right]_{\tau} + \right. \\
&\quad \left. + \frac{H[t - \tau - r]}{[(t - \tau) - r]^{1/2}} \left( -\frac{1}{2} \frac{[w_j^{\mathcal{N}}(\xi) v_h^{\mathcal{N}}(\tau)]_{\tau}}{[(t - \tau) + r]^{3/2}} - \frac{3}{2} \frac{w_j^{\mathcal{N}}(\xi) v_h^{\mathcal{N}}(\tau)}{[(t - \tau) + r]^{5/2}} \right) \right\} \\
&\quad d\xi_{\Gamma_{\mathcal{N}}} d\tau d\mathbf{x}_{\Gamma_{\mathcal{D}}} dt = \\
&= \frac{1}{2\pi} \int_0^T \int_{\Gamma_{\mathcal{D}}} w_i^{\mathcal{D}}(\mathbf{x}) v_k^{\mathcal{D}}(t) \int_0^t \int_{\Gamma_{\mathcal{N}}} \frac{\partial r}{\partial \mathbf{n}_{\xi}} \\
&\quad \left\{ \frac{H[t - \tau - r]}{[(t - \tau) - r]^{1/2}} \left( \frac{[w_j^{\mathcal{N}}(\xi) v_h^{\mathcal{N}}(\tau)]_{\tau}}{[(t - \tau) + r]^{1/2}} + \frac{3}{2} \frac{[w_j^{\mathcal{N}}(\xi) v_h^{\mathcal{N}}(\tau)]_{\tau}}{[(t - \tau) + r]^{3/2}} + \frac{3}{2} \frac{w_j^{\mathcal{N}}(\xi) v_h^{\mathcal{N}}(\tau)}{[(t - \tau) + r]^{5/2}} \right) + \right. \\
&\quad \left. + \frac{H[t - \tau - r]}{[(t - \tau) - r]^{1/2}} \left( -\frac{1}{2} \frac{[w_j^{\mathcal{N}}(\xi) v_h^{\mathcal{N}}(\tau)]_{\tau}}{[(t - \tau) + r]^{3/2}} - \frac{3}{2} \frac{w_j^{\mathcal{N}}(\xi) v_h^{\mathcal{N}}(\tau)}{[(t - \tau) + r]^{5/2}} \right) \right\} \\
&\quad d\xi_{\Gamma_{\mathcal{N}}} d\tau d\mathbf{x}_{\Gamma_{\mathcal{D}}} dt = \\
&= \int_0^T \int_{\Gamma_{\mathcal{D}}} w_i^{\mathcal{D}}(\mathbf{x}) v_k^{\mathcal{D}}(t) \int_0^t \int_{\Gamma_{\mathcal{N}}} \frac{\partial r}{\partial \mathbf{n}_{\xi}} G(r, t, \tau) \left( [w_j^{\mathcal{N}}(\xi) v_h^{\mathcal{N}}(\tau)]_{\tau} + \frac{[w_j^{\mathcal{N}}(\xi) v_h^{\mathcal{N}}(\tau)]_{\tau}}{[(t - \tau) + r]} \right) \\
&\quad d\xi_{\Gamma_{\mathcal{N}}} d\tau d\mathbf{x}_{\Gamma_{\mathcal{D}}} dt = \\
&= - \int_0^T \int_{\Gamma_{\mathcal{N}}} [w_j^{\mathcal{N}}(\mathbf{x}) v_k^{\mathcal{N}}(t)]_t \int_0^t \int_{\Gamma_{\mathcal{D}}} \frac{\partial r}{\partial \mathbf{n}_{\mathbf{x}}} G(r, t, \tau) \left( [w_i^{\mathcal{D}}(\xi) v_h^{\mathcal{D}}(\tau)]_{\tau} + \frac{w_i^{\mathcal{D}}(\xi) v_h^{\mathcal{D}}(\tau)}{(t - \tau + r)} \right) \\
&\quad d\xi_{\Gamma_{\mathcal{D}}} d\tau d\mathbf{x}_{\Gamma_{\mathcal{N}}} dt = \\
&= - \int_0^T \int_{\Gamma_{\mathcal{N}}} w_j^{\mathcal{N}}(\mathbf{x}) v_k^{\mathcal{N}}(t) (K^t [w_i^{\mathcal{D}} v_h^{\mathcal{D}}])(\mathbf{x}, t) d\mathbf{x}_{\Gamma_{\mathcal{N}}} dt = [\mathbb{E}_{\mathcal{N}\mathcal{D}}^{(\ell)}]_{ji}
\end{aligned}$$

in fact  $\partial_{\mathbf{n}_{\xi}} r = -\partial_{\mathbf{n}_{\mathbf{x}}} r$  and  $v_k^{\mathcal{D}}(t) [v_h^{\mathcal{N}}(\tau)]_{\tau} = [v_k^{\mathcal{N}}(t)]_t [v_h^{\mathcal{D}}(\tau)]_{\tau}$  as  $v_k^{\mathcal{D}}(t) = [v_k^{\mathcal{N}}(t)]_t$ .

The solution of (4.7) is obtained with a block forward substitution, i.e. at every time instant  $t_{\ell} = (\ell + 1)\Delta t$ ,  $\ell = 0, \dots, N_{\Delta t} - 1$ , one computes

$$\mathbf{z}^{(\ell)} = \mathbf{b}^{(\ell)} - \sum_{j=1}^{\ell} \mathbb{E}^{(j)} \boldsymbol{\alpha}^{(\ell-j)}$$



and then solves the reduced linear system:

$$\mathbb{E}^{(0)} \boldsymbol{\alpha}^{(\ell)} = \mathbf{z}^{(\ell)}. \quad (4.10)$$

Procedure (4.10) is a time-marching technique, where the only matrix to be inverted is the positive definite  $\mathbb{E}^{(0)}$  diagonal block, while all the other blocks are used to update at every time step the right-hand side. Owing to this procedure one can construct and store only the blocks  $\mathbb{E}^{(0)}, \dots, \mathbb{E}^{(N_{\Delta t}-1)}$  with a considerable reduction of computational cost and memory requirement.

Having set  $\Delta_{hk} = t_h - t_k$ , the matrix elements in blocks of the type  $\mathbb{E}_{\mathcal{D}\mathcal{D}}^{(\ell)}, \mathbb{E}_{\mathcal{D}\mathcal{N}}^{(\ell)}$  and  $\mathbb{E}_{\mathcal{N}\mathcal{N}}^{(\ell)}$ , after a double analytic integration in the time variables, are of the form, respectively

$$\bullet \sum_{\alpha, \beta=0}^1 (-1)^{\alpha+\beta} \int_{\Gamma_{\mathcal{D}}} w_i^{\mathcal{D}}(\mathbf{x}) \int_{\Gamma_{\mathcal{D}}} H[\Delta_{h+\alpha, k+\beta} - r] \mathbf{V}(r, t_{h+\alpha}, t_{k+\beta}) w_j^{\mathcal{D}}(\xi) d\xi_{\Gamma_{\mathcal{D}}} d\mathbf{x}_{\Gamma_{\mathcal{D}}}, \quad (4.11)$$

where

$$\mathbf{V}(r, t_h, t_k) = \frac{1}{2\pi} \left[ \log \left( \Delta_{hk} + \sqrt{\Delta_{hk}^2 - r^2} \right) - \log r \right]; \quad (4.12)$$

$$\bullet \sum_{\alpha, \beta=0}^1 (-1)^{\alpha+\beta} \int_{\Gamma_{\mathcal{D}}} w_i^{\mathcal{D}}(\mathbf{x}) \int_{\Gamma_{\mathcal{N}}} H[\Delta_{h+\alpha, k+\beta} - r] \mathbf{K}(r, t_{h+\alpha}, t_{k+\beta}) w_j^{\mathcal{N}}(\xi) d\xi_{\Gamma_{\mathcal{N}}} d\mathbf{x}_{\Gamma_{\mathcal{D}}}, \quad (4.13)$$

where

$$\mathbf{K}(r, t_h, t_k) = \frac{1}{2\pi \Delta t} \frac{\mathbf{r} \cdot \mathbf{n}_{\xi}}{r^2} \sqrt{\Delta_{hk}^2 - r^2}; \quad (4.14)$$

$$\bullet \sum_{\alpha, \beta=0}^1 (-1)^{\alpha+\beta} \int_{\Gamma_{\mathcal{N}}} w_i^{\mathcal{N}}(\mathbf{x}) \int_{\Gamma_{\mathcal{N}}} H[\Delta_{h+\alpha, k+\beta} - r] \mathbf{D}(r, t_{h+\alpha}, t_{k+\beta}) w_j^{\mathcal{N}}(\xi) d\xi_{\Gamma_{\mathcal{N}}} d\mathbf{x}_{\Gamma_{\mathcal{N}}}, \quad (4.15)$$

where

$$\begin{aligned} \mathbf{D}(r, t_h, t_k) = & \frac{1}{2\pi (\Delta t)^2} \left\{ \frac{\mathbf{r} \cdot \mathbf{n}_{\mathbf{x}} \mathbf{r} \cdot \mathbf{n}_{\xi}}{r^2} \frac{\Delta_{hk} \sqrt{\Delta_{hk}^2 - r^2}}{r^2} + \right. \\ & \left. + \frac{(\mathbf{n}_{\mathbf{x}} \cdot \mathbf{n}_{\xi})}{2} \left[ \log(\Delta_{hk} + \sqrt{\Delta_{hk}^2 - r^2}) - \log r - \frac{\Delta_{hk} \sqrt{\Delta_{hk}^2 - r^2}}{r^2} \right] \right\}. \end{aligned} \quad (4.16)$$

In the sequel I will refer to one of the double integrals in (4.11), (4.13) or (4.15), indicating it by

$$\int_{\Gamma} w_i(\mathbf{x}) \int_{\Gamma} H[\Delta_{hk} - r] \mathbf{S}(r, t_h, t_k) w_j(\xi) d\xi_{\Gamma} d\mathbf{x}_{\Gamma}, \quad (4.17)$$

where  $\mathbf{S}$  represents one of the kernels (4.12), (4.14) or (4.16) and where redundant apices  $\mathcal{D}, \mathcal{N}$  in the notation have been dropped, being clear which parts of the boundary and which test and shape functions are involved in the double integration, in relation to the fixed kernel. In the following, this simplification will be operated whenever possible.

Using the standard element by element technique, the evaluation of every double integral of the form (4.17) is reduced to the assembling of local contributions of the type

$$\int_{e_i} \tilde{w}_i^{(d_i)}(\mathbf{x}) \int_{e_j} H[\Delta_{hk} - r] \mathbf{S}(r, t_h, t_k) \tilde{w}_j^{(d_j)}(\xi) d\xi_\Gamma d\mathbf{x}_\Gamma, \quad (4.18)$$

where  $\tilde{w}_i^{(d_i)}(\mathbf{x})$  defines one of the local lagrangian basis function in the space variable of degree  $d_i$  defined over the element  $e_i$  of the boundary mesh.

Looking at (4.12), (4.14) and (4.16), observe space singularities of type  $\log r$ ,  $O(r^{-1})$  and  $O(r^{-2})$  as  $r \rightarrow 0$ , which are typical of two dimensional static kernels. Hence, there is particular interest in the efficient evaluation of double integrals of type (4.18) when  $e_i \equiv e_j$  and when  $e_i, e_j$  are consecutive. Further, notice that when the kernel is hypersingular and  $e_i \equiv e_j$  both the inner and the outer integrals are defined as Hadamard finite parts, while if  $e_i$  and  $e_j$  are consecutive, only the outer integral must be understood in the finite part sense. The correct interpretation of double integrals is the key point for any efficient numerical approach based on element by element technique (see [5]).

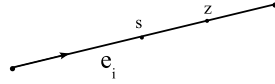
## 4.2 Evaluation of Galerkin matrix elements

Let start with an analysis of the double integration domain in (4.18), that can be rewritten in local variable of integration as

$$\int_0^{2l_i} \tilde{w}_i^{(d_i)}(s) \int_0^{2l_j} H[\Delta_{hk} - r] \mathbf{S}(r, t_h, t_k) \tilde{w}_j^{(d_j)}(z) dz ds. \quad (4.19)$$

Due to the presence of the Heaviside function  $H[\Delta_{hk} - r]$ , the double integration domain is constituted by the intersection between the rectangle  $[0, 2l_i] \times [0, 2l_j]$  and the two dimensional domain  $\Delta_{hk} - r > 0$ . Let me specify this issue with respect to the geometrical disposition of the mesh elements  $e_i, e_j$ .

**Coincident boundary elements ( $e_i \equiv e_j$ ).**



In this case, the distance between the source and the field point can be written as  $r = |s - z|$ ; hence the double integration domain is represented by the intersection between the square  $[0, 2l_i] \times [0, 2l_i]$  and the strip  $|s - z| < \Delta_{hk}$  where the Heaviside function is not trivial. In figure 4.1 these intersections for different values of  $\Delta_{hk} = t_h - t_k$  and fixed length  $2l_i$  are shown. Having set

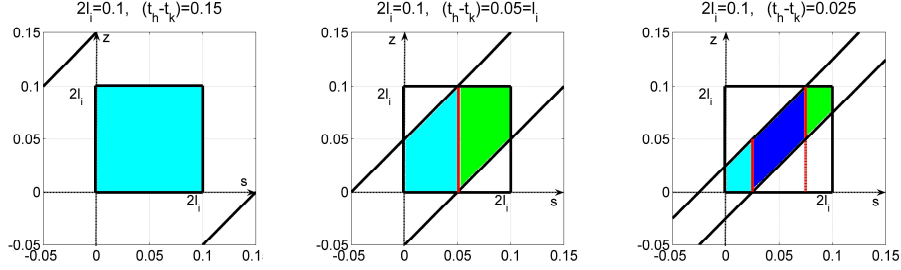


Fig. 4.1: Double integration domain (coincident elements) for different values of  $\Delta_{hk}$ . Splitting vertical lines are plotted in  $s = s_1$  and  $s = s_2$ .

$$M_s = \max(0, s - \Delta_{hk}), \quad m_s = \min(2l_i, s + \Delta_{hk}),$$

double integral (4.19) in this case becomes

$$\int_0^{2l_i} \tilde{w}_i^{(d_i)}(s) \int_{M_s}^{m_s} \mathbf{S}(r, t_h, t_k) \tilde{w}_j^{(d_j)}(z) dz ds. \quad (4.20)$$

The numerical quadrature in the outer variable of integration  $s$  has been optimally performed subdividing, when necessary, the outer interval of integration. In fact, the derivative with respect to  $s$  of the outer integrand function, after the inner integration, presents jumps in correspondence to possible subdivision points given by

$$s_1 = \Delta_{hk}, \quad s_2 = 2l_i - \Delta_{hk}.$$

Note that in this simple geometrical case, if  $\Delta_{hk} > 2l_i$  these points do not belong to the integration interval  $[0, 2l_i]$ ; if  $\Delta_{hk} = 2l_i$  these points coincide with the end-points of the integration interval  $[0, 2l_i]$ ; when  $0 < \Delta_{hk} < 2l_i$ ,  $\Delta_{hk} \neq l_i$  both points belong to  $[0, 2l_i]$ ; at last, when  $\Delta_{hk} = l_i$  only one point belong to the integration interval. Almost all these geometrical situations are shown in figure 4.1. Further, as an example, in figure 4.2, there is the behavior of the derivative

$$\frac{d}{ds} \left[ \int_{M_s}^{m_s} \log(\Delta_{hk} + \sqrt{\Delta_{hk}^2 - |s - z|^2}) \tilde{w}_j^{(0)}(z) dz \right],$$

referred to the domains of the previous figure. Hence, (4.20) will be eventually de-

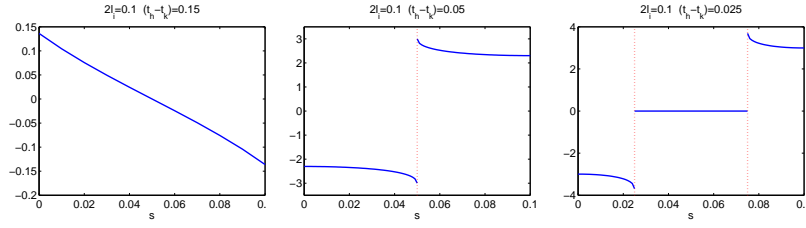


Fig. 4.2: Behavior of outer integrand function derivative for different values of  $\Delta_{hk}$ .

composed into the sum of double integrals of the form

$$\int_a^b \tilde{w}_i^{(d_i)}(s) \int_{M_s}^{m_s} \mathbf{S}(r, t_h, t_k) \tilde{w}_j^{(d_j)}(z) dz ds, \quad (4.21)$$

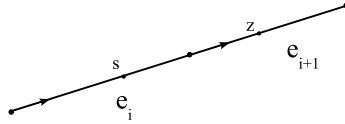
where  $[a, b] \subset [0, 2l_i]$ . Without this subdivision, one should use a lot of quadrature nodes for the outer numerical integration in order to achieve the single precision accuracy. Of course when no subdivision is needed, we will have to deal with only one double integral (4.21) where  $[a, b] \equiv [0, 2l_i]$ .

In tables 4.1-4.3 the fewer number of nodes needed to achieve single precision when using the suggested splitting is displayed in the numerical evaluation of the integral

$$\int_0^{2l_i} \tilde{w}_i^{(0)}(s) \int_{M_s}^{m_s} \log(\Delta_{hk} + \sqrt{\Delta_{hk}^2 - |s-z|^2}) \tilde{w}_j^{(0)}(z) dz ds, \quad (4.22)$$

with  $2l_i = 0.1$  and different values of  $\Delta_{hk}$  as reproduced in figures 4.1 and 4.2.

**Consecutive aligned boundary elements ( $e_j \equiv e_{i+1}$ ).<sup>1</sup>**



In this case, the distance between the source and the field point can be written as  $r = 2l_i - s + z$ ; hence the double integration domain is represented by the intersection between the rectangle  $[0, 2l_i] \times [0, 2l_{i+1}]$  and the half plane:  $z < \Delta_{hk} - 2l_i + s$ , where the Heaviside function is not trivial. This intersection will be not empty if:  $s > 2l_i - \Delta_{hk}$ . Therefore, having set

<sup>1</sup> Analogous considerations can be done for  $e_j \equiv e_{i-1}$  taking into account that the expression of the distance will be  $r = 2l_j - z + s$ .

nodes	relative error
$2^2$	$2.561123 \cdot 10^{-4}$
$4^2$	$2.225379 \cdot 10^{-7}$

Table 4.1: Relative error in numerical integration of (4.22) when  $\Delta_{hk} = 0.15$ , w.r.t. the approximated value of Mathematica  $-1.22392749 \cdot 10^{-2}$ .

nodes	relative error	nodes	relative error
$16^2$	$1.209583 \cdot 10^{-3}$	$2 \cdot (8^2)$	$1.254465 \cdot 10^{-4}$
$64^2$	$8.024902 \cdot 10^{-5}$	$2 \cdot (16^2)$	$1.685511 \cdot 10^{-5}$
$256^2$	$5.120121 \cdot 10^{-6}$	$2 \cdot (32^2)$	$2.185629 \cdot 10^{-6}$
$1024^2$	$3.123420 \cdot 10^{-7}$	$2 \cdot (64^2)$	$2.693816 \cdot 10^{-7}$

Table 4.2: Relative error in numerical integration of (4.22) when  $\Delta_{hk} = 0.05$ , w.r.t. the approximated value of Mathematica  $-1.80100286 \cdot 10^{-2}$ , on the left, without splitting and, on the right, with the foreseen splitting in two subintervals.

nodes	relative error	nodes	relative error
$16^2$	$2.409610 \cdot 10^{-3}$	$3 \cdot (8^2)$	$1.652040 \cdot 10^{-4}$
$64^2$	$2.141951 \cdot 10^{-5}$	$3 \cdot (16^2)$	$2.300028 \cdot 10^{-5}$
$256^2$	$2.029314 \cdot 10^{-6}$	$3 \cdot (32^2)$	$3.500234 \cdot 10^{-6}$
$1024^2$	$6.630974 \cdot 10^{-7}$	$3 \cdot (64^2)$	$9.424377 \cdot 10^{-7}$

Table 4.3: Relative error in numerical integration of (4.22) when  $\Delta_{hk} = 0.025$ , w.r.t. the approximated value of Mathematica  $-1.35973737 \cdot 10^{-2}$ , on the left, without splitting and, on the right, with the foreseen splitting in three subintervals.

$$s_0 = \max(0, 2l_i - \Delta_{hk}), \quad m_s = \min(2l_{i+1}, \Delta_{hk} - 2l_i + s),$$

double integral (4.19) in this case becomes

$$\int_{s_0}^{2l_i} \tilde{w}_i^{(d_i)}(s) \int_0^{m_s} \mathbf{S}(r, t_h, t_k) \tilde{w}_j^{(d_j)}(z) dz ds. \quad (4.23)$$

The numerical quadrature in the outer variable of integration  $s$  has been optimally performed subdividing, when necessary, the outer interval of integration. In fact, the derivative with respect to  $s$  of the outer integrand function, after the inner integration, presents a jump in correspondence to a possible subdivision point given by

$$s_1 = 2l_{i+1} + 2l_i - \Delta_{hk}.$$

Note that in this geometrical case, is simple to verify that if  $\Delta_{hk} < 2l_{i+1} \vee \Delta_{hk} > 2l_i + 2l_{i+1}$  this point does not belong to the integration interval  $[s_0, 2l_i]$ , while if  $2l_{i+1} < \Delta_{hk} < 2l_i + 2l_{i+1}$ ,  $s_1$  breaks in two subintervals the outer integration interval  $[s_0, 2l_i]$ . Some of these geometrical situations are shown in figure 4.3 for different values of  $\Delta_{hk}$  and fixed lengths  $2l_{i+1} > 2l_i$ . Further, as an example, in figure 4.4 there

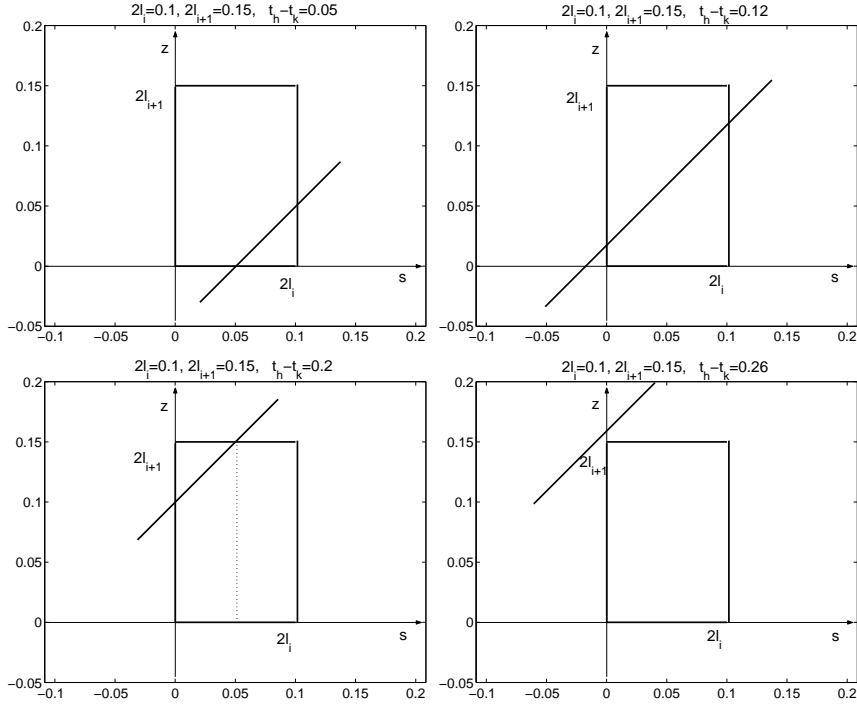


Fig. 4.3: Rectangle  $[0, 2l_i] \times [0, 2l_{i+1}]$  (consecutive aligned elements) and straight line  $z = \Delta_{hk} - 2l_i + s$  for different values of  $\Delta_{hk}$ .

is the behavior of the derivative

$$\frac{d}{ds} \left[ \int_0^{m_s} \log(\Delta_{hk} + \sqrt{\Delta_{hk}^2 - |s-z|^2}) \tilde{w}_j^{(0)}(z) dz \right],$$

referred to the domains of the previous figure. Hence, (4.23) will be eventually decomposed into the sum of double integrals of the form

$$\int_a^b \tilde{w}_i^{(d_i)}(s) \int_0^{m_s} \mathbf{S}(r, t_h, t_k) \tilde{w}_j^{(d_j)}(z) dz ds, \quad (4.24)$$

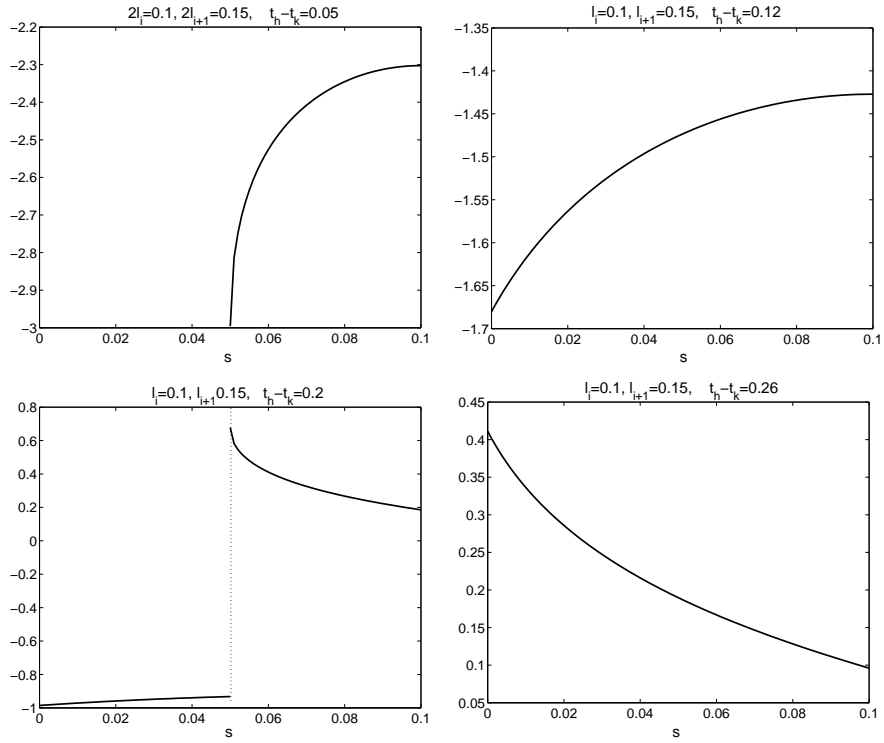
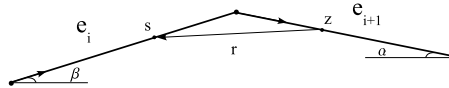


Fig. 4.4: Behavior of outer integrand function derivative for different values of  $\Delta_{hk}$ .

where  $[a, b] \subset [s_0, 2l_i]$ . Of course when no subdivision is needed, we will have to deal with only one double integral (4.24) where  $[a, b] \equiv [s_0, 2l_i]$ .

**Consecutive not aligned boundary elements ( $e_j \equiv e_{i+1}$ ).<sup>2</sup>**



In this case, having set  $\omega = \alpha + \beta$ ,  $0 < \omega < \pi$ , the distance between the source and the field point can be written as

$$r^2 = (2l_i - s)^2 + z^2 + 2(2l_i - s)z \cos \omega;$$

<sup>2</sup> Analogous considerations can be done for  $e_j \equiv e_{i-1}$  taking into account that the equation for the distance will be  $r^2 = (2l_j - z)^2 + s^2 + 2(2l_j - z)s \cos \omega$ .

hence the double integration domain is represented by the intersection between the rectangle  $[0, 2l_i] \times [0, 2l_{i+1}]$  and the elliptic domain  $r^2 - \Delta_{hk}^2 < 0$  centered in the unique singularity point  $(2l_i, 0)$ , where the Heaviside function is not trivial. The directions of the two axes of the ellipsis are  $(1, 1)$  and  $(-1, 1)$  with semi-length respectively  $(1 - \cos \omega)^{-1/2}$  and  $(1 + \cos \omega)^{-1/2}$ . Of course, when  $0 < \cos \omega < 1$  the major axis will be oriented in direction  $(1, 1)$ , when  $-1 < \cos \omega < 0$  the major axis will be oriented in direction  $(-1, 1)$ , when  $\cos \omega = 0$  the ellipsis becomes a circle. Note that the angle  $\theta = \pi - \omega$  between contiguous elements determines the eccentricity, while the increasing parameter  $\Delta_{hk}$  determines a dilation of the ellipsis. In figure 4.5, there are various types of intersections, i.e. double integration domains, for different values of  $\Delta_{hk}$  and different angles  $\theta$  between contiguous elements. Note

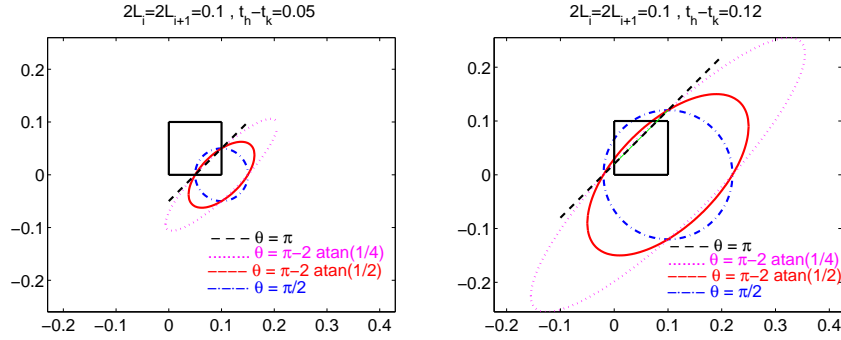


Fig. 4.5: Double integration domain (contiguous elements) for different values of  $\Delta_{hk}$  and different angles  $\theta$ .

that the inequality  $z^2 + 2(2l_i - s)z \cos \omega + (2l_i - s)^2 - \Delta_{hk}^2 < 0$  can be satisfied if and only if

$$\Delta_{hk}^2 - (2l_i - s)^2 \sin^2 \omega > 0 \quad \Leftrightarrow \quad 2l_i - \frac{\Delta_{hk}}{\sin \omega} < s < 2l_i + \frac{\Delta_{hk}}{\sin \omega}.$$

For  $s \in (0, 2l_i)$  the upper limitation for the outer variable of integration is always satisfied; then, under the restriction

$$s > 2l_i - \frac{\Delta_{hk}}{\sin \omega},$$

the inequality will be satisfied for

$$z_1^s < z < z_2^s,$$

where

$$z_{1,2}^s = -(2l_i - s) \cos \omega \mp \sqrt{\Delta_{hk}^2 - (2l_i - s)^2 \sin^2 \omega}.$$



Therefore, having set

$$s_0 = \max\left(0, 2l_i - \frac{\Delta_{hk}}{\sin \omega}\right), \quad M_s = \max(0, z_1^s), \quad m_s = \min(2l_{i+1}, z_2^s),$$

double integral (4.19) in this case becomes

$$\int_{s_0}^{2l_i} \tilde{w}_i^{(d_i)}(s) \int_{M_s}^{m_s} \mathbf{S}(r, t_h, t_k) \tilde{w}_j^{(d_j)}(z) dz ds. \quad (4.25)$$

The numerical quadrature in the outer variable of integration  $s$  has been optimally performed subdividing, when necessary, the outer interval of integration. In fact, also in this case, the derivative with respect to  $s$  of the outer integrand function, after the inner integration, presents a jump in correspondence to possible subdivision points to be searched among the solutions of the equations

$$z_1^s = 0, \quad z_2^s = 2l_{i+1},$$

formally given by

$$s_1^{1,2} = 2l_i \mp \Delta_{hk}, \quad s_2^{1,2} = 2l_i + 2l_{i+1} \cos \omega \mp \sqrt{\Delta_{hk}^2 - (2l_{i+1})^2 \sin^2 \omega}.$$

Note that  $s_1^2 \in [s_0, 2l_i]$  and solutions  $s_2^{1,2}$  are real under the restriction  $\Delta_{hk} > 2l_{i+1} \sin \omega$ .

With a deeper analysis, one obtains that:

- for  $0 < \omega < \pi/2$

only  $s_2^1$  breaks the outer integration interval  $[s_0, 2l_i]$  in two subintervals when:

$$2l_{i+1} < \Delta_{hk} < \sqrt{(2l_i)^2 + (2l_{i+1})^2 + 2(2l_i)(2l_{i+1}) \cos \omega};$$

- for  $\pi/2 < \omega < \pi$ , it happens that:

$$-s_1^1 \in [s_0, 2l_i] \text{ when } \Delta_{hk} < 2l_i;$$

$$-s_2^1 \in [s_0, 2l_i] \text{ if } \cos \omega > -\frac{2l_i}{2l_{i+1}}, \text{ when}$$

$$2l_{i+1} \sin \omega < \Delta_{hk} < \min\{2l_{i+1} \tan \omega, \sqrt{(2l_i)^2 + (2l_{i+1})^2 + 2(2l_i)(2l_{i+1}) \cos \omega}\};$$

$$-s_2^2 \in [s_0, 2l_i] \text{ when } 2l_{i+1} \sin \omega < \Delta_{hk} < 2l_{i+1}, \text{ if } \cos \omega > -\frac{2l_i}{2l_{i+1}} \text{ otherwise}$$

$$\text{when } \max\{2l_{i+1} \sin \omega, \sqrt{(2l_i)^2 + (2l_{i+1})^2 + 2(2l_i)(2l_{i+1}) \cos \omega}\} < \Delta_{hk} < 2l_{i+1}.$$

Hence, (4.25) will be eventually decomposed into the sum of double integrals of the form

$$\int_a^b \tilde{w}_i^{(d_i)}(s) \int_{M_s}^{m_s} \mathbf{S}(r, t_h, t_k) \tilde{w}_j^{(d_j)}(z) dz ds, \quad (4.26)$$

where  $[a, b] \subset [s_0, 2l_i]$ . Of course, when no subdivision is needed, one will have to deal with only one double integral (4.26) where  $[a, b] \equiv [s_0, 2l_i]$ . Note that for some values of  $s$  it could happen that  $m_s - M_s \leq 0$ : in this case the inner integral does not give any contribution to the final result and its evaluation has to be avoided.

**Disjoint elements** ( $\bar{e}_i \cap \bar{e}_j = \emptyset$ ) are investigated in appendix A.2.

### 4.3 Basic quadrature rules

To numerically evaluate double space integrals we need to use certain basic quadrature rules here briefly recalled.

1. A quadrature formula widely used to generate Galerkin matrix elements is a rule introduced in [46], that efficiently integrates functions with weak singularities at the end-points of the integration interval. In fact classical Gauss-Legendre formula, very accurate for regular integrands, loses its efficiency in presence of mild singularities of the integrand functions.

Let consider an integral of the form  $\int_0^1 f(s) ds$  where  $f(s)$  presents weak singularities at the end-points of the integration interval. Introducing a change of variable  $s = \varphi(\tilde{s})$  mapping  $(0, 1)$  onto itself, with  $\varphi'(\tilde{s}) \geq 0$ , then

$$\int_0^1 f(s) ds = \int_0^1 f(\varphi(\tilde{s})) \varphi'(\tilde{s}) d\tilde{s} \equiv \int_0^1 F(\tilde{s}) d\tilde{s}. \quad (4.27)$$

Further if

$$\varphi^{(i)}(0) = 0, \quad \varphi^{(j)}(1) = 0, \quad i = 1, \dots, p-1, \quad j = 1, \dots, q-1 \quad (4.28)$$

the function  $F(\tilde{s})$  in (4.27) can be made as smooth as we like, simply choosing integers  $p, q$  sufficiently large, to then use for the last integral in (4.27) the Gauss-Legendre rule. In the following the transformation considered will be the one proposed in [46]

$$\varphi(\tilde{s}) = \frac{(p+q-1)!}{(p-1)!(q-1)!} \int_0^{\tilde{s}} u^{p-1} (1-u)^{q-1} du, \quad p, q \geq 1. \quad (4.29)$$

Integral in (4.29) can be efficiently evaluated by a  $n$ -points Gauss-Legendre formula, with  $n = \lfloor \frac{p+q}{2} \rfloor$ .

The convergence rates related to this formula depends on convergence theorems for

the Gauss-Legendre formula when the integrand function is particularly regular at the endpoints of the domain of integration. For a deeper analysis refer to [46].

2. Another kind of quadrature rules used in the following section is the interpolatory type one, based on the zeros of Legendre polynomials. They are of the form

$$\int_{-1}^1 S(y,x)f(x) dx = \sum_{k=1}^n w_k(y)f(x_k) + R_n(f;y), \quad (4.30)$$

and are obtained by replacing  $f(x)$  by its Lagrange polynomial, of degree  $n-1$ , associated with the nodes  $\{x_k\}$ , which are the very familiar zeros of the Legendre polynomial  $P_n(x)$ , of degree  $n$  [51]. For the coefficients  $\{w_k\}$  the following expression can be easily derived [23]:

$$w_k(y) = \frac{1}{2} \lambda_k \sum_{i=0}^{n-1} (2i+1) \mu_i(y) P_i(x_k) \quad (4.31)$$

where  $\{\lambda_k\}$  denote the classical Christoffel numbers associated with the  $n$ -points Gauss-Legendre formula

$$\int_{-1}^1 f(x) dx \approx \sum_{k=1}^n \lambda_k f(x_k), \quad (4.32)$$

$P_i(x)$  is the  $i$ -th degree Legendre polynomial, and  $\mu_i(y)$  is the so-called *modified moment* of the kernel  $S(y,x)$ :

$$\mu_i(y) = \int_{-1}^1 S(y,x) P_i(x) dx. \quad (4.33)$$

The rule (4.30) has degree of exactness  $n-1$ , i.e. it is exact whenever  $f(x)$  is a polynomial of degree  $n-1$ . Expression (4.31) reduces the evaluation of  $w_k(y)$  to the knowledge of modified moments recurrence relationships which stem from the well-known three-term recurrence satisfied by Legendre polynomials [5]. The kernels  $S(y,x)$  of interest in this paper are:  $\ln(|x-a_y|)$ ,  $\ln[(x-a_y)^2 + b_y^2]$ , with  $b_y \neq 0$ , rational function containing factors of the type  $(x-a_y)$  and divisors of the type  $(x-a_y)$  and  $[(x-a_y)^2 + b_y^2]$ . Recurrence relations giving (4.33) are reported in appendix A.3.

For convergence properties of product rules, one can refer to the theorem in [6]:

**Theorem 25** Let  $f \in C^p[-1, 1]$  with  $f^{(p)} \in H_\mu[-1; 1]^3$  for some  $0 < \mu \leq 1$ . Then, if  $\int_{-1}^1 |S(y, x)|^2 dx \leq C$  for all  $y \in [-1, 1]$ ,

$$R_n(f; y) = O(n^{-p-\mu})$$

uniformly for  $y \in [-1, 1]$ . When  $S(y, x) = 1/(x - y)$ ,

$$R_n(f; y) \leq cn^{-p-\mu} \log n \begin{cases} (1-y^2)^{-1/4} \log \frac{1}{1-y^2} & |y| < 1 \\ (y^2-1)^{-1/4} & |y| > 1 \end{cases}$$

where the constant  $c$  is independent of  $n$  and  $y$ .

**3.** A third type of rule we shall need in the following is a quadrature formula for Hadamard finite-part integrals [45]:

$$\int_0^1 \frac{f(s)}{s} ds = w_0^{GR} f(0) + \sum_{k=1}^n w_k^{GR} f(s_k^{GR}) + R_n^{GR}(f) \quad (4.34)$$

$$s_k^{GR} = \frac{1+x_k}{2} \quad w_k^{GR} = \frac{\lambda_k}{2s_k} \quad k = 1, \dots, n \quad w_0^{GR} = -\sum_{k=1}^n w_k^{GR},$$

where  $x_k, \lambda_k$  are in (4.32). This rule is obtained by replacing  $f(x)$  by its  $n - th$  degree interpolation polynomial associated with the nodes  $\{0, s_1, \dots, s_n\}$ . It is a Gauss-Radau type quadrature formula, i.e. it is exact whenever  $f(x)$  is a polynomial of degree  $\leq 2n$ . The convergence property of this HFP quadrature rule can be found in [45]:

**Theorem 26** Let  $f \in C^p[0, 1]$ ,  $p \geq 1$ , with  $f^{(p)} \in H_\mu[0; 1]$  for some  $0 < \mu \leq 1$ . Then

$$R_n^{GR}(f) = O(n^{-p-\mu}).$$

#### 4.4 Numerical integration schemes

Before going into the details of numerical quadrature schemes used to integrate singular kernels, observe that in (4.12) and (4.16) there is also another function, i.e.  $\log(\Delta_{hk} + \sqrt{\Delta_{hk}^2 - r^2})$  which of course is not singular for  $r \rightarrow 0$ : nevertheless the inner numerical integration of this function has to be performed carefully even on couples of disjoint elements, when the boundary of the two dimensional region  $r < \Delta_{hk}$ , where the Heaviside function is not trivial, is contained in the rectangle  $[0, 2l_i] \times [0, 2l_j]$ .

The problem we have to deal with is due to the presence of the square root function

<sup>3</sup>  $H_\mu$  denotes the space of Hölder continuous functions of order  $\mu$ .

$\sqrt{\Delta_{hk}^2 - r^2}$ . I'm going to illustrate this issue for the case of the double integration over a couple of coincident elements  $e_i \equiv e_j$  of length  $2l_i$ , where  $r = |s - z|$  in the local variables of integration  $s, z \in (0, 2l_i)$ . The argument of  $\sqrt{\Delta_{hk}^2 - |s - z|^2}$  is always positive but it can assume very small values and in the limit for the argument tending to zero the derivative of the square root with respect to the inner variable of integration  $z$  becomes unbounded. This behavior happens along the oblique boundary of the double integration domain, as shown in figure 4.6 for different values of  $\Delta_{hk}$ , and produces a bad performance in the evaluation of

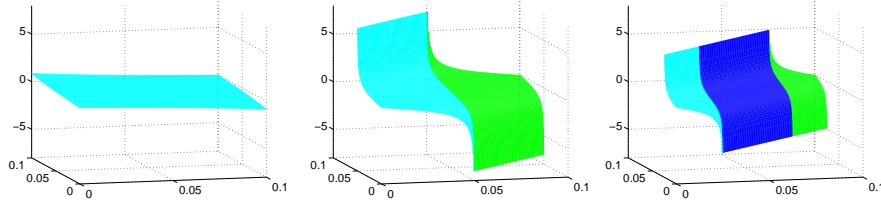


Fig. 4.6: Behavior of  $\frac{\partial}{\partial z} \sqrt{\Delta_{hk}^2 - |s - z|^2}$  for  $\Delta_{hk} = 0.15, 0.05, 0.025$ .

$$\int_a^b \tilde{w}_i^{(0)}(s) \int_{M_s}^{m_s} \log(\Delta_{hk} + \sqrt{\Delta_{hk}^2 - |s - z|^2}) \tilde{w}_j^{(0)}(z) dz ds, \quad (4.35)$$

even of classical Gauss-Legendre quadrature formula, in the sense that one should use a lot of quadrature nodes to achieve the single precision accuracy. To overcome this difficulty, consider, for the inner integration, the regularization procedure (4.27), which suitably pushes the Gaussian nodes towards the end-points of the interval  $[M_s, m_s]$  and modify the Gaussian weights in order to regularize integrand functions with mild boundary “singularities”. The outer integral is performed with a classical Gauss-Legendre rule. In figure 4.7, the computational costs of Gaussian quadrature formula alone and regularization procedure just explained are shown in relation to the achievement of the single precision accuracy (horizontal line) in the evaluation of the double integral (4.35) for  $\Delta_{hk} = 0.15, 0.05, 0.025$ . The presence of the square root function together with singular kernels forces to adopt the above procedure for the numerical treatment of double integrals of those kernels on disjoint elements, while on coincident and consecutive elements we will have to treat strong singularities and hyper singularities together with the “mild” singularities of  $\sqrt{\Delta_{hk}^2 - r^2}$ .

Looking at (4.12), (4.14) and (4.16), I have here to consider, up to suitable constants, the numerical treatment of kernels of the type

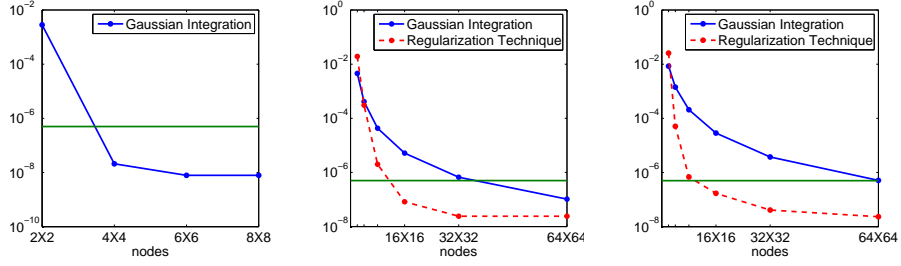


Fig. 4.7: Computational cost of Gaussian quadrature and regularization procedure, for  $\Delta_{hk} = 0.15, 0.05, 0.025$ .

$$\log r, \quad \frac{\mathbf{r} \cdot \mathbf{n}_\xi}{r^2} \sqrt{\Delta_{hk}^2 - r^2}, \quad \left[ \frac{\mathbf{r} \cdot \mathbf{n}_x \mathbf{r} \cdot \mathbf{n}_\xi}{r^2} - \frac{\mathbf{n}_x \cdot \mathbf{n}_\xi}{2} \right] \frac{\sqrt{\Delta_{hk}^2 - r^2}}{r^2}, \quad (4.36)$$

which present weak, Cauchy type and hyper singularities respectively when  $r \rightarrow 0$ ; hence these types of singularities arise in the double integration over coincident or adjacent boundary elements, while they haven't to be considered on a couple of disjoint elements.

#### CASE I: $\log(r)$ kernel

##### Coincident boundary elements:

we have to numerically evaluate

$$\int_a^b \tilde{w}_i^{(d_i)}(s) \int_{M_s}^{m_s} \log(|z-s|) \tilde{w}_j^{(d_j)}(z) dz ds. \quad (4.37)$$

*Outer integral:* regularization procedure (4.27)

*Inner integral:*  $(d_j + 1)$ -points product rule (4.30) for logarithmic kernel

##### Consecutive aligned boundary elements:

defining  $a_s = s - 2l_i$ , we have to numerically evaluate

$$\int_a^b \tilde{w}_i^{(d_i)}(s) \int_0^{m_s} \log(|z-a_s|) \tilde{w}_j^{(d_j)}(z) dz ds. \quad (4.38)$$

- If  $b = 2l_i$

*Outer integral:* regularization procedure (4.27)

*Inner integral:*  $(d_j + 1)$ -points product rule (4.30) for logarithmic kernel

- if  $b \neq 2l_i$

*Outer integral:* Gauss-Legendre formula

*Inner integral:* Gauss-Legendre formula

**Consecutive not aligned boundary elements:**

having set  $a_s = -(2l_i - s) \cos \omega$  and  $b_s = (2l_i - s) \sin \omega$ , we have to numerically evaluate

$$\frac{1}{2} \int_a^b \tilde{w}_i^{(d_i)}(s) \int_{M_s}^{m_s} \log[(z - a_s)^2 + b_s^2] \tilde{w}_j^{(d_j)}(z) dz ds. \quad (4.39)$$

- If  $b = 2l_i$  and  $M_s = 0$

*Outer integral:* regularization procedure (4.27)

*Inner integral:*  $(d_j + 1)$ -points product rule (4.30) for logarithmic kernel

- if  $b \neq 2l_i$  or  $M_s \neq 0$

*Outer integral:* Gauss-Legendre formula

*Inner integral:* Gauss-Legendre formula

$$\text{CASE II: } \frac{\mathbf{r} \cdot \mathbf{n}_\xi}{r^2} \sqrt{\Delta_{hk}^2 - r^2} \text{ kernel}$$

Note that, due to the presence of the scalar product  $\mathbf{r} \cdot \mathbf{n}_\xi$ , the coincident and consecutive aligned elements cases have not to be considered.

**Consecutive not aligned boundary elements:**

having set  $a_s = -(2l_i - s) \cos \omega$  and  $b_s = (2l_i - s) \sin \omega$ , we have to numerically evaluate

$$\int_a^b \tilde{w}_i^{(d_i)}(s) \int_{M_s}^{m_s} \frac{-b_s}{(z - a_s)^2 + b_s^2} \sqrt{\Delta_{hk}^2 - ((z - a_s)^2 + b_s^2)} \tilde{w}_j^{(d_j)}(z) dz ds. \quad (4.40)$$

Two subcases arise:

**a) the boundary of the two dimensional region  $r < \Delta_{hk}$  is not contained in the rectangle  $[a, b] \times [M_s, m_s]$ , i.e.  $M_s = 0$ ,  $m_s = 2l_{i+1}$**

- If  $b = 2l_i$

*Outer integral:* regularization procedure (4.27)

*Inner integral:* product rule (4.30) for  $[(z - a_s)^2 + b_s^2]^{-1}$  kernel.

- If  $b \neq 2l_i$

*Outer integral:* Gauss-Legendre formula

*Inner integral:* Gauss-Legendre formula

**b) the boundary of the two dimensional region  $r < \Delta_{hk}$  is contained in the rectangle  $[a, b] \times [M_s, m_s]$**

• If  $b = 2l_i$  and  $M_s = 0$

we can rewrite the double integral (4.40) adding and subtracting in the interior integral the Taylor expansion of second order centered in  $(s, z) = (2l_i, 0)$  of the function

$\sqrt{\Delta_{hk}^2 - ((z - a_s)^2 + b_s^2)} \tilde{w}_j^{(d_j)}(z)$ :

$$\begin{aligned} & - \int_a^{2l_i} b_s \tilde{w}_i^{(d_i)}(s) \int_0^{m_s} \frac{\sqrt{\Delta_{hk}^2 - ((z - a_s)^2 + b_s^2)} \tilde{w}_j^{(d_j)}(z) - \Delta_{hk} \tilde{w}_j^{(d_j)}(0) - \Delta_{hk} \tilde{w}_j^{(d_j)}(0) z}{(z - a_s)^2 + b_s^2} dz ds \\ & + \Delta_{hk} \tilde{w}_j^{(d_j)}(0) \int_a^{2l_i} -b_s \tilde{w}_i^{(d_i)}(s) \int_0^{m_s} \frac{1}{(z - a_s)^2 + b_s^2} dz ds \\ & + \Delta_{hk} \tilde{w}_j^{(d_j)}(0) \int_a^{2l_i} -b_s \tilde{w}_i^{(d_i)}(s) \int_0^{m_s} \frac{z}{(z - a_s)^2 + b_s^2} dz ds \\ & =: I_1 + I_2 + I_3. \end{aligned}$$

For the numerical evaluation of  $I_1$

*Outer integral:* Gauss-Legendre formula

*Inner integral:* regularization procedure (4.27), because of the square root “mild” singularity

For  $I_2$ , after an analytical inner integration:

$$I_2 = -\Delta_{hk} \tilde{w}_j^{(d_j)}(0) \int_a^{2l_i} \tilde{w}_i^{(d_i)}(s) \left[ \arctan\left(\frac{m_s - a_s}{b_s}\right) + \arctan\left(\frac{a_s}{b_s}\right) \right] ds$$

and we can use a Gauss-Legendre formula.

For  $I_3$ , after an analytical inner integration:

$$\begin{aligned} I_3 & = -\Delta_{hk} \tilde{w}_j^{(d_j)}(0) \int_a^{2l_i} \tilde{w}_i^{(d_i)}(s) a_s \left[ \arctan\left(\frac{m_s - a_s}{b_s}\right) + \arctan\left(\frac{a_s}{b_s}\right) \right] ds \\ & \quad - \Delta_{hk} \tilde{w}_j^{(d_j)}(0) \int_a^{2l_i} \tilde{w}_i^{(d_i)}(s) \frac{b_s}{2} \left[ \log((m_s - a_s)^2 + b_s^2) - \log(a_s^2 + b_s^2) \right] ds \\ & =: I_3^1 + I_3^2. \end{aligned}$$



For the numerical evaluation of  $I_3^1$  we can use a Gauss-Legendre formula, while for  $I_3^2$  we can use regularization procedure (4.27), because of the logarithmic “mild” singularities.

Tables 4.4 and 4.5 are referred to the discretization parameters  $\omega = \pi/2$ ,  $2l_i = 2l_{i+1} = 0.1$ ,  $\Delta_{hk} = 0.05$ ,  $d_i = 0$ ,  $d_j = 1$  (in the considered case,  $I_2 = 0$  because  $\tilde{\omega}_j^{(1)}(0) = 0$  and  $I_3^1 = 0$  because  $\cos \omega = 0$ ).

nodes	$p = q = 1$	$p = q = 2$	$p = q = 3$
$4^2$	$1.098022 \cdot 10^{-6}$	$2.118745 \cdot 10^{-7}$	$4.748094 \cdot 10^{-8}$
$8^2$	$1.824366 \cdot 10^{-7}$	$7.264172 \cdot 10^{-9}$	$7.741366 \cdot 10^{-9}$
$16^2$	$2.558711 \cdot 10^{-8}$	$2.437165 \cdot 10^{-10}$	$2.444638 \cdot 10^{-10}$
$32^2$	$3.379819 \cdot 10^{-9}$	$3.301006 \cdot 10^{-12}$	$3.299448 \cdot 10^{-12}$

Table 4.4: Relative Error w.r.t. the integral value  $I_1 = 3.315728 \cdot 10^{-4}$  evaluated with Mathematica.

nodes	$p = 1, q = 1$	$p = 1, q = 2$	$p = 1, q = 3$
8	$1.956603 \cdot 10^{-4}$	$6.938891 \cdot 10^{-7}$	$1.205578 \cdot 10^{-7}$
16	$1.372090 \cdot 10^{-5}$	$1.132429 \cdot 10^{-7}$	$1.105648 \cdot 10^{-7}$
32	$1.011936 \cdot 10^{-6}$	$1.105737 \cdot 10^{-7}$	$1.105621 \cdot 10^{-7}$
64	$1.686180 \cdot 10^{-7}$	$1.105622 \cdot 10^{-7}$	$1.105621 \cdot 10^{-7}$

Table 4.5: Relative Error w.r.t. the integral value  $I_3^2 = 9.947183 \cdot 10^{-4}$  evaluated with Mathematica.

- Otherwise, i.e. the singularity point is not contained in the domain of integration, for the numerical evaluation of (4.40) we can proceed as follows:

*Outer integral:* Gauss-Legendre formula

*Inner integral:* regularization procedure (4.27), because of the square root “mild” singularity.

$$\text{CASE III: } \left[ \frac{\mathbf{r} \cdot \mathbf{n}_x \mathbf{r} \cdot \mathbf{n}_\xi}{r^2} - \frac{\mathbf{n}_x \cdot \mathbf{n}_\xi}{2} \right] \frac{\sqrt{\Delta_{hk}^2 - r^2}}{r^2} \text{ kernel}$$

#### Coincident boundary elements:

note that in this configuration  $\mathbf{r} \cdot \mathbf{n}_x = \mathbf{r} \cdot \mathbf{n}_\xi = 0$  and  $\mathbf{n}_x \cdot \mathbf{n}_\xi = 1$ ; we have to numerically evaluate

$$\int_a^b \tilde{w}_i^{(d_i)}(s) \int_{M_s}^{m_s} -\frac{\sqrt{\Delta_{hk}^2 - r^2}}{2r^2} \tilde{w}_j^{(d_j)}(z) dz ds. \quad (4.41)$$

Two subcases arise:

**a) the boundary of the two dimensional region  $r < \Delta_{hk}$  is not contained in the rectangle  $[a, b] \times [M_s, m_s]$ , i.e.  $M_s = 0, m_s = 2l_i$**

we can rewrite the double integral (4.41) adding and subtracting in the interior integral the Taylor expansion of first order centered in  $z = s$  of the function  $\sqrt{\Delta_{hk}^2 - |z - s|^2} \tilde{w}_j^{(d_j)}(z)$ <sup>4</sup>:

$$\begin{aligned} & - \int_a^b \tilde{w}_i^{(d_i)}(s) \int_{M_s}^{m_s} \frac{\sqrt{\Delta_{hk}^2 - |z - s|^2} \tilde{w}_j^{(d_j)}(z) - \Delta_{hk} \tilde{w}_j^{(d_j)}(s)}{2|z - s|^2} dz ds + \\ & - \frac{\Delta_{hk}}{2} \int_a^b \tilde{w}_i^{(d_i)}(s) \tilde{w}_j^{(d_j)}(s) \int_{M_s}^{m_s} \frac{1}{|z - s|^2} dz ds =: I_1 + I_2. \end{aligned}$$

For the numerical evaluation of  $I_1$

*Outer integral:* regularization procedure (4.27)

*Inner integral:* product rule (4.30) for  $[(z - a_s)^2 + b_s^2]^{-1}$  kernel

For  $I_2$ , after an analytical inner integration:

$$I_2 = -\frac{\Delta_{hk}}{2} \int_a^b \tilde{w}_i^{(d_i)}(s) \tilde{w}_j^{(d_j)}(s) \left[ \frac{1}{s - m_s} - \frac{1}{s - M_s} \right] ds =: I_2^1 + I_2^2.$$

If  $m_s = 2l_i$  and  $b = 2l_i$ , then  $I_2^1$  can be evaluated by the HFP formula (4.34) otherwise with the Gauss-Legendre formula.

If  $M_s = 0$  and  $a = 0$  then  $I_2^2$  can be evaluated by the HFP formula (4.34) otherwise with the Gauss-Legendre formula.

**b) the boundary of the two dimensional region  $r < \Delta_{hk}$  is contained in the rectangle  $[a, b] \times [M_s, m_s]$**

we can rewrite the double integral (4.41) adding and subtracting in the interior integral the Taylor expansion of second order centered in  $z = s$  of the two variables function  $\sqrt{\Delta_{hk}^2 - |z - s|^2} \tilde{w}_j^{(d_j)}(z)$ :

---

<sup>4</sup> Note that here, and in the following cases a), the expansion subtracted has order one to satisfy for the difference the hypothesis of theorem 25; in cases b) one or two more terms will be subtracted, this because it is important to have the interior integral with at most weak singularities at the endpoints of the domain of integration for the convergence of the regularization procedure (4.27).

$$\begin{aligned}
& - \int_a^b \tilde{w}_i^{(d_i)}(s) \int_{M_s}^{m_s} \frac{\sqrt{\Delta_{hk}^2 - |z-s|^2} \tilde{w}_j^{(d_j)}(z) - \Delta_{hk} \tilde{w}_j^{(d_j)}(s) - \Delta_{hk} \tilde{w}_j^{\prime(d_j)}(s)(z-s)}{2|z-s|^2} dz ds \\
& - \frac{\Delta_{hk}}{2} \int_a^b \tilde{w}_i^{(d_i)}(s) \tilde{w}_j^{(d_j)}(s) \int_{M_s}^{m_s} \frac{1}{|z-s|^2} dz ds \\
& - \frac{\Delta_{hk}}{2} \int_a^b \tilde{w}_i^{(d_i)}(s) \tilde{w}_j^{\prime(d_j)}(s) \int_{M_s}^{m_s} \frac{1}{|z-s|} dz ds \\
& =: I_1 + I_2 + I_3.
\end{aligned}$$

For the numerical evaluation of  $I_1$

*Outer integral:* Gauss-Legendre formula

*Inner integral:* regularization procedure (4.27), because of the square root ‘‘mild’’ singularity

For  $I_2$ , after an analytical inner integration:

$$I_2 = -\frac{\Delta_{hk}}{2} \int_a^b \tilde{w}_i^{(d_i)}(s) \tilde{w}_j^{(d_j)}(s) \left[ \frac{1}{s-m_s} - \frac{1}{s-M_s} \right] ds =: I_2^1 + I_2^2.$$

If  $m_s = 2l_i$  and  $b = 2l_i$  then  $I_2^1$  can be evaluated by the HFP formula (4.34) otherwise with the Gauss-Legendre formula.

If  $M_s = 0$  and  $a = 0$  then  $I_2^2$  can be evaluated by the HFP formula (4.34) otherwise with the Gauss-Legendre formula.

For  $I_3$ , after an analytical inner integration:

$$I_3 = -\frac{\Delta_{hk}}{2} \int_a^b \tilde{w}_i^{(d_i)}(s) \tilde{w}_j^{\prime(d_j)}(s) [\log|m_s - s| - \log|M_s - s|] ds =: I_3^1 + I_3^2.$$

If  $m_s = 2l_i$  and  $b = 2l_i$  then  $I_3^1$  can be evaluated by the regularization procedure (4.27) otherwise with the Gauss-Legendre formula only.

If  $M_s = 0$  and  $a = 0$  then  $I_3^2$  can be evaluated by the regularization procedure (4.27) otherwise with the Gauss-Legendre formula only.

**Consecutive aligned boundary elements:**

defining  $a_s = s - 2l_i$ , we have to numerically evaluate

$$\int_a^b \tilde{w}_i^{(d_i)}(s) \int_0^{m_s} \frac{\sqrt{\Delta_{hk}^2 - (z - a_s)^2}}{2(z - a_s)^2} \tilde{w}_j^{(d_j)}(z) dz ds. \quad (4.42)$$

Two subcases arise:

**a) the boundary of the two dimensional region  $r < \Delta_{hk}$  is not contained in the rectangle  $[a, b] \times [M_s, m_s]$ , i.e.  $b = 2l_i$ ,  $M_s = 0$ ,  $m_s = 2l_{i+1}$**

we can rewrite the double integral (4.42) adding and subtracting in the interior integral the Taylor expansion of first order centered in  $(s, z) = (2l_i, 0)$  of the function  $\sqrt{\Delta_{hk}^2 - (z - a_s)^2} \tilde{w}_j^{(d_j)}(z)$ :

$$\begin{aligned} & - \int_a^{2l_i} \tilde{w}_i^{(d_i)}(s) \int_0^{m_s} \frac{\sqrt{\Delta_{hk}^2 - (z - a_s)^2} \tilde{w}_j^{(d_j)}(z) - \Delta_{hk} \tilde{w}_j^{(d_j)}(0)}{2(z - a_s)^2} dz ds + \\ & - \frac{\Delta_{hk}}{2} \tilde{w}_j^{(d_j)}(0) \int_a^{2l_i} \tilde{w}_i^{(d_i)}(s) \int_0^{m_s} \frac{1}{(z - a_s)^2} dz ds =: I_1 + I_2. \end{aligned}$$

For the numerical evaluation of  $I_1$

*Outer integral:* regularization procedure (4.27)

*Inner integral:* product rule (4.30) for  $[z - a_s]^{-1}$

For  $I_2$ , after an analytical inner integration:

$$I_2 = -\frac{\Delta_{hk}}{2} \tilde{w}_j^{(d_j)}(0) \int_a^{2l_i} \tilde{w}_i^{(d_i)}(s) \left[ \frac{1}{2l_i - s} - \frac{1}{2l_i - s + m_s} \right] ds =: I_2^1 + I_2^3$$

$I_2^1$  can be evaluated by the HFP formula (4.34) and  $I_2^3$  with the Gauss-Legendre formula.

**b) the boundary of the two dimensional region  $r < \Delta_{hk}$  is contained in the rectangle  $[a, b] \times [M_s, m_s]$**

• If  $b = 2l_i$

we can rewrite the double integral (4.42) adding and subtracting in the interior integral the Taylor expansion of second order centered in  $(s, z) = (2l_i, 0)$  of the two variables function  $\sqrt{\Delta_{hk}^2 - (z - a_s)^2} \tilde{w}_j^{(d_j)}(z)$ :

$$\begin{aligned}
& - \int_a^{2l_i} \tilde{w}_i^{(d_i)}(s) \int_0^{m_s} \frac{\sqrt{\Delta_{hk}^2 - (z - a_s)^2} \tilde{w}_j^{(d_j)}(z) - \Delta_{hk} \tilde{w}_j^{(d_j)}(0) - \Delta_{hk} \tilde{w}_j^{\prime(d_j)}(0)z}{2(z - a_s)^2} dz ds \\
& + \frac{\Delta_{hk}}{2} \tilde{w}_j^{(d_j)}(0) \int_a^{2l_i} -\tilde{w}_i^{(d_i)}(s) \int_0^{m_s} \frac{1}{(z - a_s)^2} dz ds \\
& + \frac{\Delta_{hk}}{2} \tilde{w}_j^{\prime(d_j)}(0) \int_a^{2l_i} -\tilde{w}_i^{(d_i)}(s) \int_0^{m_s} \frac{z}{(z - a_s)^2} dz ds \\
& =: I_1 + I_2 + I_3.
\end{aligned}$$

For the evaluation of  $I_1$

*Outer integral:* Gauss-Legendre formula

*Inner integral:* regularization procedure (4.27), because of the square root “mild” singularity

For  $I_2$ , after an analytical inner integration:

$$I_2 = -\frac{\Delta_{hk}}{2} \tilde{w}_j^{(d_j)}(0) \int_a^{2l_i} \tilde{w}_i^{(d_i)}(s) \left[ \frac{1}{2l_i - s} - \frac{1}{2l_i - s + m_s} \right] ds =: I_2^1 + I_2^3$$

$I_2^1$  can be evaluated by the HFP formula (4.34) and  $I_2^3$  with the Gauss-Legendre formula.

For  $I_3$ , after an analytical inner integration:

$$\begin{aligned}
I_3 & = -\frac{\Delta_{hk}}{2} \tilde{w}_j^{\prime(d_j)}(0) \int_a^{2l_i} \tilde{w}_i^{(d_i)}(s) \left[ \frac{(m_s - a_s) \log(m_s - a_s) - m_s}{m_s - a_s} - \log(-a_s) \right] ds \\
& =: I_3^1 + I_3^2.
\end{aligned}$$

For the numerical evaluation of  $I_3^1$  we can use a Gauss-Legendre formula, while for  $I_3^2$  we can use the regularization procedure (4.27).

• Otherwise, i.e. the singularity point is not contained in the domain of integration, for the numerical evaluation of (4.42) we can proceed as follows:

*Outer integral:* Gauss-Legendre formula

*Inner integral:* regularization procedure (4.27), because of the square root “mild” singularity.

**Consecutive not aligned boundary elements:**

having set  $a_s = -(2l_i - s) \cos \omega$  and  $b_s = (2l_i - s) \sin \omega$ , we have to numerically evaluate

$$\int_a^b \tilde{w}_i^{(d_i)}(s) \int_{M_s}^{m_s} \left[ -\frac{\mathbf{n}_x \cdot \mathbf{n}_\xi}{2} + \frac{\mathbf{r} \cdot \mathbf{n}_x \mathbf{r} \cdot \mathbf{n}_\xi}{r^2} \right] \frac{\sqrt{\Delta_{hk}^2 - r^2}}{r^2} \tilde{w}_j^{(d_j)}(z) dz ds \quad (4.43)$$

$$= \int_a^b \tilde{w}_i^{(d_i)}(s) \int_{M_s}^{m_s} -\frac{\cos \omega}{2} \frac{\sqrt{\Delta_{hk}^2 - ((z - a_s)^2 + b_s^2)}}{((z - a_s)^2 + b_s^2)} \tilde{w}_j^{(d_j)}(z) dz ds \quad (4.44)$$

$$+ \int_a^b \tilde{w}_i^{(d_i)}(s) \int_{M_s}^{m_s} (-b_s z \sin \omega) \frac{\sqrt{\Delta_{hk}^2 - ((z - a_s)^2 + b_s^2)}}{((z - a_s)^2 + b_s^2)^2} \tilde{w}_j^{(d_j)}(z) dz ds \quad (4.45)$$

$$=: \tilde{I} + I$$

Here I will describe the numerical treatment of  $\tilde{I}$ ; that one used for  $I$  is analogous and it is reported in appendix A.4. Two subcases arise:

**a) the boundary of the two dimensional region  $r < \Delta_{hk}$  is not contained in the rectangle  $[a, b] \times [M_s, m_s]$ , i.e.  $M_s = 0$ ,  $m_s = 2l_{i+1}$**

• If  $b = 2l_i$  and  $M_s = 0$

we can rewrite the double integral (4.44) adding and subtracting in the interior integral the Taylor expansion of first order centered in  $(s, z) = (2l_i, 0)$  of the two variables function  $\sqrt{\Delta_{hk}^2 - ((z - a_s)^2 + b_s^2)} \tilde{w}_j^{(d_j)}(z)$ :

$$\begin{aligned} \tilde{I} &= -\frac{\cos \omega}{2} \int_a^{2l_i} \tilde{w}_i^{(d_i)}(s) \int_0^{m_s} \frac{\sqrt{\Delta_{hk}^2 - ((z - a_s)^2 + b_s^2)} \tilde{w}_j^{(d_j)}(z) - \Delta_{hk} \tilde{w}_j^{(d_j)}(0)}{(z - a_s)^2 + b_s^2} dz ds + \\ &+ \frac{\Delta_{hk} \cos \omega}{2} \tilde{w}_j^{(d_j)}(0) \int_a^{2l_i} -\tilde{w}_i^{(d_i)}(s) \int_0^{m_s} \frac{1}{(z - a_s)^2 + b_s^2} dz ds =: \tilde{I}_1 + \tilde{I}_2 + \tilde{I}_3. \end{aligned}$$

For the numerical evaluation of  $\tilde{I}_1$

*Outer integral:* Gauss-Legendre formula

*Inner integral:* product rule (4.30) for  $[(z - a_s)^2 + b_s^2]^{-1}$  kernel

For  $\tilde{I}_2$ , after an analytical inner integration:

$$\tilde{I}_2 = -\frac{\Delta_{hk} \cos \omega}{2} \tilde{w}_j^{(d_j)}(0) \int_a^{2l_i} \tilde{w}_i^{(d_i)}(s) [f(m_s) - f(0)] ds$$

with

$$f(s) = \frac{1}{b_s} \operatorname{atan} \left( \frac{z - a_s}{b_s} \right)$$

that can be evaluated by the HFP formula (4.34).

- Otherwise, i.e. the singularity point is not contained in the domain of integration, for the numerical evaluation of (4.44) we can proceed as follows:

*Outer integral:* Gauss-Legendre formula

*Inner integral:* Gauss-Legendre formula.

**b) the boundary of the two dimensional region  $r < \Delta_{hk}$  is contained in the rectangle  $[a, b] \times [M_s, m_s]$**

- If  $b = 2l_i$  and  $M_s = 0$

we can rewrite the double integral (4.44) adding and subtracting in the interior integral the Taylor expansion of second order centered in  $(s, z) = (2l_i, 0)$  of the two variables function  $\sqrt{\Delta_{hk}^2 - ((z - a_s)^2 + b_s^2)} \tilde{w}_j^{(d_j)}(z)$ :

$$\begin{aligned} \tilde{I} &= -\frac{\cos \omega}{2} \int_a^{2l_i} \tilde{w}_i^{(d_i)}(s) \int_0^{m_s} \frac{1}{(z - a_s)^2 + b_s^2} \\ &\quad 0 \left[ \sqrt{\Delta_{hk}^2 - ((z - a_s)^2 + b_s^2)} \tilde{w}_j^{(d_j)}(z) - \Delta_{hk} \tilde{w}_j^{(d_j)}(0) - \Delta_{hk} \tilde{w}_j^{(d_j)'}(0) z \right] dz ds \\ &\quad + \frac{\Delta_{hk} \cos \omega}{2} \tilde{w}_j^{(d_j)}(0) \int_a^{2l_i} -\tilde{w}_i^{(d_i)}(s) \int_0^{m_s} \frac{1}{(z - a_s)^2 + b_s^2} dz ds \\ &\quad + \frac{\Delta_{hk} \cos \omega}{2} \tilde{w}_j^{(d_j)'}(0) \int_a^{2l_i} -\tilde{w}_i^{(d_i)}(s) \int_0^{m_s} \frac{z}{(z - a_s)^2 + b_s^2} dz ds \\ &=: \tilde{I}_1 + \tilde{I}_2 + \tilde{I}_3. \end{aligned}$$

For the numerical evaluation of  $\tilde{I}_1$

*Outer integral:* Gauss-Legendre formula

*Inner integral:* regularization procedure (4.27), because of the square root “mild” singularity

For  $\tilde{I}_2$ , after an analytical inner integration:

$$\tilde{I}_2 = -\frac{\Delta_{hk} \cos \omega}{2} \tilde{w}_j^{(d_j)}(0) \int_a^{2l_i} \tilde{w}_i^{(d_i)}(s) [f(m_s) - f(0)] ds$$

with

$$f(s) = \frac{1}{b_s} \operatorname{atan} \left( \frac{z - a_s}{b_s} \right)$$

that can be evaluated by the HFP formula (4.34).

For  $\tilde{I}_3$ , after an analytical inner integration:

$$\tilde{I}_3 = -\frac{\Delta_{hk} \cos \omega}{2} \tilde{w}_j^{(d_j)}(0) \int_a^{2l_i} \tilde{w}_i^{(d_i)}(s) [f(m_s) - f(0)] ds$$

with

$$f(s) = -\frac{\cos \omega}{\sin \omega} \operatorname{atan} \left( \frac{z - a_s}{b_s} \right) + \frac{1}{2} \log((z - a_s)^2 + b_s^2)$$

that can be evaluated by the regularization procedure (4.27) for the logarithm and with the Gauss-Legendre formula.

• Otherwise, i.e. the singularity point is not contained in the domain of integration, for the numerical evaluation of (4.44) we can proceed as follows:

*Outer integral:* Gauss-Legendre formula

*Inner integral:* Gauss-Legendre formula.



# A

## Appendix

### A.1 Remarks on energy coerciveness in 1D

The coerciveness of the quadratic form  $a_{\mathcal{E}}(\varphi, \varphi)$ , defined in (2.12), asserts a coerciveness property of the total energy of the solution  $u$  to problem (2.1). This follows at once from the equality

$$a_{\mathcal{E}}(\varphi, \varphi) = \mathcal{E}(T).$$

Thus, remembering (2.4), theorem 19 assures that

$$\mathcal{E}(T) \geq c(T) \left\| \left[ \frac{\partial u}{\partial \mathbf{n}} \right] \right\|_{L^2(\Sigma)}^2. \quad (\text{A.1})$$

The purpose of this section is to point out some interesting facts about the different contributions to inequality (A.1) of the external and internal energies, defined respectively as

$$\mathcal{E}_+(t) := \frac{1}{2} \int_{\mathbb{R} \setminus (0,L)} (u_t(x,t)^2 + u_x(x,t)^2) dx, \quad \mathcal{E}_-(t) := \frac{1}{2} \int_0^L (u_t(x,t)^2 + u_x(x,t)^2) dx.$$

We shall see that the main contribution to inequality (A.1) is provided by the external energy. Indeed, for any given time  $T$ , one may replace in (A.1) the global energy  $\mathcal{E}(T)$  with  $\mathcal{E}_+(T)$ , provided a slightly larger coerciveness constant  $\tilde{c}(T)$  takes the place of  $c(T)$ . On the contrary, interactions of reflected waves make the contribution of the internal energy  $\mathcal{E}_-(T)$  almost negligible at least for large times  $T \gg L$ . More precisely, for any  $T$  greater than  $L$ , we have (see (A.4) below):

$$\mathcal{E}_-(T) = \frac{1}{4} \int_{T-L}^T |\varphi(t)|^2 dt, \quad (\text{A.2})$$

thus  $\mathcal{E}_-(T)$  vanishes provided  $\varphi(t) = 0$  in the “small” interval  $(T - L, T)$ .

Although these arguments rely upon particular features of the one dimensional d’Alembert equation, they could suggest a possible approach even for the much more difficult cases of the two or three dimensional wave equation. In fact also in the  $n$ -dimensional case, at least for non trapping domains, the external energy at a given time is strictly positive and thus may be viewed as a possible coercive quadratic form in the single layer potential variable  $\varphi$  with respect to a suitable norm  $|\cdot|_W$ . Of course, in the  $n$ -dimensional case the main open problem is the identification of the functional space  $W$ .

Start by observing that the solution  $u^+$  to problem (2.1), on each external interval is a simple progressive wave, that is

$$u^+(x, t) = \begin{cases} g_{\mathcal{D}}^L(t + L - x) & \text{for } x > L, \\ g_{\mathcal{D}}^0(t + x) & \text{for } x < 0. \end{cases}$$

Thus, at the boundary points  $x = 0, x = L$ , on has

$$\frac{\partial u^+}{\partial \mathbf{n}} = -g_{\mathcal{D},t} = -(V\varphi)_t, \quad t \in [0, T].$$

On the other hand, from the energy identity on the external domain and remembering the definition of the operator  $A$ ,

$$\mathcal{E}_+(T) = - \int_0^T \frac{\partial u^+}{\partial \mathbf{n}} \cdot g_{\mathcal{D},t} dt = \int_0^T |(V\varphi)_t|^2 dt = \langle A\varphi, A\varphi \rangle_{L^2(\Sigma)} = \langle A^*A\varphi, \varphi \rangle_{L^2(\Sigma)}. \quad (\text{A.3})$$

Therefore, as claimed before,  $\mathcal{E}_+(T)$  may be viewed as a coercive quadratic form with coerciveness constant  $\tilde{c}(T) = 1/\|A^{-1}\|^2$ .

Let consider the internal energy. From a simple computation,

$$A^*A\varphi(t) = A_s\varphi(t) - \frac{1}{4}H[t - T + L]\varphi(t),$$

which, owing to (A.3), yields for  $\mathcal{E}_-(T)$  the following simple expression:

$$\mathcal{E}_-(T) = \mathcal{E}(T) - \mathcal{E}_+(T) = \langle (A_s - A^*A)\varphi, \varphi \rangle_{L^2(\Sigma)} = \frac{1}{4} \int_0^T H[t - T + L] |\varphi(t)|^2 dt, \quad (\text{A.4})$$

and (A.2) is proved.

I’m going to conclude this section with other two remarks. Even though the internal energy is in general only nonnegative, it still enjoys some coerciveness property adding to  $\mathcal{E}_-(T)$  its integral with respect to time as in the following

**Theorem 27** *For every  $T > 0$ , one has*

$$|\varphi|_{L^2(\Sigma)}^2 \leq 4\mathcal{E}_-(T) + \frac{8}{L} \int_0^T \mathcal{E}_-(t) dt. \quad (\text{A.5})$$

*Proof.* Instead of using directly the identity (A.4), derive (A.5) from a simple application of the multipliers technique. Let define the function

$$q(x) = \frac{2}{L} \left(x - \frac{2}{L}\right), \quad 0 < x < L,$$

and evaluate through integrations by parts the integral

$$\int_0^T \int_0^L \left(u_{tt}(x,t) - u_{xx}(x,t)\right) q(x) u_x(x,t) dx dt = 0$$

in terms of space and space-time integrals of quadratic forms, either on the boundary or on the interval  $(0, L)$ . The function  $u$  will be assumed regular enough to perform all the integration by parts; the estimate (A.5) then will follow by a density argument.

$$\begin{aligned} & \int_0^T \int_0^L u_{tt}(x,t) q(x) u_x(x,t) dx dt = \\ & \int_0^T \int_0^L [u_t(x,t) q(x) u_x(x,t)]_t dx dt - \int_0^T \int_0^L q(x) u_t(x,t) u_{xt}(x,t) dx dt = \\ & \int_0^L q(x) u_t(x,t) u_x(x,t) dx \Big|_{t=T} - \frac{1}{2} \int_0^T \int_0^L [q(x) u_t^2(x,t)]_x dx dt + \frac{1}{2} \int_0^T \int_0^L q_x(x) u_t^2(x,t) dx dt = \\ & \int_0^L q(x) u_t(x,t) u_x(x,t) dx \Big|_{t=T} - \frac{1}{2} \int_0^T |g_t(t)|^2 dt + \frac{1}{2} \int_0^T \int_0^L q_x(x) u_t^2(x,t) dx dt. \end{aligned} \quad (\text{A.6})$$

On the other hand

$$\begin{aligned} & \int_0^T \int_0^L u_{xx}(x,t) q(x) u_x(x,t) dx dt = \\ & \frac{1}{2} \int_0^T \int_0^L [q(x) u_x^2(x,t)]_x dx dt - \frac{1}{2} \int_0^T \int_0^L q_x(x) u_x^2(x,t) dx dt = \\ & \frac{1}{2} \int_0^T (u_x^2(0,t) + u_x^2(L,t)) dx - \frac{1}{2} \int_0^T \int_0^L q_x(x) u_x^2(x,t) dx dt. \end{aligned} \quad (\text{A.7})$$

Thus, summing the equalities (A.6) and (A.7), we get the identity

$$\int_0^L q(x) u_t(x,t) u_x dx \Big|_{t=T} + \frac{2}{L} \int_0^T \mathcal{E}_-(t) dt = \frac{1}{2} \int_0^T |g_t(t)|^2 dt + \frac{1}{2} \int_0^T \left| \frac{\partial u^-}{\partial n}(t) \right|^2 dt, \quad (\text{A.8})$$

and taking into account (A.3),

$$\int_0^L q(x) u_t(x,t) u_x(x,t) dx \Big|_{t=T} + \frac{2}{L} \int_0^T \mathcal{E}_-(t) dt = \frac{1}{2} \int_0^T \left( \left| \frac{\partial u^+}{\partial n} \right|^2 + \left| \frac{\partial u^-}{\partial n} \right|^2 \right) dt. \quad (\text{A.9})$$

By applying the Cauchy-Schwarz inequality in the term of (A.9) containing the product  $u_t u_x$ , and using the following inequality

$$|\varphi|^2 = \left| \frac{\partial u^-}{\partial n} - \frac{\partial u^+}{\partial n} \right|^2 \leq 2 \left( \left| \frac{\partial u^-}{\partial n} \right|^2 + \left| \frac{\partial u^+}{\partial n} \right|^2 \right),$$

the inequality (A.5) is proved.

Finally, by combining the identity (A.3), the energy identity (2.10) and the inequality (A.5), we obtain an alternative proof of the coerciveness estimate (2.15) which does not rely on the algebraic features of the operator  $A_s$ . In fact, by an application of the Cauchy-Schwarz inequality in (2.10),

$$\mathcal{E}(t) \leq \left( \int_0^t |\varphi(\tau)|^2 d\tau \right)^{1/2} \left( \int_0^t |g_{\mathcal{D},t}(\tau)|^2 d\tau \right)^{1/2} \leq |\varphi|_{L^2(\Sigma)} |g_{\mathcal{D},t}|_{L^2(\Sigma)}.$$

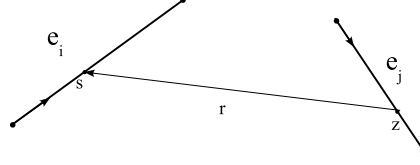
Therefore, since  $\mathcal{E}_-(t) \leq \mathcal{E}(t)$ , we get from (A.5) and (A.3)

$$|\varphi|_{L^2(\Sigma)}^2 \leq 4\mathcal{E}_-(T) + \frac{8T}{L} |\varphi|_{L^2(\Sigma)} \sqrt{\mathcal{E}_+(T)},$$

which yields the following inequality where the internal and external energies play a distinguished role:

$$|\varphi|_{L^2(\Sigma)}^2 \leq 8\mathcal{E}_-(T) + \frac{64T^2}{L^2} \mathcal{E}_+(T).$$

Note that the constant  $(8 + 64T^2/L^2)^{-1}$  is not optimal, nevertheless as function of the ratio  $T/L$  has the same asymptotic behavior of  $c(T)$  in (2.16).

**A.2 Integration over disjoint elements ( $\bar{e}_i \cap \bar{e}_j = \emptyset$ )**

Having indicated with  $(x_{i-1}^1, x_{i-1}^2)$ ,  $(x_i^1, x_i^2)$  the end-points of  $e_i$  and with  $(\xi_{j-1}^1, \xi_{j-1}^2)$ ,  $(\xi_j^1, \xi_j^2)$  the end-points of  $e_j$ , the distance between the source and the field points can be written as

$$r^2 = [A + Bs - Cz]^2 + [D + Es - Fz]^2,$$

where

$$A = x_{i-1}^1 - \xi_{j-1}^1, \quad B = \frac{x_i^1 - x_{i-1}^1}{2\ell_i}, \quad C = \frac{\xi_j^1 - \xi_{j-1}^1}{2\ell_j},$$

$$D = x_{i-1}^2 - \xi_{j-1}^2, \quad E = \frac{x_i^2 - x_{i-1}^2}{2\ell_i}, \quad F = \frac{\xi_j^2 - \xi_{j-1}^2}{2\ell_j}.$$

The double integration domain is the intersection between the rectangle  $[0, 2\ell_i] \times [0, 2\ell_j]$  and the two dimensional domain

$$r < \Delta_{hk} \quad \Leftrightarrow \quad [A + Bs - Cz]^2 + [D + Es - Fz]^2 < \Delta_{hk}^2, \quad (\text{A.10})$$

where the Heaviside function is not trivial. Using the relations

$$B^2 + E^2 = 1, \quad C^2 + F^2 = 1,$$

with a straightforward calculation, the result is that the inequality (A.10) is satisfied if and only if

$$\Delta_{hk}^2 - ((BF - EC)s + FA - CD)^2 > 0,$$

that implies restriction on the outer variable of integration  $s$  when  $BF - EC \neq 0$ ; more precisely:

$$\text{if } BF - EC > 0, \quad m := \frac{-\Delta_{hk} - (FA - CD)}{BF - EC} < s < \frac{\Delta_{hk} - (FA - CD)}{BF - EC} =: M$$

$$\text{if } BF - EC < 0, \quad m := \frac{\Delta_{hk} - (FA - CD)}{BF - EC} < s < \frac{-\Delta_{hk} - (FA - CD)}{BF - EC} =: M.$$

Under these restrictions, the inequality (A.10) will be satisfied for

$$z_1^s < z < z_2^s,$$

where

$$z_{1,2}^s = (AC + FD) + (BC + EF)s \mp \sqrt{\Delta_{hk}^2 - ((BF - EC)s + FA - CD)^2}. \quad (\text{A.11})$$

Therefore, having set

$$\begin{aligned} s_0 &= \max(0, m), & s_1 &= \min(2l_i, M), \\ M_s &= \max(0, z_1^s), & m_s &= \min(2l_j, z_2^s), \end{aligned}$$

double integral (4.19) in this case becomes

$$\int_{s_0}^{s_1} \tilde{w}_i^{(d_i)}(s) \int_{M_s}^{m_s} \mathcal{S}(r, t_h, t_k) \tilde{w}_j^{(d_j)}(z) dz ds. \quad (\text{A.12})$$

The numerical quadrature in the outer variable of integration  $s$  has been optimally performed subdividing, when necessary, the outer interval of integration. In fact, the derivative with respect to  $s$  of the outer integrand function, after the inner integration, presents a jump in correspondence to possible subdivision points to be searched among the solutions of the equations

$$z_1^s = 0, \quad z_2^s = 2l_j,$$

formally given by

$$\begin{aligned} s_1^{1,2} &= -(AB + ED) \mp \sqrt{\Delta_{hk}^2 + (AB + ED)^2 - A^2 - D^2}, \\ s_2^{1,2} &= G \mp \sqrt{\Delta_{hk}^2 + G^2 - (FA - CD)^2 - (2l_j - AC - FD)^2}, \end{aligned}$$

where  $G = (BC + EF)(2l_j - AC - FD) - (BF - EC)(FA - CD)$ .

When one or more of these solutions are real and belong to the outer interval of integration, (A.12) will be decomposed into the sum of double integrals of the form

$$\int_a^b \tilde{w}_i^{(d_i)}(s) \int_{M_s}^{m_s} \mathbf{S}(r, t_h, t_k) \tilde{w}_j^{(d_j)}(z) dz ds, \quad (\text{A.13})$$

where  $[a, b] \subset [s_0, s_1]$ . Of course, when no subdivision is needed, one will have to deal with only one double integral (A.13) where  $[a, b] \equiv [s_0, s_1]$ . Note that for some values of  $s$  it could happen that  $m_s - M_s \leq 0$ : in this case the inner integral does not give any contribution to the final result and its evaluation has to be avoided.

### A.3 Recurrence relations for product rules

- $S(y, x) = \ln(|x - a_y|)$

In [18] the following recursive relation has been derived to compute the modified moments:

$$\begin{cases} \mu_0(y) = (1 + a_y) \ln(1 + a_y) + (1 - a_y) \ln(1 - a_y) - 2 \\ \mu_j(y) = \frac{1}{2j} Q_{j-1}^{(1,1)}(a_y), \quad j \geq 1 \end{cases}$$

where the quantities:

$$\begin{cases} Q_0^{(1,1)}(a_y) = (1 - a_y^2) \ln \frac{1 - a_y}{1 + a_y} - 2a_y \\ Q_1^{(1,1)}(a_y) = 2a_y Q_0^{(1,1)}(a_y) + \frac{8}{3} \\ Q_j^{(1,1)}(a_y) = \frac{j+1}{j(j+2)} [(2j+1)a_y Q_{j-1}^{(1,1)}(a_y) - j Q_{j-2}^{(1,1)}(a_y)], \quad j \geq 2 \end{cases}$$

are Jacobi functions of second kind [51].

- $S(y, x) = \ln[(x - a_y)^2 + b_y^2]$ ,  $b_y \neq 0$

Here:

$$\begin{aligned} \mu_0(y) &= (1 - a_y) \ln[(1 - a_y)^2 + b_y^2] + (1 + a_y) \ln[(1 + a_y)^2 + b_y^2] + \\ &\quad + 2b_y \left[ \arctan \frac{1 + a_y}{b_y} + \arctan \frac{1 - a_y}{b_y} \right] - 4 \\ \mu_j(y) &= \frac{1}{j} \int_{-1}^1 \frac{(1 - x^2)(x - a_y)}{(x - a_y)^2 + b_y^2} P_{j-1}^{(1,1)}(x) dx, \quad j \geq 1, \end{aligned}$$

where  $\{P_j^{(1,1)}(x)\}$  are Jacobi polynomials [51], which are related to Legendre polynomials through:

$$P_j(x) = -\frac{1}{2j} \frac{d}{dx} [(1 - x^2) P_{j-1}^{(1,1)}(x)], \quad j \geq 1.$$

Having defined:

$$m_j(y) = \int_{-1}^1 (1 - x^2)(x - a_y) P_j^{(1,1)}(x) dx = \begin{cases} -\frac{4}{3} a_y & j = 0 \\ \frac{8}{15} & j = 1 \\ 0 & j \geq 2 \end{cases}$$

modified moments  $\mu_j(y)$  follows from these latter quantities by means of the procedure described in (2iii) below.

- rational function containing factors of the type  $(x - a_y)$  and divisors of the type  $(x - a_y)$  and  $[(x - a_y)^2 + b_y^2]$ .

Let assume to know the quantities:

$$m_j(y) = \int_{-1}^1 S(y, x) p_j(x) dx$$

associated with a given set of polynomials satisfying a recurrence relation of the form:

$$\begin{cases} p_0(x) = 1 \\ p_1(x) = k_1^{(1)}x + k_0^{(1)} \\ p_{j+1}(x) = \alpha_j x p_j(x) - \beta_j p_{j-1}(x), \quad j \geq 1. \end{cases}$$

Then, in the case of new kernels of the form:

$$(2i) \quad \bar{S}(y, x) = S(y, x)(x - a_y)$$

$$(2ii) \quad \bar{S}(y, x) = \frac{S(y, x)}{(x - a_y)}, \quad a_y \neq \pm 1$$

$$(2iii) \quad \bar{S}(y, x) = \frac{S(y, x)}{[(x - a_y)^2 + b_y^2]}, \quad b_y \neq 0,$$

one has, respectively:

$$(2i) \quad \begin{cases} \bar{m}_0(y) = \frac{1}{k_1^{(1)}} m_1(y) - \left( \frac{k_0^{(1)}}{k_1^{(1)}} + a_y \right) m_0(y) \\ \bar{m}_j(y) = \frac{1}{\alpha_j} m_{j+1}(y) - a_y m_j(y) + \frac{\beta_j}{\alpha_j} m_{j-1}(y), \quad j \geq 1 \end{cases}$$

$$(2ii) \quad \bar{m}_j(y) = q_j(a_y), \quad \text{with}$$

$$\begin{cases} q_0(z) = \int_{-1}^1 \frac{S(y, x)}{x - z} dx \\ q_1(z) = p_1(z) q_0(z) + k_1^{(1)} m_0(y) \\ q_{j+1}(z) = \alpha_j z q_j(z) - \beta_j q_{j-1}(z) + \alpha_j m_j(y), \quad j \geq 1, \end{cases}$$



when  $z \in (-1, 1)$  the integral defining  $q_0(z)$  ought to be defined in the Cauchy principal value sense;

$$(2iii) \quad \begin{cases} \bar{m}_0(y), \bar{m}_1(y) & \text{must be computed explicitly} \\ \bar{m}_2(y) = \alpha_0 \alpha_1 (m_0(y) + a_y \bar{m}_1(y)) - [\alpha_0 \alpha_1 (a_y^2 + b_y^2) + \beta_1] \bar{m}_0(y) \\ \bar{m}_j(y) = \frac{q_j^I(a_y + ib_y)}{b_y}, & j \geq 3 \end{cases}$$

where

$$\begin{aligned} q_0^R(z_y) &= \frac{1}{\alpha_0} \bar{m}_1(y) - a_y \bar{m}_0(y) \\ q_0^I(z_y) &= b_y \bar{m}_0(y) \\ q_1^R(z_y) &= \frac{1}{\alpha_1} \bar{m}_2(y) - a_y \bar{m}_1(y) + \frac{\beta_1}{\alpha_1} \bar{m}_0(y) \\ q_1^I(z_y) &= b_y \bar{m}_1(y) \\ q_{j+1}^R(z_y) &= \alpha_j a_y q_j^R(z_y) - \alpha_j b_y q_j^I(z_y) - \beta_j q_{j-1}^R(z_y) + \alpha_j m_j(y) \\ q_{j+1}^I(z_y) &= \alpha_j a_y q_j^I(z_y) + \alpha_j b_y q_j^R(z_y) - \beta_j q_{j-1}^I(z_y), \quad j \geq 1. \end{aligned}$$

**Remark.** The considered kernels have real or complex poles outside (except for the logarithmic kernel and (2ii) above, if  $a_y \in (-1, 1)$ ) the interval of integration. Whenever these singularities are very close to the interval of integration, the corresponding kernels cannot be considered *smooth*, in the sense that any standard quadrature rule, for instance the Gauss-Legendre formula, would perform poorly. Therefore it would require a large number of points to achieve the required accuracy [44]. For this reason, unless the poles are *sufficiently* far away from the region of integration, one should use the product rules presented in subsection 4.3.

#### A.4 Numerical integration of (4.45)

For the evaluation of  $I$  the standard two subcases arise:

**a) the boundary of the two dimensional region  $r < \Delta_{hk}$  is not contained in the rectangle  $[a, b] \times [M_s, m_s]$**

- If  $b = 2l_i$  and  $M_s = 0$

we can rewrite the double integral (4.45) adding and subtracting in the interior integral the Taylor expansion of first order centered in  $(s, z) = (2l_i, 0)$  of the two variables function  $\sqrt{\Delta_{hk}^2 - ((z - a_s)^2 + b_s^2)} \tilde{w}_j^{(d_j)}(z)$  because in this term the singularity in the interior integral is stronger:

$$I = \int_a^{2l_i} \tilde{w}_i^{(d_i)}(s) \int_0^{m_s} \frac{(b_s z \sin \omega) \left[ \tilde{w}_j^{(d_j)}(z) \sqrt{\Delta_{hk}^2 - ((z - a_s)^2 + b_s^2)} - \Delta_{hk} \tilde{w}_j^{(d_j)}(0) \right]}{((z - a_s)^2 + b_s^2)^2} dz ds$$

$$+ \Delta_{hk} \tilde{w}_j^{(d_j)}(0) \int_a^{2l_i} -\tilde{w}_i^{(d_i)}(s) \int_0^{m_s} \frac{z (b_s \sin \omega)}{((z - a_s)^2 + b_s^2)^2} dz ds =: I_1 + I_2.$$

For the numerical evaluation of  $I_1$

*Outer integral:* regularization procedure (4.27)

*Inner integral:* product rule (4.30) for  $[(z - a_s)^2 + b_s^2]^{-1}$  kernel

For  $I_2$ , after an analytical inner integration:

$$I_2 = -\Delta_{hk} \tilde{w}_j^{(d_j)}(0) \int_a^{2l_i} \tilde{w}_i^{(d_i)}(s) (b_s \sin \omega) [f(m_s) - f(0)] ds$$

with

$$f(s) = \frac{za_s - (a_s^2 + b_s^2)}{2b_s^2((z - a_s)^2 + b_s^2)} - \frac{\cos \omega}{2b_s^2 \sin \omega} \operatorname{atan} \left( \frac{z - a_s}{b_s} \right)$$

that can be evaluated by the HFP formula (4.34) and the Gauss-Legendre formula.

- Otherwise, i.e. the singularity point is not contained in the domain of integration, for the numerical evaluation of (4.45) we can proceed as follows:

*Outer integral:* Gauss-Legendre formula

*Inner integral:* Gauss-Legendre formula.

**b) the boundary of the two dimensional region  $r < \Delta_{hk}$  is contained in the rectangle  $[a, b] \times [M_s, m_s]$**

- If  $b = 2l_i$  and  $M_s = 0$

we can rewrite the double integral (4.45) adding and subtracting in the interior integral the Taylor expansion of third order centered in  $(s, z) = (2l_i, 0)$  of the two variables function  $\sqrt{\Delta_{hk}^2 - ((z - a_s)^2 + b_s^2)} \tilde{w}_j^{(d_j)}(z)$  because in this term the singularity in the interior integral is stronger:

$$\begin{aligned}
I = & \int_a^{2l_i} \tilde{w}_i^{(d_i)}(s) \int_0^{m_s} \frac{(b_s z \sin \omega)}{((z - a_s)^2 + b_s^2)^2} \left[ \tilde{w}_j^{(d_j)}(z) \sqrt{\Delta_{hk}^2 - ((z - a_s)^2 + b_s^2)} \right. \\
& \left. - \Delta_{hk} \tilde{w}_j^{(d_j)}(0) - \Delta_{hk} \tilde{w}_j^{\prime(d_j)}(0) z - \frac{z^2}{2} \left( \tilde{w}_j^{\prime\prime(d_j)}(0) \Delta_{hk} - \frac{\tilde{w}_j^{(d_j)}(0)}{\Delta_{hk}} \right) \right] dz ds \\
& + \Delta_{hk} \tilde{w}_j^{(d_j)}(0) \int_a^{2l_i} -\tilde{w}_i^{(d_i)}(s) \int_0^{m_s} \frac{z(b_s \sin \omega)}{((z - a_s)^2 + b_s^2)^2} dz ds \\
& + \Delta_{hk} \tilde{w}_j^{\prime(d_j)}(0) \int_a^{2l_i} -\tilde{w}_i^{(d_i)}(s) \int_0^{m_s} \frac{z^2(b_s \sin \omega)}{((z - a_s)^2 + b_s^2)^2} dz ds \\
& + \Delta_{hk} \left( \tilde{w}_j^{\prime\prime(d_j)}(0) \Delta_{hk} - \frac{\tilde{w}_j^{(d_j)}(0)}{\Delta_{hk}} \right) \int_a^{2l_i} -\tilde{w}_i^{(d_i)}(s) \int_0^{m_s} \frac{z^3(b_s \sin \omega)}{((z - a_s)^2 + b_s^2)^2} dz ds \\
= & I_1 + I_2 + I_3 + I_4.
\end{aligned}$$

For the numerical evaluation of  $I_1$

*Outer integral:* Gauss-Legendre formula

*Inner integral:* regularization procedure (4.27), because of the square root “mild” singularity

For  $I_2$ , after an analytical inner integration:

$$I_2 = -\Delta_{hk} \tilde{w}_j^{(d_j)}(0) \int_a^{2l_i} \tilde{w}_i^{(d_i)}(s) (b_s \sin \omega) [f(m_s) - f(0)] ds$$

with

$$f(s) = \frac{za_s - (a_s^2 + b_s^2)}{2b_s^2((z - a_s)^2 + b_s^2)} - \frac{\cos \omega}{2b_s^2 \sin \omega} \operatorname{atan} \left( \frac{z - a_s}{b_s} \right)$$

that can be evaluated by the HFP formula (4.34) and the Gauss-Legendre formula.

For  $I_3$ , after an analytical inner integration:

$$I_3 = -\Delta_{hk} \tilde{w}_j^{(d_j)}(0) \int_a^{2l_i} \tilde{w}_i^{(d_i)}(s) (b_s \sin \omega) [f(m_s) - f(0)] ds$$

with

$$f(s) = \frac{-a_s + z(\cos^2 \omega - \sin^2 \omega)}{2 \sin^2 \omega ((z - a_s)^2 + b_s^2)} - \frac{1}{2b_s} \operatorname{atan} \left( \frac{z - a_s}{b_s} \right)$$

that can be evaluated with the Gauss-Legendre formula.

For  $I_4$ , after an analytical inner integration:

$$I_4 = -\Delta_{hk} \left( \tilde{w}_j^{(d_j)}(0) \Delta_{hk} - \frac{\tilde{w}_j^{(d_j)}(0)}{\Delta_{hk}} \right) \int_a^{2l_i} \tilde{w}_i^{(d_i)}(s) (b_s \sin \omega) [f(m_s) - f(0)] ds$$

with

$$f(s) = \frac{1}{2} \log((z - a_s)^2 + b_s^2) - \frac{(\cos^3 \omega + 3 \sin^2 \omega \cos \omega)}{2 \sin^3 \omega} \operatorname{atan} \left( \frac{z - a_s}{b_s} \right) + \frac{a_s^4 - b_s^4 - z a_s^3 - 3 z a_s b_s^2}{2 b_s^2 ((z - a_s)^2 + b_s^2)}$$

that can be evaluated by the product rule (4.30) for  $\log((z - a_s)^2 + b_s^2)$  kernel and the Gauss-Legendre formula.

Tables A.1-A.4 show the efficiency of the adopted quadrature techniques and in particular the convenience in using the regularization procedure (4.27) in evaluating  $I_1$  as underlined by the decreasing of relative errors with the varying of  $p$  and  $q$  parameters in table A.1 (to fix  $p = q = 1$  means to use the standard Gauss Legendre formula).

The sequence of the following four tables A.1-A.4 is referred to the discretization parameters  $\omega = \pi/2$ ,  $2l_i = 2l_{i+1} = 0.1$ ,  $\Delta_{hk} = 0.05$ .

• Otherwise, i.e. the singularity point is not contained in the domain of integration, for the numerical evaluation of (4.45) we can proceed as follows:

*Outer integral:* Gauss-Legendre formula

*Inner integral:* regularization procedure (4.27), because of the square root “mild” singularity.

nodes	$p = q = 1$	$p = q = 2$	$p = q = 3$
$8^2$	$1.051507 \cdot 10^{-3}$	$1.804700 \cdot 10^{-3}$	$2.610697 \cdot 10^{-3}$
$16^2$	$3.925552 \cdot 10^{-5}$	$3.467667 \cdot 10^{-5}$	$1.969021 \cdot 10^{-5}$
$32^2$	$2.071282 \cdot 10^{-6}$	$2.857438 \cdot 10^{-7}$	$2.749069 \cdot 10^{-8}$

Table A.1: Relative Error w.r.t. the exact integral value  $I_1 = 6.156878 \cdot 10^{-3}$ .

nodes	1	2
	$1.068267 \cdot 10^{-2}$	$1.232387 \cdot 10^{-15}$

Table A.2: Relative Error w.r.t. the exact integral value  $I_2 = 3.476736 \cdot 10^{-1}$ .

nodes	2	4	8
	$3.427467 \cdot 10^{-5}$	$1.183973 \cdot 10^{-5}$	$3.091870 \cdot 10^{-6}$

Table A.3: Relative Error w.r.t. the exact integral value  $I_3 = 2.261957 \cdot 10^{-2}$ .

nodes	8	16	32
	$4.801363 \cdot 10^{-4}$	$3.318646 \cdot 10^{-5}$	$2.193332 \cdot 10^{-6}$

Table A.4: Relative Error w.r.t. the exact integral value  $I_4 = 8.178796 \cdot 10^{-3}$ .

## References

1. A.I. Abreu, J.A.M. Carrer, and W.J. Mansur. Scalar wave propagation in 2D: a bem formulation based on the operational quadrature method. *Eng. Anal. Bound. Elem.*, 27:101–105, 2003.
2. A. Aimi and M. Diligenti. A new space-time energetic formulation for wave propagation analysis in layered media by BEMs. *Int. J. for Num. Meth. in Eng.*, 75(9):1102–1127, 2008.
3. A. Aimi, M. Diligenti, C. Guardasoni, I. Mazzieri, and S. Panizzi. An energy approach to space-time Galerkin BEM for wave propagation problems. *Internat. J. Numer. Methods Engrg.*, available online, 2009.
4. A. Aimi, M. Diligenti, C. Guardasoni, and S. Panizzi. A space-time energetic formulation for wave propagation analysis by BEM's. *Riv. Mat. Univ. Parma*, 8(7):171–207, 2008.
5. A. Aimi, M. Diligenti, and G. Monegato. New numerical integration schemes for applications of Galerkin BEM to 2D problems. *Internat. J. Numer. Methods Engrg.*, 40:1977–1999, 1997.
6. A. Aimi, M. Diligenti, and G. Monegato. Numerical integration schemes for the BEM solution of hypersingular integral equations. *Internat. J. Numer. Methods Engrg.*, 45(12):1807–1830, 1999.
7. H. Antes. A boundary element procedure for transient wave propagations in two-dimensional isotropic media. *Finite Elem. Anal. Des.*, 1:313–322, 1985.
8. H. Antes, G. Beer, and W. Moser. A Duhamel integral based approach to one-dimensional wave propagation analysis in layered media. *Comput. Mech.*, 35(2):115–126, 2005.
9. A. Bachelot, L. Bounhoure, and A. Pujols. Time dependent integral method for Maxwell's system. In *Mathematical and numerical aspects of wave propagation*. SIAM, Philadelphia, 1995.
10. A. Bamberger and T. Ha Duong. Formulation variationnelle espace-temps pour le calcul par potentiel retardé de la diffraction d'une onde acoustique. I. *Math. Methods Appl. Sci.*, 8(3):405–435, 1986.
11. A. Bamberger and T. Ha Duong. Formulation variationnelle pour le calcul de la diffraction d'une onde acoustique par une surface rigide. *Math. Methods Appl. Sci.*, 8(4):598–608, 1986.
12. E. Bécache. A variational boundary integral equation method for an elastodynamic antiplane crack. *Internat. J. Numer. Methods Engrg.*, 36(6):969–984, 1993.
13. E. Bécache. Equations intégrales pour l'équation des ondes. INRIA, Paris, janvier 1994.
14. B. Birgisson, E. Siebrits, and A. P. Peirce. Elastodynamic direct boundary element methods with enhanced numerical stability properties. *Internat. J. Numer. Methods Engrg.*, 46(6):871–888, 1999.
15. G. Chen and J. Zhou. *Boundary element methods*. Computational Mathematics and Applications. Academic Press Ltd., London, 1992.
16. I. Chudinovich. Boundary equations in dynamic problems of the theory of elasticity. *Acta Appl. Math.*, 65(1-3):169–183, 2001. Special issue dedicated to Antonio Avantaggiati on the occasion of his 70th birthday.
17. P.G. Ciarlet. *Introduction à l'analyse numérique matricielle et à l'optimisation*. Masson, Paris, 1985.
18. V. Colombo and G. Monegato. Product integration for linear transport equation in slab geometry. *Numer. Math.*, 52:219–240, 1988.
19. M. Costabel. Developments in boundary element methods for time-dependent problems. In *Problems and methods in mathematical physics*, volume 134, pages 17–32. Teubner-Texte Math., 1994.
20. M. Costabel. *Time-dependent problems with the boundary integral equations method*. John Wiley and Sons, 2004.
21. B. Davies. *Integral Transforms and their Applications*. Springer-Verlag, New York, 2002.
22. D.G. Duffy. *Green's functions with applications*. Chapman & Hall/CRC, 2001.
23. D. Elliot and D.F. Paget. Product-integration rules and their occurrence. *BIT*, 16:32–40, 1976.
24. A. Frangi. Elastodynamics by BEM: a new direct formulation. *Internat. J. Numer. Methods Engrg.*, 45(6):721–740, 1999.

25. A. Frangi. “Causal” shape functions in the time domain boundary element method. *Comput. Mech.*, 25(6):533–541, 2000.
26. A. Frangi and G. Novati. On the numerical stability of time-domain elastodynamic analyses by BEM. *Comput. Methods Appl. Mech. Engrg.*, 173(3-4):403–417, 1999.
27. W.H.J. Fuchs. On the eigenvalues of an integral equation arising in the theory of band-limited signals. *J. Math. Analysis Appl.*, 9:533–541, 1964.
28. R. Gallego and J. Domínguez. Hypersingular BEM for transient elastodynamics. *Internat. J. Numer. Methods Engrg.*, 39(10):1681–1705, 1996.
29. T. Ha Duong. On the transient acoustic scattering by a flat object. *Japan J. Appl. Math.*, 7:489–513, 1990.
30. T. Ha Duong. On retarded potential boundary integral equations and their discretization. In *Topics in computational wave propagation. Direct and inverse problems*. Davies P., Duncan D., Martin P. and Rynne B. (eds). Springer-Verlag, 2003.
31. N.M. Hung. On the smoothness of a solution of the Dirichlet problem for hyperbolic systems in domains with a non-smooth boundary. *Russian Mathematical Surveys*, 53(2):387–389, 1998.
32. U. Iturraran-Viveros and F.J. Sanchez-Sesma. Variational formulation for every nonlinear problem. *Geophys. J. Int.*, 162:379–393, 2005.
33. I. Lasiecka and R. Triggiani. Sharp regularity theory for second order hyperbolic equations of Neumann type. I.  $L_2$  nonhomogeneous data. *Ann. Mat. Pura Appl. (4)*, 157:285–367, 1990.
34. I. Lasiecka and R. Triggiani. Regularity theory of hyperbolic equations with nonhomogeneous Neumann boundary conditions. II. General boundary data. *J. Differential Equations*, 94(1):112–164, 1991.
35. I. Lasiecka, J.L. Lions, and R. Triggiani. Non homogeneous boundary value problems for second order hyperbolic operators. *J. Math. Pures et Appl.*, 65:149–192, 1986.
36. G. Lebeau and M. Schatzman. A wave problem in a half-space with a unilateral constraint at the boundary. *J. Differential Equations*, 53:309–361, 1984.
37. J.-L. Lions and E. Magenes. *Problèmes aux limites non homogènes et applications. Vol. 1.* Travaux et Recherches Mathématiques, No. 17. Dunod, Paris, 1968.
38. J.-L. Lions and E. Magenes. *Problèmes aux limites non homogènes et applications. Vol. 2.* Travaux et Recherches Mathématiques, No. 18. Dunod, Paris, 1968.
39. C. Lubich. Convolution quadrature and discretized operational calculus. I. *Numer. Math.*, 52(2):129–145, 1988.
40. C. Lubich. Convolution quadrature and discretized operational calculus. II. *Numer. Math.*, 52(4):413–425, 1988.
41. C. Lubich. On the multistep time discretization of linear initial-boundary value problems and their boundary integral equations. *Numer. Math.*, 67:365–389, 1994.
42. G. Maier, M. Diligenti, and A. Carini. A variational approach to boundary element elastodynamic analysis and extension to multidomain problems. *Comput. Methods Appl. Mech. Engrg.*, 92(2):193–213, 1991.
43. S. Miyatake. Neumann operator for wave equation in a half space and microlocal orders of singularities along the boundary. In *Seminaire sur les Equations aux Dérivées Partielles*, Exp. No. XVI, page 8 pp. Ecole Polytech., Palaiseau, 1993.
44. G. Monegato. Quadrature formulas for functions with poles near the interval of integration. *Math. Comp.*, 47:137–158, 1986.
45. G. Monegato. The numerical evaluation of 2-D Cauchy principal value integral arising in boundary integral equation methods. *Math. Comp.*, 62(206):765–777, 1994.
46. G. Monegato and L. Scuderi. Numerical integration of functions with boundary singularities. *J. Comput. Appl. Math.*, 112(1-2):201–214, 1999.
47. R. Sakamoto. Dirichlet-Neumann problem in a domain with piecewise-smooth boundary. *Tsukuba J. Math.*, 26(2):387–406, 2002.
48. F.J. Sanchez-Sesma and U. Iturraran-Viveros. Scattering and diffraction of SH waves by a finite crack: an analytical solution. *Geophys. J. Int.*, 145:749–758, 2001.
49. M. Schanz and H. Antes. A new visco- and elastodynamic time domain: boundary element formulation. *Comput. Mech.*, 20(5):452–459, 1997.

50. D. Slepian. Some comments on Fourier analysis. *Uncertainty and Modelling, SIAM Review*, 25(3):379–393, 1983.
51. G. Szegő. *Orthogonal polynomials*. American Mathematical Society, Providence, R.I., fourth edition, 1975. American Mathematical Society, Colloquium Publications, Vol. XXIII.
52. G. Yu, W. J. Mansur, J. A. M. Carrer, and L. Gong. Stability of Galerkin and collocation time domain boundary element method as applied to the scalar wave equation. *Comput. & Structures*, 74(4):495–506, 2000.
53. Ch. Zhang. A 2d hypersingular time-domain bem for transient elastodynamic crack analysis. *Wave Motion*, 35(1):17–40, 2002.